

# Climate Change in Central and South America: Recent Trends, Future Projections, and Impacts on Regional Agriculture

Working Paper No. 73

CGIAR Research Program on Climate Change,  
Agriculture and Food Security (CCAFS)

Jose A Marengo  
Sin Chan Chou  
Roger R Torres  
Angelica Giarolla  
Lincoln M Alves  
Andre Lyra



RESEARCH PROGRAM ON  
**Climate Change,  
Agriculture and  
Food Security**



Working Paper

# Climate Change in Central and South America: Recent Trends, Future Projections, and Impacts on Regional Agriculture

Working Paper No. 73

CGIAR Research Program on Climate Change, Agriculture and Food Security (CCAFS)

Jose A Marengo

Sin Chan Chou

Roger R Torres

Angelica Giarolla

Lincoln M Alves

Andre Lyra

**Correct citation:**

Marengo JA, Chou SC, Torres RR, Giarolla A, Alves LM, Lyra A. 2014. *Climate Change in Central and South America: Recent Trends, Future Projections, and Impacts on Regional Agriculture*. CCAFS Working Paper no. 73. CGIAR Research Program on Climate Change, Agriculture and Food Security (CCAFS). Copenhagen, Denmark. Available online at: [www.ccafs.cgiar.org](http://www.ccafs.cgiar.org)

Titles in this Working Paper series aim to disseminate interim climate change, agriculture and food security research and practices and stimulate feedback from the scientific community.

This document is published by the CGIAR Research Program on Climate Change, Agriculture and Food Security (CCAFS), which is a strategic partnership of CGIAR and Future Earth, led by the International Center for Tropical Agriculture (CIAT). CCAFS is supported by the CGIAR Fund, the Danish International Development Agency (DANIDA), the Australian Government Overseas Aid Program (AusAid), Irish Aid, Environment Canada, Ministry of Foreign Affairs for the Netherlands, Swiss Agency for Development and Cooperation (SDC), Instituto de Investigação Científica Tropical (IICT), UK Aid, the Government of Russia and the European Union (EU). The Program is carried out with technical support from the International Fund for Agricultural Development (IFAD).

**Contact:**

CCAFS Coordinating Unit - Faculty of Science, Department of Plant and Environmental Sciences, University of Copenhagen, Rolighedsvej 21, DK-1958 Frederiksberg C, Denmark. Tel: +45 35331046; Email: [ccaafs@cgiar.org](mailto:ccaafs@cgiar.org)

Creative Commons License



This Working Paper is licensed under a Creative Commons Attribution – NonCommercial–NoDerivs 3.0 Unported License.

Articles appearing in this publication may be freely quoted and reproduced provided the source is acknowledged. No use of this publication may be made for resale or other commercial purposes.

© 2014 CGIAR Research Program on Climate Change, Agriculture and Food Security (CCAFS). CCAFS Working Paper no. 73.

**DISCLAIMER:**

CCAFS working papers are not necessarily peer reviewed. Any opinions stated herein are those of the author(s) and do not necessarily reflect the policies or opinions of CCAFS, donor agencies, or partners. All images remain the sole property of their source and may not be used for any purpose without written permission of the source.

## **Abstract**

This report investigates the climate of two target regions of the CGIAR Research Program on Climate Change, Agriculture and Food Security (CCAFS): Central and South America (CA and SA, respectively). The report assesses the implications of climate change for agriculture, with a particular focus on those aspects of climate change that will have greatest impact on the crops currently grown in each region. The study investigated the ability of General Circulation Models (GCMs) and downscaled climate change scenarios to reproduce already observed climates, to establish the reliability of future climate projections, as well as projections of how associated crops might grow under future conditions.

## **Keywords**

Climate change; extremes; General Circulation Model; climate vulnerability; adaptation; agriculture impacts

## About the authors

Jose A. Marengo, PhD in Meteorology from the University of Wisconsin-Madison, USA. His research work includes climate forecasting, climate and global change and studies linked to impacts, vulnerability and adaptation to climate variability and change, with emphasis on weather and climate extremes. He is currently a Senior Scientist at the Earth System Science Center (CCST) of the National Institute for Space Research (INPE). He is member of international panels such as IPCC, IAI, IGBP and others related to climate change and impacts.

Sin Chan Chou, Ph.D. in Meteorology from the University of Reading, UK. Currently she is a Senior Scientist at the Center for Weather Forecasts and Climate Studies (CPTEC) at the National Institute for Space Research. She has experience in Meteorology, with emphasis on regional atmospheric modeling, acting on the field of weather and climate forecast and well as climate change projections, and on model development. She is a member of international panels such as IPCC.

Roger R. Torres, PhD in Meteorology from the National Institute for Space Research (INPE), Brazil. His research experience includes climatology, regional modeling of weather and climate, and climate variability and change. He is currently working as professor at the Natural Resources Institute of the Federal University of Itajuba (Unifei), Brazil.

Angélica Giarolla, PhD in Agricultural Engineering from the State University of Campinas, Brazil. With experience in agrometeorology, crop modeling, climatic risk in agriculture, weather forecast for agriculture and climate change. She is currently working at the Center for Earth System Science, National Institute for Space Research (CCST/INPE), Brazil.

Lincoln M. Alves, M.S. in Meteorology and PhD student in Meteorology at the National Institute for Space Research (INPE). He has experience with climate modeling, seasonal climate forecasts and in regional modeling and development of regional climate change scenarios in South America.

Andre Lyra, M.S. in Meteorology and PhD student in Earth System Science at the National Institute for Space Research (CCST/INPE). He has experience in regional modeling and in the development of regional climate change scenarios in South America.

## Acknowledgements

The research leading to these results shown on this publication has received funding from the European Community's Seventh Framework Programme (FP7/2007–2013) under Grant Agreement No. 212492: CLARIS LPB, Europe-South America Network for Climate Change Assessment and Impact Studies in La Plata Basin. Additional funding was provided by Rede-CLIMA, the National Institute of Science and Technology (INCT) for Climate Change funded by CNPq Grant Number 573797/2008-0 and FAPESP Grant Number 57719-9, the FAPESP-Assessment of Impacts and Vulnerability to Climate Change in Brazil and strategies for Adaptation Options Project.

The CGIAR Research Program on Climate Change, Agriculture and Food Security (CCAFS) is a strategic partnership of CGIAR and Future Earth, led by the International Center for Tropical Agriculture (CIAT).

The Program is carried out with funding by the CGIAR Fund, the Danish International Development Agency (DANIDA), the Australian Government Overseas Aid Program (AusAid), Irish Aid, Environment Canada, Ministry of Foreign Affairs for the Netherlands, Swiss Agency for Development and Cooperation (SDC), Instituto de Investigação Científica Tropical (IICT), UK Aid, the Government of Russia and the European Union (EU). The Program is carried out with technical support from the International Fund for Agricultural Development (IFAD).

# Contents

Abstract.....	3
Keywords .....	3
About the authors.....	4
Acknowledgements.....	5
<b>Contents</b> .....	<b>6</b>
Acronyms.....	7
Figure index .....	9
Table index.....	14
1. Introduction.....	15
2. Objectives .....	17
3. Observed trends in climate.....	19
3.1 Climate trends .....	19
3.2 Climate extremes trends.....	21
4. Global Climate Model Evaluation: from IPCC AR4 to IPCC AR5.....	24
4.1 SRES and RCPs scenarios and climate change projections.....	26
4.2 Comparisons between CMIP3 and CMIP5 models .....	27
5. High-resolution climate change projections for CA and SA: Downscaling of the HAdGEM2 ES using the Eta regional model.....	47
5.1 Models used for the climate downscaling (HadGEM2 ES and Eta).....	47
5.2 Climate change projections for CA and SA derived from the Eta-HAdGEM2-ES .....	49
6. Impacts of climate change in agriculture in CA and SA.....	66
6.1 General overview .....	66
6.2 Degree of vulnerability of specific crops production in CA and SA .....	69
7. Main results and key advances that can be expected from the climate modelling community in the next few years .....	76
References.....	80

## Acronyms

CA	Central America
CCAFS	CGIAR Research Program on Climate Change, Agriculture and Food Security
CCS	Climate Change Studies
CDD	Consecutive dry days
CDKN	Climate and Development Knowledge Network
CIAT	Centro Inter Americano de Agricultura Tropical
CMIP3	Couple Model Intercomparison Program Version 3
CMIP5	Couple Model Intercomparison Program Version 5
CPTEC	Centro de Previsão de Tempo e Estudos Climáticos
ECLAC	Economical Council for Latin America
ENSO	El Nino Southern Oscillation
GCMs	General circulation models
GDP	Gross Domestic Product.
GHG	Greenhouse Gases
HadAM3P	Hadley Center Atmospheric Global Model Version 3
HadGEM2 ES	Hadley Center Global Environmental Model Version 2-Earth System
DJF	December-January-February
INPE	Instituto Nacional de Pesquisa Espaciais
ITCZ	Intertropical Convergence Zone
IPCC AR4	Intergovernmental Panel on Climate Change Fourth Assessment Report
IPCC AR5	Intergovernmental Panel on Climate Change Fifth Assessment Report
ITCZ	Intertropical convergence zone
JJA	June-July-August
NAMS	North American Monsoon System
PCMDI	Program for Climate Model Diagnosis and Intercomparison
PRECIS	Providing Regional Climates for Impacts Studies



RIOCC	Red Internacional de Oficinas sobre Cambio Climático
RCM	Regional climate model
RCP	Representative Concentration Pathway
SA	South America
SACZ	South Atlantic Convergence Zone
SAMS	South American Monsoon System
SENAMHI	Servicio Nacional de Meteorología Hidrología-Peru
SESA	South Eastern South America
SOI	Southern Oscillation Index
SRES	Special Report Emission Scenario
SST	Sea surface temperature
SMA	Soil Moisture Anomalies
SREX	IPCC Special Reports on Extremes
UK	United Kingdom
WG1IPCC	Working Group 1
WG2IPCC	Working Group 2

## Figure index

Figure 1. Location of the region of the study: Central and South America

Figure 2. Observed worldwide (a) annual temperature (1901-2013) and (b) rainfall trends (1951-2012). (IPCC WG1, Chapter 21, 2013)

Figure 3. Trends (in annual days per decade) for annual series of percentile temperature indices for 1951–2010: cool nights (TN10p), warm nights (TN90p), cool days (TX10p), and warm days (TX90p). Trends were calculated only for grid boxes with sufficient data (at least 66% of years having data during the period, and the last year of the series is no earlier than 2003). Hatching indicates regions where trends are significant at the 5% level. Note that for the global average time series only grid boxes with at least 90% of temporal coverage are used, i.e., 99 years during 1901–2010. Color scale (days) is shown on the lower site of the upper (cool days and nights) and lower (warm days and nights) panels. (Donat et al 2013).

Figure 4. Decadal trends and global average time series for annual indices: Number of heavy precipitation days (R10) in days, contribution from very wet days (R95pTOT) in %, consecutive dry days (CDD) in days. Trend and time series calculations as described in Figure 3 (Donat et al 2013)

Figure 5. Greenhouse gases concentration and global warming for SREX scenarios used in the IPCC AR4 CMIP3 model runs (IPCC 2007).

Figure 6. Representation of the RCPs (Representative Concentration Pathways) used by IPCC AR5 (Van Vuuren et al 2011)

Figure 7. Changes in mean temperature (colour lines) and uncertainties (shades) relative to 1986–2005, for the SRES IPCC AR4 and RCPs of IPCC AR5. The number of models is indicated among brackets. The boxes on the right side of the panel show the mean and the whiskers show the standard deviation on the projected warming by 2100 (Knutti and Sedlacek 2013).

Figure 8. Observed (a-e) and CMIP3 ensemble mean (f-j) patterns of seasonal precipitation and bias (k-o) for 1961-1990. Bias was calculated as the difference between simulation (ensemble mean) and observation (CRU-TS 3.0). Symbols DJF, MAM, JJA, SON, and ANO, represent the periods from December to February, March to May, June to August, September to November, and annual mean, respectively. Units are in millimeters per day.

Figure 9. The same as in Figure 8, but for seasonal surface air temperature (in degrees Celsius).

Figure 10. Study domain. Rectangles indicate some sub-regions of interest: Mexico and Central America (MX), North-western South America (N), Amazon Basin (AM), Northeast Brazil (NE), Central-Western South America (CO), south-eastern and southern Brazil (SE and S, respectively), and a rectangle containing the full extent of the Brazilian territory (BR).

Figure 11. Annual cycle of observed precipitation (blue) and historical simulations (gray) of 24 GCMs from the CMIP3 dataset averaged over the sub-regions described in Fig. 4.2.3 for 1961-1990. The

black bold line represents the CMIP3 GCMs ensemble mean. The mean GCMs root mean square error ((RMSE) $\bar{}$ ) is indicated below each region acronym. Units are in mm day<sup>-1</sup>.

Figure 12. The same as in Figure 11, but for seasonal surface air temperature (in degrees Celsius).

Figure 13. Observed (a-e) and CMIP5 ensemble mean (f-j) patterns of seasonal precipitation and bias (k-o) for 1961-1990. Bias was calculated as the difference between simulation (ensemble mean) and observation (CRU-TS 3.0). Symbols DJF, MAM, JJA, SON, and ANO, represent the periods from December to February, March to May, June to August, September to November, and annual mean, respectively. Units are in millimeters per day.

Figure 14. The same as in Figure 13, but for seasonal surface air temperature (in degrees Celsius).

Figure 15. Annual cycle of observed precipitation (blue) and historical simulations (gray) of 24 GCMs from the CMIP5 dataset averaged over the sub-regions described in Fig. 4.2.3 for 1961-1990. The black bold line represents the CMIP5 GCMs ensemble mean. The mean GCMs root mean square error ((RMSE) $\bar{}$ ) is indicated below each region acronym. Units are in mm day<sup>-1</sup>.

Figure 16. The same as in Figure 15, but for seasonal surface air temperature (in degrees Celsius).

Figure 17. Projected annual changes in some indices for daily T<sub>min</sub> for 2081-2100 with respect to 1980-1999, based on 14 GCMs contributing to the CMIP3: fraction of warm days (days in which T<sub>max</sub> exceeds the 90th percentile of that day of the year, calculated from the 1961-1990 reference period); fraction of cold days (days in which T<sub>max</sub> is lower than the 10th percentile of that day of the year, calculated from the 1961-1990 reference period); percentage of days with T<sub>max</sub> >30°C; fraction of warm nights (days at which T<sub>min</sub> exceeds the 90th percentile of that day of the year, calculated from the 1961-1990 reference period); fraction of cold nights (days at which T<sub>min</sub> is lower than the 10th percentile of that day of the year, calculated from the 1961-1990 reference period); percentage of days with T<sub>min</sub> >20°C. The changes are computed for the annual time scale, as the fractions/percentages in the 2081-2100 period (based on simulations under emission scenario SRES A2) minus the fractions/percentages of the 1980-1999 period (from corresponding simulations for the 20th century). Warm night and cold night changes are expressed in units of standard deviations, derived from detrended per year annual or seasonal estimates, respectively, from the three 20-year periods 1980-1999, 2046-2065, and 2081-2100 pooled together. T<sub>min</sub> >20°C changes are given directly as differences of percentage points. Color shading is only applied for areas where at least 66% (i.e., 10 out of 14) of the GCMs agree in the sign of the change; stippling is applied for regions where at least 90% (i.e., 13 out of 14) of the GCMs agree in the sign of the change (IPCC SREX 2012).

Figure 18. Projected annual and seasonal changes in three indices for daily precipitation for 2081-2100 with respect to 1980-1999, based on 17 GCMs contributing to the CMIP3: wet-day intensity, percentage of days with precipitation above the 95% quantile of daily wet day precipitation for that day of the year, calculated from the 1961-1990 reference period; right column: fraction of days with precipitation higher than 10 mm. The changes are computed for the annual time scale as the fractions/percentages in the 2081-2100 period (based on simulations under emission scenario SRES A2) minus the fractions/percentages of the 1980-1999 period (from corresponding simulations for the 20th century). Changes in wet-day intensity and in the fraction of days with Pr >10 mm are expressed in units of standard deviations, derived from detrended per year annual or seasonal estimates,

respectively, from the 2081-2100 pooled together. Changes in percentages of days with precipitation above the 95% quantile are given directly as differences in percentage points. Color shading is only applied for areas where at least 66% (i.e., 12 out of 17) of the GCMs agree on the sign of the change; stippling is applied for regions where at least 90% (i.e., 16 out of 17) of the GCMs agree on the sign of the change (IPCC SREX 2012).

Figure 19. Projected annual changes in dryness assessed from two indices. Upper panels: Change in annual maximum number of consecutive dry days (CDD: days with precipitation <1 mm); lower panel: Changes in soil moisture (soil moisture anomalies, SMA). Increased dryness is indicated with yellow to red colors; decreased dryness with green to blue. Projected changes are expressed in units of standard deviation of the interannual variability in the three 20-year periods 1980–1999, 2046–2065, and 2081–2100. The figures show changes for two time horizons, 2046–2065 and 2081–2100, as compared to late 20th-century values (1980–1999), based on GCM simulations under emissions scenario SRES A2 relative to corresponding simulations for the late 20th century. Results are based on 17 (CDD) and 15 (SMA) GCMs contributing to the CMIP3. Colored shading is applied for areas where at least 66% (12 out of 17 for CDD, 10 out of 15 for SMA) of the models agree on the sign of the change; stippling is added for regions where at least 90% (16 out of 17 for CDD, 14 out of 15 for SMA) of all models agree on the sign of the change. Grey shading indicates where there is insufficient model agreement (<66%). (IPCC SREX 2012).

Figure 20. Seasonal (DJF and JJA) air temperature anomalies from 23 CMIP5 models for CA and SA for the RCP8.5 scenario. Units are in oC, and color scale is shown on the lower side of the panel. Name of the model is shown at the left side of each map. Projections are for 2071-2100 relative to 1961-90.

Figure 21. Seasonal (DJF and JJA) rainfall anomalies from 23 CMIP5 models for CA and SA for the RCP8.5 scenario. Units are in mm/day, and color scale is shown on the lower side of the panel. Name of the model is shown at the left side of each map. Projections are for 2071-2100 relative to 1961-90.

Figure 22. Seasonal (DJF and JJA) air temperature anomalies from the mean of 23 CMIP5 models for CA and SA for the RCP8.5 scenario for the short (2010-40), medium (2041-70) and long term (2071-2110) relative to 1961-90 (first and third columns). Maps of standard deviation are shown in second and fourth columns. Units are in oC, and color scale is shown on the lower side of the panels. Arrows indicate the correspondence between the maps and the color for means and standard deviation.

Figure 23. Seasonal (DJF and JJA) rainfall anomalies from the mean of 23 CMIP5 models for CA and SA for the RCP8.5 scenario for the short (2010-40), medium (2041-70) and long term (2071-2110) relative to 1961-90 (first and third columns). Maps of agreement between models for increase or decrease of precipitation. Units are in mm/day for rainfall and in n% for the model agreement. Color scale is shown on the lower side of the panels. Arrows indicate the correspondence between the maps and the color for means and model agreements.

Figure 24. The multimodal median of temporally averaged changes in tropical nights (days), fraction of warm nights (%), warm day spell duration (days), and fraction of cold nights (%), over the period 2081–2100 relative to 1981-2000, for RCP8.5. All changes are significant at the 5% significance level. Stippling indicates grid points with changes that are not significant at the 5% significance level (modified from Sillman et al. 2013).

Figure 25. Same as Figure 24, but for total wet day precipitation (%), fraction of days with  $pp > 10$  mm (days), percentage of days with  $Pr > 9Q85$  and consecutive dry days. All changes are significant at the 5% significance level. Stippling indicates grid points with changes that are not significant at the 5% significance level (modified from Sillman et al. 2013).

Figure 26. Comparisons between observed CRU rainfall and simulated rainfall from the Global HadGEM2 ES and from the downscaling of the HadGEM2 ES using the Eta regional model. Regions are shown in Figure 10.

Figure 27. Comparisons between present time (1961-90) CRU and future (2011-2040, 2041-870 and 2071-2100) annual cycle of rainfall and simulated rainfall from the Global HadGEM2 ES and from the downscaling of the HadGEM2 ES using the Eta regional models. Regions are shown in Figure 10.

Figure 28. Comparisons between observed CRU rainfall and simulated rainfall from the Global HadGEM2 ES and from the downscaling of the HadGEM2 ES using the Eta regional models for both CA and SA, during austral summer DJF.

Figure 29. Comparisons between observed CRU rainfall and simulated rainfall from the Global HadGEM2 ES and from the downscaling of the HadGEM2 ES using the Eta regional models for both CA and SA, during austral winter (boreal summer) JJA.

Figure 30. Comparisons between observed CRU temperature and simulated temperature from the Global HadGEM2 ES and from the downscaling of the HadGEM2 ES using the Eta regional models for both CA and SA, during austral summer DJF.

Figure 31. Comparisons between observed CRU temperature and simulated rainfall from the Global HadGEM2 ES and from the downscaling of the HadGEM2 ES using the Eta regional models for both CA and SA, during austral winter JJA.

Figure 32. Comparisons between present time 1961-90 CRU rainfall and projections from the from the downscaling of the HadGEM2 ES using the Eta regional models for 2011-40, 2041-70 and 2071-2100, for the RCP4.5 scenario. Regions are shown in Figure 10.

Figure 33. Comparisons between present time 1961-90 CRU temperature and projections from the from the downscaling of the HadGEM2 ES using the Eta regional models for 2011-40, 2041-70 and 2071-2100, for the RCP4.5 scenario. Regions are shown in Figure 10.

Figure 34. Seasonal rainfall anomalies for DJF, MAM, JJA and SON for 2011-40 relative to 1961-90, for the RCP8.5 derived from the downscaling of the HadGEM2 ES using the Eta regional models for both CA and SA. Units are in mm/day

Figure 35. Seasonal rainfall anomalies for DJF, MAM, JJA and SON for 2041-70 relative to 1961-90, for the RCP8.5 derived from the downscaling of the HadGEM2 ES using the Eta regional models for both CA and SA. Units are in mm/day

Figure 36. Seasonal rainfall anomalies for DJF, MAM, JJA and SON for 2071-2100 relative to 1961-90, for the RCP8.5 derived from the downscaling of the HadGEM2 ES using the Eta regional models for both CA and SA. Units are in mm/day.

Figure 37. Seasonal temperature anomalies for DJF, MAM, JJA and SON for 2011-2040 relative to 1961-90, for the RCP8.5 derived from the downscaling of the HadGEM2 ES using the Eta regional models for both CA and SA. Units are in °C.

Figure 38. Seasonal temperature anomalies for DJF, MAM, JJA and SON for 2041-2070 relative to 1961-90, for the RCP8.5 derived from the downscaling of the HadGEM2 ES using the Eta regional models for both CA and SA. Units are in °C.

Figure 39. Seasonal temperature anomalies for DJF, MAM, JJA and SON for 2071-2100 relative to 1961-90, for the RCP8.5 derived from the downscaling of the HadGEM2 ES using the Eta regional models for both CA and SA. Units are in °C.

Figure 40: Observed and simulated variations in past and projected future annual average temperature over the Central and South American regions defined in IPCC (IPCC SREX 2012). Black lines show various estimates from observational measurements. Shading denotes the 5-95 percentile range of climate model simulations driven with "historical" changes in anthropogenic and natural drivers (63 simulations), historical changes in "natural" drivers only (34), the "RCP2.6" emissions scenario (63), and the "RCP8.5" (63). Data are anomalies from the 1986-2006 average of the individual observational data (for the observational time series) or of the corresponding historical all forcing simulations. Further details are given in Margrin et al (2014).

Figure 41. Number of days considering maximum temperatures above 34°C during the months of September, October, November and December (Flowering and ripening stages for coffee crop in Sao Paulo State-Brazil). Source: Rodrigues et al. (2011).

Figure 42. Number of days considering maximum temperatures above 34°C during the months of September, October, November and December (Flowering and ripening stages for coffee crop in Sao Paulo State-Brazil). Source: Rodrigues et al. (2011).

Figure 43. Duration of soybean life cycle (in days) for 2 locations in Parana State- Brazil, based on A1B Scenarios generated by Eta-HadCM3 model. Source: Tavares et al. (2010).

Figure 44. Grain ripening of coffee arabica, where the grains go from "cherry" stage to dried fruits according to air temperature. (Pezzopane et al, 2003).

Figure 45. Coffee crop intercalated with a) Banana and b) Grevillea as a way to evaluate the microclimate in this crop system and adaptation to high temperatures. Source: Valentini (2009); IAC/APTA.

Figure 46. Projected changes in annual average temperature and precipitation. CMIP5 multi-model mean projections of annual average temperature changes (left panel) and average percent change in annual mean precipitation (right panel) for 2046-2065 and 2081-2100 under RCP2.6 and 8.5. Solid colors indicate areas with very strong agreement, where the multi-model mean change is greater than twice the baseline variability, and >90% of models agree on sign of change. Colors with white dots

indicate areas with strong agreement, where >66% of models show change greater than the baseline variability and >66% of models agree on sign of change. Gray indicates areas with divergent changes, where >66% of models show change greater than the baseline variability, but <66% agree on sign of change. Colors with diagonal lines indicate areas with little or no change, less than the baseline variability in >66% of models. (There may be significant change at shorter timescales such as seasons, months, or days.). Analysis uses model data and methods building from IPCC WG2 AR5 (Magrin et al 2014).

## Table index

Table 1. Observed changes in temperature and precipitation extremes, including dryness in regions of Latin America since 1950, with the period 1961-1990 used as a baseline (see Box 3.1 in Chapter 3 of IPCC SREX; 2012) for more information).

Table 2. shows projected changes in temperature and precipitation extremes, including dryness in Latin America. The projections are for the period 2071-2100 (compared with 1961-1990) or 2080-2100 (compared with 1980-2000) and are based on GCM and RCM outputs run under the A2/A1B emissions scenario (see Box 3.1 in Chapter 3 of IPCC SREX 2012; for more information).

Table 3. List of CMIP3 global models used on this report, showing horizontal resolution (latitude/longitude), SRES emission scenarios, and number of realizations. The models are organized according to their horizontal resolution (Torres and Marengo 2013).

Table 4. List of CMIP5 global models used on this report, showing horizontal resolution (latitude/longitude), RCPs (RCPs 2.6, 4.5, 6.0, 8.5). The models are organized according to their horizontal resolution (Torres and Marengo 2013).

Table 5. Overview of considered extremes and summary of observed and projected changes on global scale (CDKN 2013).

# 1. Introduction

Central America (CA) consists of seven countries: Belize, Costa Rica, El Salvador, Guatemala, Honduras, Nicaragua, and Panama. Part of the Mesoamerican biodiversity hotspot, which extends from northern Guatemala through central Panama (Fig. 1), CA is bordered by Mexico to the north, the Caribbean Sea to the east, the North Pacific Ocean to the west, and Colombia to the south-east, which is also the most southern point of North America. CA has an area of 524,000 square kilometers (202,000 sq. mi), or almost 0.1% of the Earth's surface. As of 2009, its population was estimated at 41,739,000, with a density of 77 people per square kilometer. South America (SA) includes twelve sovereign states: Argentina, Bolivia, Brazil, Chile, Colombia, Ecuador, Guyana, Paraguay, Peru, Suriname, Uruguay, Venezuela and French Guiana, an overseas region of France. SA has an area of 17,840,000 square kilometers (6,890,000 sq. mi), and as of 2005 its population has been estimated at more than 371,090,000. SA ranks fourth in area globally (after Asia, Africa, and North America) and fifth in population (after Asia, Africa, Europe, and North America).

CA and SA are highly heterogeneous in terms of climate, ecosystems, human population distribution, and cultural traditions. The CA and SA region harbors unique ecosystems, the highest biodiversity in the planet, and has a variety of ecoclimatic gradients. A large portion of the region is located in the tropics, a climate dominated by convergence zones such as the Inter-tropical Convergence Zone (ITCZ), and the South Atlantic Convergence Zone (SACZ).

The summer circulation in tropical and sub-tropical CA and Mexico is dominated by the North America Monsoon System, which affects Mexico and parts of CA, and the South America Monsoon System, which affects tropical and sub-tropical SA east of the Andes. CA is also affected by tropical storms and hurricanes during summer time.



These monsoon climates are closely interconnected with ocean-atmosphere interactions over the tropical and sub-tropical oceans. Low Level Jets in SA east of the Andes, and in North America east of the Rockies, Baja California and over the Intra-Americas Seas transport moisture from warm oceans to contribute to continental rainfall. Most of the rainfall is concentrated in the convergence zones or by topography, leading to strong spatial and temporal rainfall contrasts. These include the expected sub-tropical arid regions of northern Mexico and Patagonia, the driest desert in the world in northern Chile, and a tropical semi-arid region of north-east Brazil located next to humid Amazonia and one of the wettest areas in the world in western Colombia.

Figure 1. Location of the region of the study: Central and South America

A changing climate leads to variation in the frequency, intensity, spatial extent, duration, and timing of weather and climate extremes. The increased exposure of people and economic assets to these



changes has been the major cause of long-term increases in economic losses from climate-related disasters. Furthermore, assessments have indicated that in many regions of the world, socio-economic factors will be among the main drivers of future increases in related losses. Many countries in CA and SA face severe challenges in coping with climate-related disasters (IPCC SREX 2012, IPCC 2007, 2014). Flash floods and landslides due to intense rainfall have affected the entire region, and have been costly both in terms of money and human life. Seasonal floods and droughts have also affected regions such as Amazonia, the Andean Valleys, the La Plata Basin and Northeast Brazil, and regions of Central America, with huge impacts on the national and regional economies (Magrin et al 2014, IPCC SREX 2012).

Vulnerability and exposure are dynamic and depend on economic, social, demographic, cultural, institutional, and governance factors. Individuals and communities are also differentially exposed based on factors such as wealth, education, gender, age, class/caste, and health. Lack of resilience and capacity to anticipate, cope with, and adapt to extremes are important factors of vulnerability. For example, a tropical cyclone and hurricanes can have very different impacts depending on where and when they make landfall. Similarly, heat waves and intense rainfall can have very different impacts on different population groups depending on their vulnerability and exposure, as well as their income and education levels. Extreme impacts on human, ecological, or physical systems can therefore result from individual extreme weather or climate events, from non-extreme events where exposure and vulnerability are high, or from a compounding of events or their impacts (flash floods, landslides). High vulnerability and exposure are generally the outcome of skewed development processes, for example, environmental mismanagement, demographic change, rapid and unplanned urbanization, failed governance, and a scarcity of livelihood options.

This can result in settlements in hazard prone areas, the creation of unsafe dwellings, slums and scattered districts, poverty, and lack of awareness of risks. For example, those with awareness, transferable livelihoods, money and access to transport can move away from disaster and live more comfortably out of danger. Those without these assets may be forced to locate their homes in hazard prone areas where they are more vulnerable and exposed to climate extremes. They will also have to deal with the impacts of disaster on the ground, including no water, food, sanitation or shelter. Agriculture in CA and SA is highly vulnerable to climate variability, as floods, dry spells, droughts, and both cold and heat waves have affected agricultural production. Climate change can potentially exacerbate or ameliorate these stresses, depending on the direction and magnitude of changes to climate in variables of relevance to crop growth, and also as a consequence of the impacts of secondary factors such flood and heat-wave damage. According to IPCC AR5 (Magrin et al. 2014), changes in agricultural productivity with consequences for food security associated with climate change are expected to exhibit large spatial variability in CA and SA. Increases in production and more intense use of land, particularly in tropical areas, have led to problems of compaction, salinization, desertification, soil erosion, water pollution, and negative effects on biodiversity and human health. In south-eastern SA, where climate change projections indicate more rainfall, average productivity could be sustained or increased until the mid-century. In CA, northeast of Brazil and parts of the Andean region, increases in temperature and decreases in rainfall could reduce productivity in the short-term (by 2030), threatening the food security of the poorest population. Considering that SA will be a key food-producing region in the future, one of the challenges is going to be increasing food and bioenergy quality and production while maintaining environmental sustainability under climate change. Some adaptation measures include crop, risk, and water use management along with genetic improvement.

Therefore, the aim of this report is:

- (i) to provide an initial assessment of recent observed trends and projected future changes in climate and in extremes, specifically focused on the CA and SA regions,
- (ii) to summarize the key advances that can be expected in climate model information over the next few years in CA and SA
- (iii) to assess the potential changes of key crop yields in CA and SA

The report is laid out as follows. Section 1 provides background on the climate of CA and SA, with a particular focus on current knowledge of climate variability and change in the regions and their associations with impacts-vulnerability-adaptation on the agriculture sector. Section 2 introduces the objectives of this study. Section 3 examines recent trends in basic climatic variables—precipitation and temperature and also trends in several indices of extreme climate events. Section 4 reviews the performance of global climate models from CMIP3 (A1 and B2 scenarios) and CMIP5 (RCP 2.5 and 8.5) through a review of the literature, and through original analysis of model performance over CA and SA. Focus is on the simulation of present climate by the CMIP3 and CMIP5 models, and also projections for future climate (temperature and rainfall) until the end of the 21st Century. Section 5 examines the projections of temperature and precipitation for CA and SA and its sub-regions from the period 1961-90 (present climate) and 2010–2100 including how climate and extremes change in future decades, derived from the downscaling of the HadGEMi ES global model using the Eta regional model. Section 6 identifies climatic thresholds for key crops in CA and SA, and compares the present day and potential future spatial patterns of climatically suitable areas for various crops important for the agriculture of SA and CA. Section 6 summarizes the main results of the report and discusses the key advances that can be expected from the climate modelling community in the next few years.

## 2. Objectives

This report summarizes the results of studies on observed climate trends during the last 60 years or so, as well as future climate change projections for CA and SA (from Mexico southwards) up to 2100, using the latest climate change projections from the global CMIP5 models reported in the WG1 and WG2 of the from the IPCC AR5 released in 2014, the global CMIP3 models reported at the WG1 and 2, and the IPCC Special report on extremes (IPCC SREX 2012). We also show the results of the most recent experiences of downscaling developed at INPE using the Eta regional model nested in the HadGEM2-ES from the UK, one of the IPCC AR5 models. High-resolution projections have been used on impacts and vulnerability studies in Brazil and South America, regarding impacts of climate change in biodiversity in Amazonia, agriculture, human health and migration, energy, tropical Andes and on the economy of climate change (Marengo et al 2012, Chou et al 2012).

For the observational part of this study, we used the recent results of observed trends in extremes from 1951-2010 from Donat et al (2013) and various other studies referred to in IPCC (2007, 2014). For the modeling we use projections of climate and extremes using the IPCC AR4 models for the IPCC SREX for two of the SRES (Special Report Emission Scenarios) scenarios, as well as the 22 global climate models of the IPCC AR5 WG2 models for two RCPs (Representative Concentration Pathways, Moss et al 2010) emission scenarios developed to assess changes in wet and dry seasons. The analyses are focused on the short term (2010-204), medium term (2040-2070), and long term (2070-2100). We then project changes in temperature and rainfall using the results of the downscaling

of the HadGEM2 ES model from the UK using the Eta regional model from INPE, run at a resolution of 20 km latitude-longitude.

The focus of this report, according to the needs of CIAT-CCAFS covers:

- a) An outline of current trends in climate and extreme events (mainly temperature and precipitation) from the beginning of the twentieth century onwards based on observations and previously published studies.
- b) An evaluation of CMIP5 and CMIP3 global coupled climate models' climatology for the region, and assessment of their projections up to the end of the XX Century. Focus will be on temperature and precipitation, robust indicators of conditions that are related to agricultural production impacts and food security considerations, possibly with regard to crop tolerances and thresholds. These might include changes in wet and dry seasons, precipitation, maximum and minimum temperatures, frequency of dry spells, and threshold temperature exceedance, for example (some of these diagnostics may already be in the literature).
- c) A brief indication of how the science of climate modeling may develop in the next five years that could increase knowledge of changes in climate and climate variability in CA and SA in the decades leading up to the middle of the century. Of particular interest would be aspects that are salient for agriculture, such as spatial scale and higher-order statistics of rainfall that impact crops, as well as possible advances in process-based understanding, climate model diagnostics, and empirical methods useful for both detecting ongoing change and quantifying uncertainty.

For objective (a), since we do not have access to meteorological data from each of the region's countries, we do a comprehensive analyses of trends of extremes available in the published literature reflected in recent IPCC reports (2007, 2012, 2013, 2014), as well as the extensive literature reviewed on those on extremes. Based on this review, we prepare summary maps to identify observed trends and changes on extremes and levels of confidence of those changes in the regions during the last 50 to 60 years. The evaluation includes some interpretation of the state of knowledge about mechanisms of change (particularly for rainfall and temperature), including attention to competing mechanisms that tend to have opposite effects, and some treatment of the uncertainty of the projected impacts at relevant time scales. Indications of areas of considerable disagreement between models at the regional level would be very helpful (e.g. projected changes in the amplitude of future El Niño events).

For objective (b), we assess various CMIP3 and CMIP5 models for the region and sub regions, for medium and long-term horizons. The focus is on changes in precipitation, temperature, changes in dry and wet seasons, and surface wind circulation, in order to identify mechanisms responsible for changes in rainfall. In addition, we show projections for future climate in the region that includes most of Mexico to South America, derived from the downscaling of the HadGEM2 ES (UK model that is part of CMIP5) for the region using the Eta Regional model used by INPE, to analyze projected changes in climate for the medium and long term horizons, and for the same variables listed above, but with a higher space resolution (20 km). For objective (c), we consider the experience of INPE and other climate centers in the region on climate model development and the production of climate change scenarios.

### 3. Observed trends in climate

#### 3.1 Climate trends

Figures 2a and 2b summarize some of the observed trends in temperature and rainfall in the world (IPCC 2013). In the CA and SA region, from 1901 to 2012, temperatures have increased between 0.5 to 3oC, with the more significant increases in tropical South America. On rainfall, the most consistent signals are a gradual rainfall increase in SESA, and northern South America, as well over Northeast Brazil and the Northwest Coast of Peru and Ecuador. Reductions have been detected over northern and southern Chile, Northern Argentina and Southern Mexico and parts of CA, where the North American Monsoon System (NAMS) is located.

Since around 1950, in CA and the North American Monsoon System (NAMS), rainfall has been increasingly delayed and has become more irregular in space and time, while the intensity of rainfall has been increasing during the onset season. Arias et al. (2012) relate those changes to decadal rainfall variations in NAMS.

The West coast of South America experienced a prominent but localized coastal cooling of about 1oC during the past 30-50 years extending from central Peru down to central Chile. This occurs in connection with an increased upwelling of coastal waters favored by the more intense trade winds (Falvey and Garreaud, 2009; Gutiérrez et al, 2011a; Gutiérrez et al, 2011b; Kosaka and Xie, 2013; Narayan et al, 2010; Schulz et al, 2012).

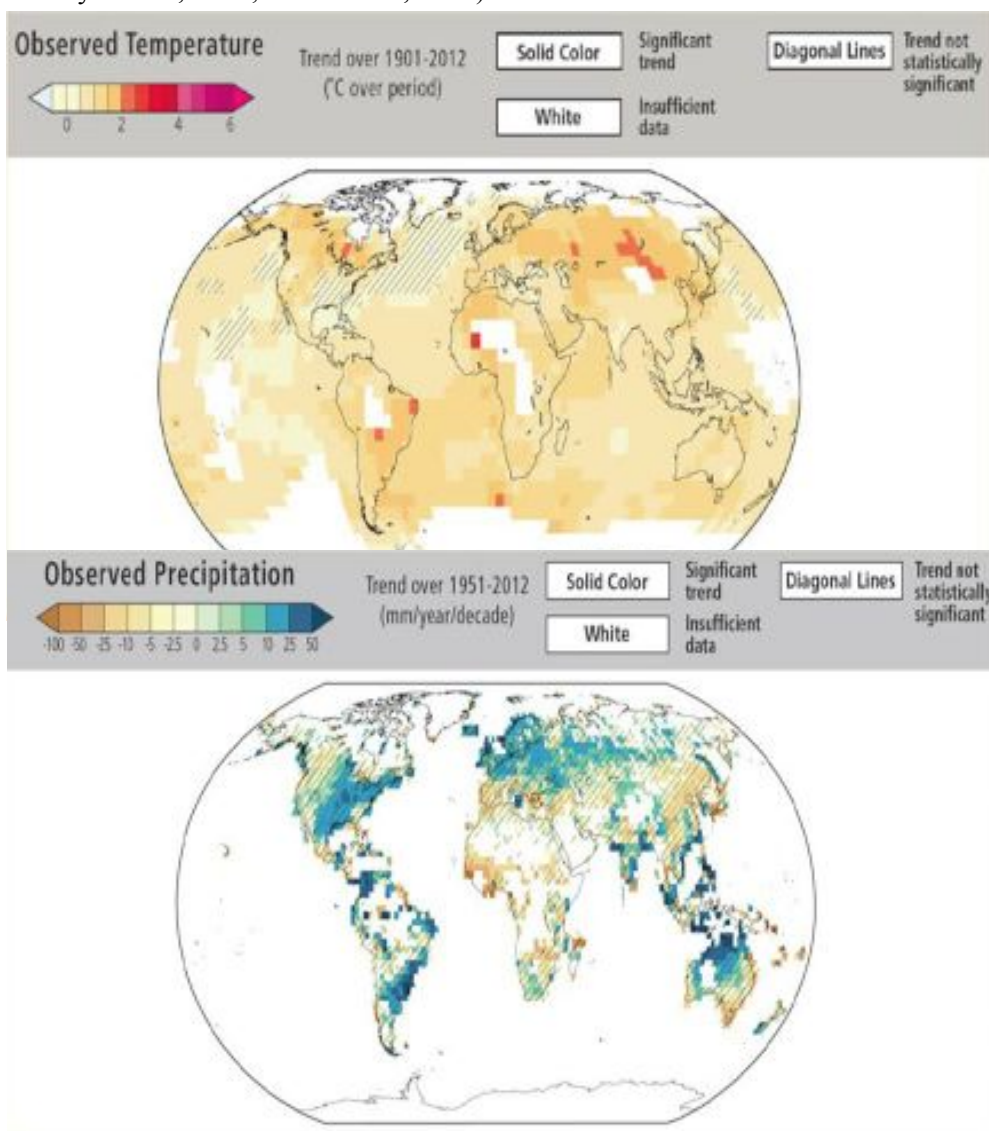


Figure 2. Observed worldwide (a) annual temperature (1901-2013) and (b) rainfall trends (1951-2012). (IPCC 2013)

In the extremely arid northern coast of Chile, rainfall, temperature, and cloudiness show strong interannual and decadal variability, and since the mid-70s, the minimum daily temperature, cloudiness and precipitation have decreased. In central Chile, a negative precipitation trend was observed over the period 1935-1976, and an increase after 1976, while further south, the negative trend in rainfall that prevailed since the 1950s has intensified by the end of the 20th century (Quintana and Aceituno, 2012). Increases in precipitation were observed in Southeastern SA, northwest Peru and Ecuador; while decreases were registered in southern Chile, southwest Argentina, southern Peru and western CA since 1960. Mean warming was near to 0.1°C/decade. The glacier-retreat trend has intensified, reaching critical conditions in the Andean countries.

To the east of the Andes, Northeast Brazil exhibits large interannual rainfall variability, with a slight decrease since the 1970s (Marengo et al. 2013). Droughts in this region (e.g. 1983, 1987, 1998) have been associated with El Niño and/or a warmer Tropical North Atlantic Ocean. However, not all El Niño years result in drought in Northeast Brazil, as the drought 2012-2013 occurred during La Niña (Marengo et al, 2013). Regarding seasonal extremes in the Amazon region, two major droughts and three floods have affected the region from 2005 to 2012, although these events have been related to natural climate variability rather than to deforestation (Espinoza et al 2011, 2012, 2013; Lewis et al 2011; Marengo et al 2008, 2012, 2013; Satyamurty et al 2013).

In the central Andes, in the Mantaro Valley (Peru), precipitation shows a strong negative trend, while warming is also detected (SENAMHI 2007). In the southern Andes of Peru air temperatures have increased during 1964-2006, but no clear signal on precipitation changes has been detected (Marengo et al 2009a, b). In the northern Andes (Colombia, Ecuador), changes in temperature and rainfall in 1961-90 have been identified by Villacís (2008). In the Patagonia region, Masiokas et al (2008) have identified an increase of temperature together with precipitation reductions during 1912-2002. Vuille et al (2008) found that climate in the tropical Andes has changed significantly over the past 50–60 years. Temperature in the Andes has increased by approximately 0.1°C/ decade, with only two of the last 20 years being below the 1961–90 average. Precipitation has slightly increased in the second half of the 20th century in the inner tropics and decreased in the outer tropics. The general pattern of moistening in the inner tropics and drying in the subtropical Andes is dynamically consistent with observed changes in the large-scale circulation, suggesting a strengthening of the tropical atmospheric circulation. A positive and significant trend in mean temperature of 0.09 oC/decade during 1965-2007 has been detected over the Peruvian Andes by Lavado et al (2012).

For the Amazon basin, Marengo (2004) and Satyamurty et al (2010) concluded that no systematic unidirectional long-term trends towards drier or wetter conditions in both the northern and southern Amazon have been identified since the 1920s. Rainfall fluctuations are more characterized by inter-annual scales linked to ENSO or decadal variability. Analyzing a narrower time period, Espinoza et al (2009a; 2009b) found that mean rainfall in the Amazon basin for 1964–2003 has decreased, with stronger amplitude after 1982, especially in the Peruvian western Amazonia (Lavado et al 2012), consistent with reductions in convection and cloudiness in the same region (Arias et al 2012).

On the impacts of land use changes on variability in the climate and hydrology of Amazonia, Zhang et al (2009) suggest that biomass-burning aerosols can work against the seasonal monsoon circulation transition, thus re-enforcing the dry season rainfall pattern for Southern Amazonia. Wang et al (2011) suggests the importance of deforestation and vegetation dynamics on decadal variability of rainfall in the region. Costa and Pires (2010) have suggested a possible decrease in precipitation due to soybean

expansion in Amazonia, mainly as a consequence of its very high albedo. In the SAMS region, positive trends in rainfall extremes have been identified in the last 30 years with a pattern of increasing frequency and intensity of heavy rainfall events, and earlier onsets and late demise of the rainy season.

### **3.2 Climate extremes trends**

According to IPCC WG2 AR4 and AR5 (Magrin et al 2007, 2014), during the last decades of the 20th century, unusual extreme weather events have been severely affecting CA and SA contributing greatly to the strengthening of the vulnerability of human systems to natural disasters.

For CA, Aguilar et al (2005) show that for the 1961–2003 period, climate trends reveal a general warming trend in the region. The occurrence of extreme warm maximum and minimum temperatures has increased while extremely cold temperature events have decreased. Precipitation indices, despite the large and expected spatial variability, indicate that although no significant increases in the total amount are found, rainfall events are intensifying and the contribution of wet and very wet days are enlarging. Temperature and precipitation indices were correlated with northern and equatorial Atlantic and Pacific Ocean sea surface temperatures. However, those indices having the largest significant trends (percentage of warm days, precipitation intensity, and contribution from very wet days) have low correlations to El Niño–Southern Oscillation. Additionally, precipitation indices show a higher correlation with tropical Atlantic sea surface temperatures.

In SA, Vincent et al (2005) examined daily temperature extremes trends over 1960–2000. The results indicate no consistent changes in the indices based on daily maximum temperature while significant trends were found in the indices based on daily minimum temperature. Significant increasing trends in the percentage of warm nights and decreasing trends in the percentage of cold nights were observed at many stations. It seems that this warming is mostly due to more warm nights and fewer cold nights during the summer (DJF) and winter (JJA). The stations with significant trends appear to be located closer to the west and east coasts of South America. For rainfall extremes, Haylock et al (2006) identify trends for extremes that are generally the same as those for total annual rainfall, with a change to wetter conditions in Ecuador and northern Peru and the region of southern Brazil, Paraguay, Uruguay, and northern and central Argentina. A decrease was observed in southern Peru and southern Chile, with the latter showing significant decreases in many indices. A canonical correlation analysis between each of the indices and sea surface temperatures (SSTs) revealed two large-scale patterns that have contributed to the observed trends in the rainfall indices. A coupled pattern with ENSO-like SST loadings and rainfall loadings showing similarities with the pattern of the observed trend reveals that the change to a generally more negative Southern Oscillation index (SOI) has had an important effect on regional rainfall trends. A significant decrease in many of the rainfall indices at several stations in southern Chile and Argentina can be explained by a canonical pattern reflecting a weakening of the continental trough leading to a southward shift in storm tracks. The observed trend toward wetter conditions in the southwest and drier conditions in the northeast could again be explained by changes in ENSO.

More recently, as reported the IPCC SREX (IPCC SREX2012) and IPCC AR5 WG2 (Magrin et al 2014) shows that for CA and SA a changing climate leads to changes in the frequency, intensity, spatial extent or duration of weather and climate extremes, and can result in unprecedented extremes. Levels of confidence in historical changes depend on the availability of high quality and homogeneous data, and relevant model projections. This has been a major challenge in CA and SA,

where a lack of long-term homogeneous and continuous climate and hydrological records, and of complete studies on trends, have not allowed for an identification of trends in extremes, particularly in CA.

Recent observational studies show increases in warm days and decreases in cold days, as well as increases on warm nights and decreases in cold nights in CA and SA, Northern South America, Northeast Brazil, South-eastern South America and the west coast of South America. Table 1 (CDKN 2013, IPCC SREX 2012) summarizes observed trends in temperature (cold days and nights, warm days and nights, heat waves), and rainfall extremes (heavy precipitation and droughts) in CA and SA. It is detected that while in some regions there is a tendency for warmer conditions; in others the signal is unclear. While signals for rainfall and dryness are inconsistent in some places, due to lack of good data coverage, the tendency is for increases in rainfall extremes and drought since 1950.

Table 1. Observed changes in temperature and precipitation extremes, including dryness in regions of Latin America since 1950, with the period 1961-1990 used as a baseline (see Box 3.1 in Chapter 3 of IPCC SREX 2012 and CDKN 2013) for more information).

Region and Sub-region	Trends in maximum temperature (warm and cold days) <sup>a</sup>	Trends in minimum temperature (warm and cold nights) <sup>a</sup>	Trends in the heat waves/warm spells <sup>a</sup>	Trends in heavy precipitation (rain, snow) <sup>a</sup>	Trends in dryness and drought <sup>a</sup>
Amazon	Insufficient evidence to identify a significant trend	Insufficient evidence to identify a significant trend	Insufficient evidence	Increase in many areas, decrease in a few areas	Decrease in dryness for much of the region. Some opposite trends and inconsistencies
Northeastern Brazil	Increases in the number of warm days	Increases in the number of warm nights	Insufficient evidence	Increases in many areas, decreases in a few areas	Varying and inconsistent trends
Southeastern South America	Spatially varying trends (increases in some areas, decreases in others)	Increases in number of warm nights (decreases in number of cold nights)	Spatially varying trends (increases in some areas, decreases in others)	Increases in northern areas Insufficient evidence in southern areas	Varying and inconsistent trends
West Coast South America	Spatially varying trends (increases in some areas, decreases in others)	Increases in number of warm nights (decrease in number of cold nights)	Insufficient evidence	Increases in some areas, decreases in others	Varying and inconsistent trends
Central America and Mexico	Increases in the number of warm days, decreases in the number of cold days	Increases in number of warm nights (decrease in number of cold nights)	Spatially varying trends (increases in some areas, decreases in others)	Increases in many areas, decreases in few areas	Varying and inconsistent trends

**Symbols**

- Increasing trend
- Decreasing trend
- Varying trend
- Inconsistent trend/insufficient evidence
- No or only slight change

**Level of confidence in findings**

- Low confidence
- Medium confidence
- High confidence

In CA, there is *low confidence* that any observed long-term increase in tropical cyclone activity is robust, after accounting for past changes in observing capabilities. In other regions, such as the Amazon region, *insufficient evidence*, inconsistencies among studies and detected trends result in *low confidence* of observed rainfall trends.

In CA and SA, decadal variability and changes in extremes have been affecting large sectors of the population, especially those more vulnerable and exposed to climate hazards.

In the La Plata Basin in South-eastern South America, various studies have documented interannual and decadal scale circulation changes that have led to decreases in the frequency of cold nights in austral summer, as well as to increases in warm nights and minimum temperatures during the last 40 years. Simultaneously, a reduction in the number of dry months in the warm season is found since the mid-1970s, while heavy rain frequency is increasing in this region.

Figure 3 shows the observed trends in temperature extremes defined by Frich et al (2002) and derived by Donat et al (2013) for 1951-2010. Besides the fact that there are regions without data coverage, the figures suggest an increase in the frequency of warm nights and to a lesser degree of warm days in CA and SA, where changes are more intense in Northern and South-eastern South America. On the other hand a reduction in the frequency of cold days and in less degree in cold nights is noted. This is consistent with the observed warming of those regions.

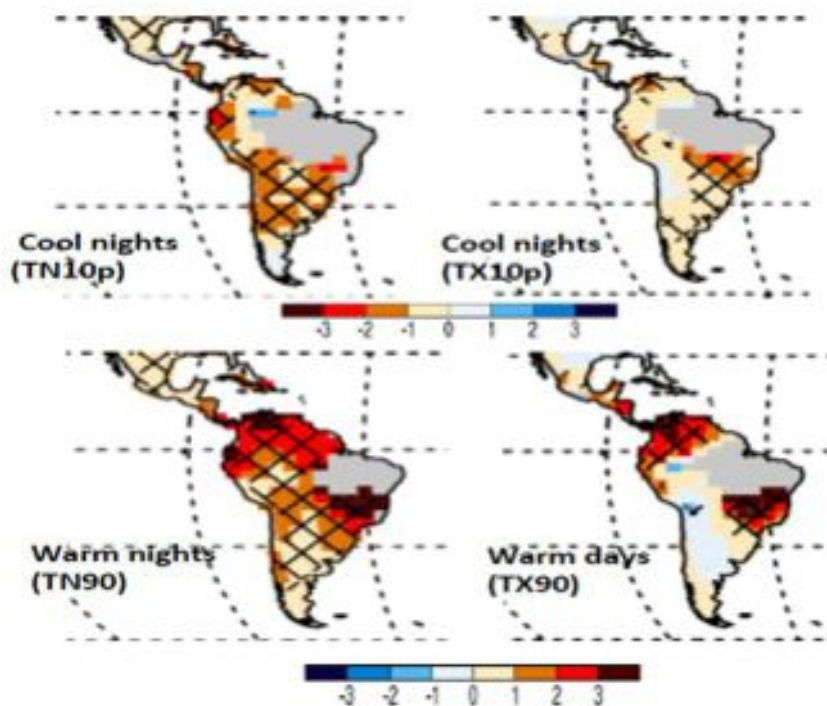


Figure 3. Trends (in annual days per decade) for annual series of percentile temperature indices for 1951– 2010: cool nights (TN10p), warm nights (TN90p), cool days (TX10p), and warm days (TX90p). Trends were calculated only for grid boxes with sufficient data (at least 66% of years having data during the period, and the last year of the series is no earlier than 2003). Hatching indicates regions where trends are significant at the 5% level. Note that for the global average time series only grid boxes with at least 90% of temporal coverage are used, i.e., 99 years during 1901– 2010. Color scale (days) is shown on the lower site of the upper (cool days and nights) and lower (warm days and nights) panels (Donat et al 2013)

On rainfall extremes, Figure 4, the rainfall data coverage is less comprehensive than in the case of temperature. Donat et al (2013) show an increase in the frequency of rainfall extremes in south-eastern SA, as well as in the northern coast of Peru, Ecuador and Colombia and in CA from Honduras to Panama. With regard to dry spells (CDD), there is an increase in the frequency of dry spells in south-eastern SA and in the northern coast of Peru and Ecuador, suggesting that in those regions a concentration of rainfall extremes is observed over the span of a few days, with longer dry spells in between. This situation favours the possibility of floods and landslides triggered by intense rainfall extremes, as already observed in South and Central America. With longer warm and dry spells, there



is a significant impact on human health and agriculture, since these episodes are characterized by dry air and high maximum temperatures and low soil moisture, responsible for drought, increased risk of fires and biomass burning, and higher risk of allergies and respiratory diseases due to smoke.

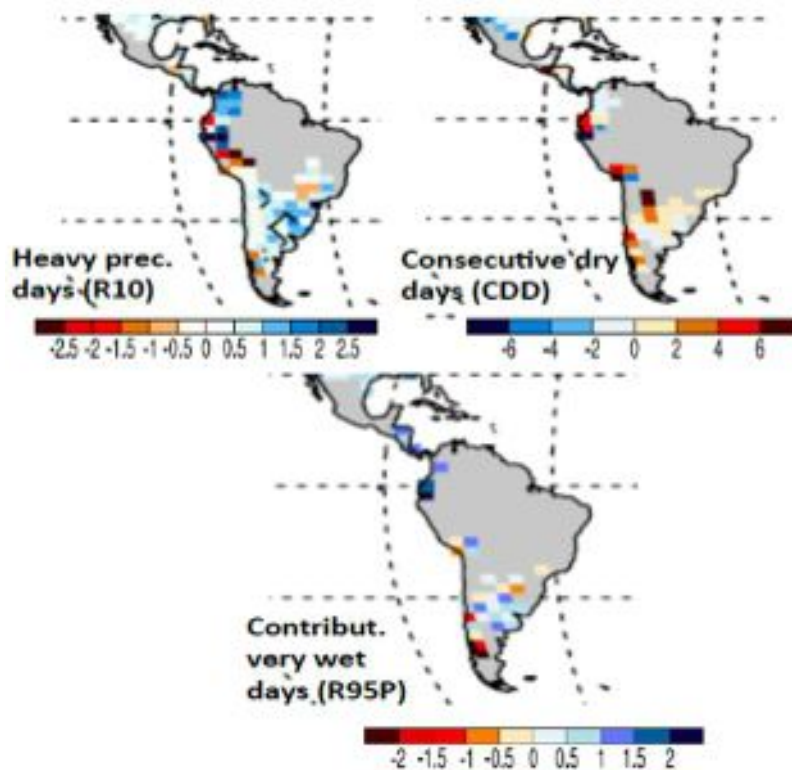


Figure 4. Decadal trends and global average time series for annual indices: Number of heavy precipitation days (R10) in days, contribution from very wet days (R95pTOT) in %, consecutive dry days (CDD) in days. Trend and time series calculations as described in Figure 3 (Donat et al 2013)

Extreme events have the greatest impacts on sectors that are closely linked with or dependent on the climate, for example water, agriculture and food security, forestry, health, and tourism. There is high confidence that changes in the climate could seriously affect water management systems, as well as food and energy security in CA and SA.

## 4. Global Climate Model Evaluation: from IPCC AR4 to IPCC AR5















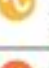












According to the IPCC AR4 (IPCC 2007) and IPCC SREX (IPCC SREX 2012), mean warming for CA and SA at the end of 21st century could reach 1°C to 4°C (SRES B2) or 2°C to 6°C (SRES A2) (*medium confidence*). Rainfall anomalies (positive or negative) will be larger for tropical SA, as in the Amazon and Northeast Brazil region. The frequency and intensity of weather and climate extremes is *likely* to increase (*medium confidence*). For extremes the IPCC SREX (IPCC SREX 2012), projections for the end of the 21st century for differing emissions scenarios (SRES A2 and A1B) show that for all CA and SA, models project substantial warming in temperature extremes.

Table 2 shows that as derived from CMIP3 models and from downscaled scenarios, there are positive trends in extreme temperature indices and heat waves, and also in some rainfall extreme indices, while


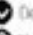



droughts trends are still uncertain. There is still *low confidence* in changes on El Nino frequency and intensity and on changes in the intensity and frequency of tropical storms and hurricanes in CA.

It is *likely* that increases in the frequency and magnitude of warm daily temperature extremes and decreases in cold extremes will occur in the 21st century on the global scale. With *medium confidence*, it is *very likely* that the length, frequency and/or intensity of heat waves will experience a large increase over most of SA, with weaker tendency towards increasing in South-eastern South America. With *low confidence*, the models also project an increase of the proportion of total rainfall from heavy falls for SA and the West coast of South America; while for Amazonia and the rest of South and Central there are not consistent signals of change. In some regions, there is *low confidence* in projections of changes in fluvial floods. Confidence is low due to limited evidence and because the causes of regional changes are complex. There is *medium confidence* that droughts will intensify along the 21st century in some seasons and areas due to reduced precipitation and/or increased evapotranspiration in Amazonia and Northeast Brazil.




Table 2 shows projected changes in temperature and precipitation extremes, including dryness in Latin America. The projections are for the period 2071-2100 (compared with 1961-1990) or 2080-2100 (compared with 1980-2000) and are based on GCM and RCM outputs run under the A2/A1B emissions scenario (see Box 3.1 in Chapter 3 of IPCC SREX, 2012 and CDKN 2013 for more information).

Region and Sub-region	Trends in maximum temperature (the frequency of warm and cold days)**	Trends in minimum temperature (the frequency of warm and cold nights)**	Trends in the heat waves/warm spells**	Trends in heavy precipitation (rain, snow)**	Trends in dryness and drought**
Amazon	 Warm days likely to increase (cold days likely decrease)	 Very likely increase in warm nights (likely decrease in cold nights)	 Likely more frequent and longer heat waves and warm spells	 Tendency for increases in heavy precipitation events	 Inconsistent trends
Northeastern Brazil	 Warm days likely to increase (cold days likely decrease)	 Likely increase in warm nights (likely decrease in cold nights)	 Likely more frequent and longer heat waves and warm spells in some studies. Non-significant signal in others.	 Slight or no change	 Increase in dryness
Southeastern South America	 Warm days likely to increase (cold days likely decrease)	 Very likely increase in warm nights (likely decrease in cold nights)	 Tendency for more frequent and longer heat waves and warm spells	 Increases in northern areas  Insufficient evidence in southern areas	 Inconsistent trends
West Coast South America	 Warm days likely to increase (cold days likely decrease)	 Likely increase in warm nights (likely decrease in cold nights)	 Likely more frequent and longer heat waves and warm spells	 Increases in tropics  Insufficient evidence in extratropics	 Varying and inconsistent trends
Central America and Mexico	 Warm days likely to increase (cold days likely decrease)	 Likely increase in warm nights (likely decrease in cold nights)	 Likely more frequent, longer and/or more intense heat waves/warm spells in most of the region	 Inconsistent trends	 Increase in dryness in Central America and Mexico, with less confidence in trend in extreme South of region

**Symbols**

-  Increasing trend
-  Decreasing trend
-  Varying trend
-  Inconsistent trend/insufficient evidence
-  No or only slight change

**Level of confidence in findings**

-  Low confidence
-  Medium confidence
-  High confidence

## 4.1 SRES and RCPs scenarios and climate change projections

The global climate models from IPCC AR4 were run using the emission scenarios SRES-Special Report Emission Scenarios (Nakicenovic et al 2000). The different SRES scenarios show various types of trajectories or environmental realities that depend on the levels of emissions (Figure 5). Some of these scenarios, defined as A1, A2, A1B, B1 or B2 among others are available on the IPCC web site. The SRES represent socio-economic scenarios that consider society development, population growth and the degree of greenhouse gases emissions. The high emission scenario is referred to as A2 and a low emission scenario is B2, and they were used in the generation of the first high resolution future climate change scenarios using the HadAM3P global model and three regional models: PRECIS, Eta-CCS e RegCM3 (Marengo et al 2010), for the 2071-2100 time slice. After that, the Eta model was run with the A1B scenario with the HadCM3 for 2010-2100 (Marengo et al 2012, Chou et al 2012).

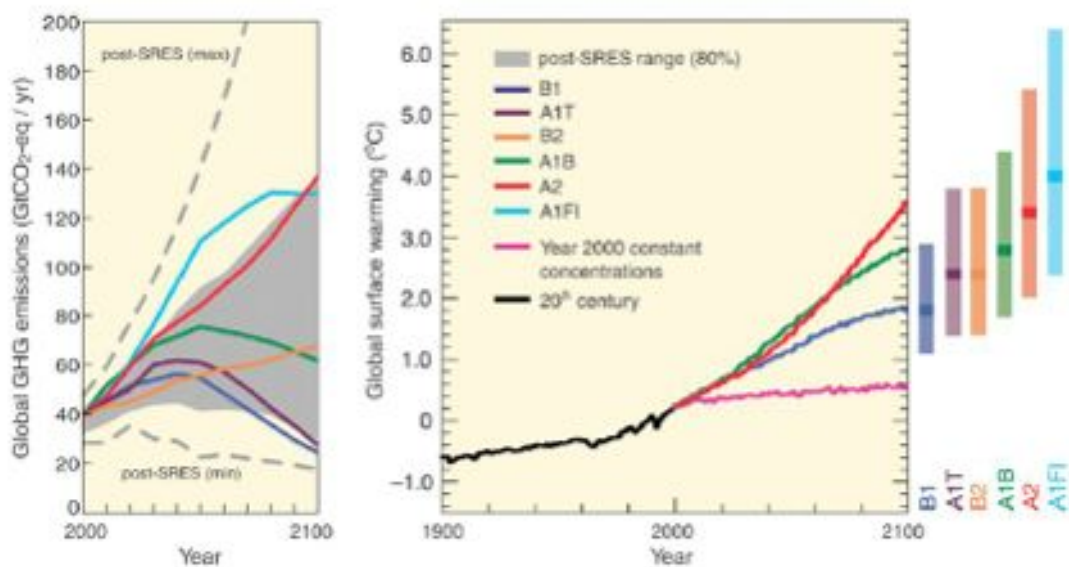


Figure 5. Greenhouse gases concentration and global warming for SRES scenarios used in the IPCC AR4 CMIP3 model runs (IPCC 2007).

For the IPCC AR5 model runs, the scenarios used are RCP-*Representative Concentration Pathways* (Van Vuuren et al 2011) that have replaced the SRES emission scenarios (Figure 6). The RCPs represent radiative forcing (right side), where the RCP2.6 represents a scenario with low emissions and low radiative forcing (similar to SRES B1 or B2). The RCP8.5 represents a larger radiative forcing and is similar to a high emission scenario (SRES A1 or A2). The RCP4.5 scenario would be similar to a A1B medium emission scenario.

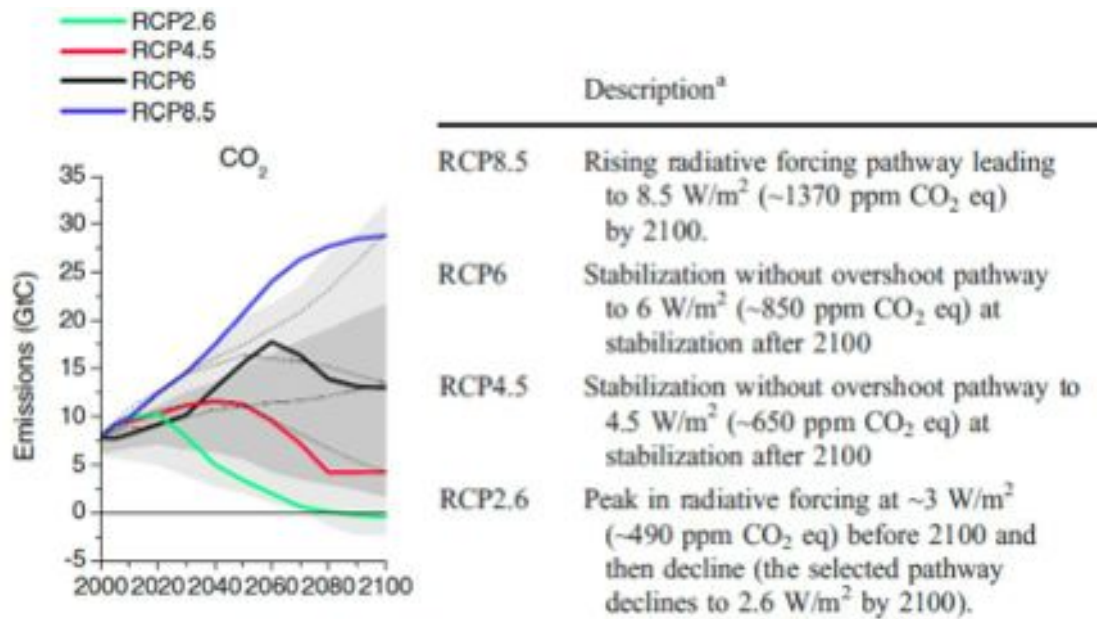


Figure 6. Representation of the RCPs (Representative Concentration Pathways) used by IPCC AR5 (Van Vuuren et al 2011)

A comparison between the warming projected by 2100 derived from the SRES scenarios used in IPCC AR4 and the RCPs used in the IPCC AR5 is shown in Figure 7. By 2100 the RCPs seem to show the highest warming.

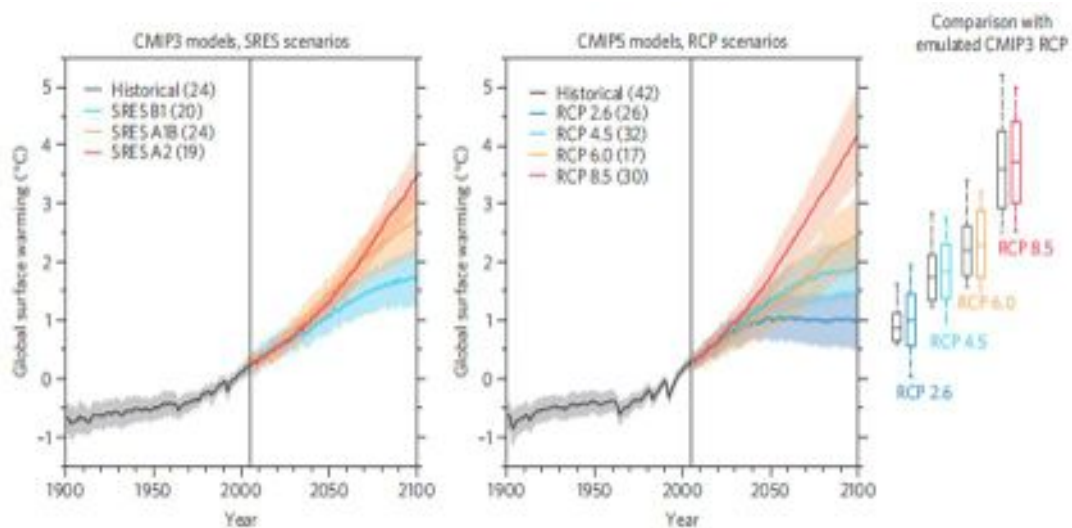


Figure 7. Changes in mean temperature (color lines) and uncertainties (shades) and uncertainties relative to 1986–2005, for the SRES IPCC AR4 and RCPs do IPCC AR5. The number of models is indicated among brackets. The boxes on the right side of the panel show the mean and the whiskers show the standard deviation on the projected warming by 2100 (Knutti and Sedlacek 2013).

## 4.2 Comparisons between CMIP3 and CMIP5 models

The horizontal resolution of the CMIP5 models is slightly higher than that of the CMIP3 models, and the experiments using CMIP5 models are more comprehensive, including experiments for seasonal climate forecast at the decadal time scale, which make it possible for scientists to explore a wide range of scientific questions (Taylor et al 2012). Some of the main improvements of CMIP5 models

include more detailed coupling with oceans, the inclusion of the carbon cycle and the use of more complete radiative forcing due to a better modeling of the aerosol effects from time series of volcanic and solar forcing in most of the models (Taylor et al 2012; Knutti and Sedlacek 2013; Sillmann et al 2013). Tables 3 and 4 show a list of CMIP3 and CMIP 5 models, indicating names and horizontal resolution.

Table 3. List of CMIP3 global models used on this report showing horizontal resolution (latitude/longitude), SRES emission scenarios, and number of realizations. The models are organized according to their horizontal resolution (Torres and Marengo, 2013).

<b>Models</b>	<b>Resolution</b>	<b>20C3M</b>	<b>A2</b>	<b>A1B</b>	<b>B1</b>
INM-CM3.0	5 ° x 4 °	1	1	1	1
GISS-EH	5 ° x 4 °	5	-	3	-
GISS-ER	5 ° x 4 °	9	1	2	1
GISS-AOM	4 ° x 3 °	2	-	2	2
CGCM3.1(T47)	3.8 ° x 3.8 °	5	5	5	5
MIUB-ECHO-G	3.8 ° x 3.8 °	5	3	3	3
UKMO-HadCM3	3.8 ° x 2.5 °	2	1	1	1
IPSL-CM4	3.8 ° x 2.5 °	1	1	1	1
FGOALS-g1.0	2.8 ° x 3 °	3	-	2	3
MRI-CGCM2.3.2	2.8 ° x 2.8 °	5	5	5	5
CGCM3.1(T63)	2.8 ° x 2.8 °	1	-	1	1
CNRM-CM3	2.8 ° x 2.8 °	1	1	1	1
MIROC3.2(medres)	2.8 ° x 2.8 °	2	3	3	3
PCM	2.8 ° x 2.8 °	4	4	4	2
GFDL-CM2.0	2.5 ° x 2 °	3	1	1	1
GFDL-CM2.1	2.5 ° x 2 °	3	1	1	1
BCCR-BCM2.0	1.9 ° x 1.9 °	1	1	1	1
CSIRO-MK3.0	1.9 ° x 1.9 °	3	1	1	1
CSIRO-MK3.5	1.9 ° x 1.9 °	3	1	1	1
ECHAM5	1.9 ° x 1.9 °	4	3	4	3
UKMO-HadGEM1	1.9 ° x 1.3 °	2	1	1	-
CCSM3	1.4 ° x 1.4 °	7	4	7	9
ECHAM4	1.1 ° x 1.1 °	1	1	1	-
MIROC3.2(hires)	1.1 ° x 1.1 °	1	-	1	1

Table 4. – List of CMIP5 global models used on this report, showing horizontal resolution (latitude/longitude), RCPs (RCPs 2.6, 4.5, 6.0, 8.5). The models are organized according to their horizontal resolution (Torres and Marengo, 2013).

Models	Resolution (lat/lon)	Historical	RCP			
			2.6	4.5	6.0	8.5
FGOALS-g2	3.1 ° x 2.8 °	4	1	1	-	1
BCC-CSM1-1	2.8 ° x 2.8 °	3	1	1	1	1
CanESM2	2.8 ° x 2.8 °	5	5	5	-	5
MIROC-ESM	2.8 ° x 2.8 °	3	1	1	1	1
FIO-ESM	2.8 ° x 2.8 °	1	1	1	1	1
MIROC-ESM-CHEM	2.8 ° x 2.8 °	1	1	1	1	1
GFDL-CM3	2.0 ° x 2.5 °	5	1	1	1	1
GFDL-ESM2G	2.0 ° x 2.5 °	1	1	1	1	-
Giss-E2-R	2.0 ° x 2.5 °	5	1	5	1	1
GFDL-ESM2M	2.0 ° x 2.5 °	1	1	1	1	1
IPSL-CM5A-LR	1.9 ° x 3.8 °	4	1	3	1	3
NorESM1-M	1.9 ° x 2.5 °	3	1	1	1	1
CSIRO-Mk3-6-0	1.9 ° x 1.9 °	10	10	10	10	10
MPI-ESM-LR	1.9 ° x 1.9 °	3	3	3	-	3
INMCM4	1.5 ° x 2.0 °	1	-	1	-	1
CNRM-CM5	1,4 ° x 1,4 °	1	1	1	-	1
MIROC5	1.4 ° x 1.4 °	1	1	1	1	1
IPSL-CM5A-MR	1.3 ° x 2.5 °	1	1	1	-	1
HadGEM2-CC	1.3 ° x 1.9 °	1	-	1	-	1
HadGEM2-ES	1.3 ° x 1.9 °	4	1	1	1	4
ACCESS1.0	1.3 ° x 1.9 °	1	-	1	-	1
EC-EARTH	1.1 ° x 1.1 °	1	1	1	-	1
MRI-CGCM3	1.1 ° x 1.1 °	5	1	1	1	1
CCSM4	0.9 ° x 1.3 °	6	5	5	5	5

In the following, we analyze climate simulations of the 20th and 21<sup>st</sup> century performed by CMIP3 A1B scenario and CMIP5 RC8.5 models. While more than one realization is available for some models, we analyze only the first ensemble member of each model simulation as a first-order assessment. The CMIP3 and CMIP5 model output is available from the data archives of the Program for Climate Model Diagnosis and Intercomparison (PCMDI, <http://www.pcmdi.llnl.gov>) and the Earth System Grid data distribution portal (ESG, <http://www.earthsystemgrid.org>).

Climate changes simulated in the CMIP3 and CMIP5 ensembles are not directly comparable because of the differences in prescribed forcing agents (e.g., CO<sub>2</sub> and aerosols) between the SRES and RCP scenarios. Furthermore, the models may respond differently to a specific radiative forcing due to different model-specific climate sensitivities. However, based on the underlying radiative forcing (or

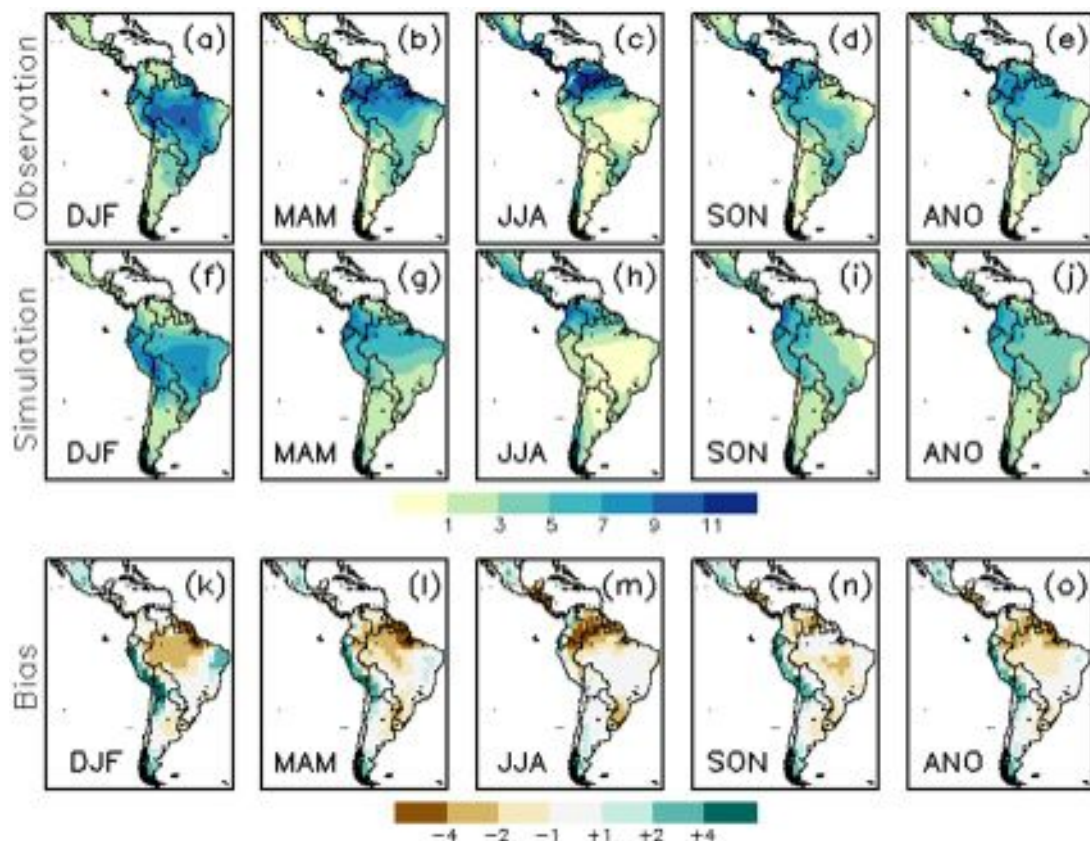
CO2 concentrations), one can compare projected changes in the temperature and precipitation indices and provide an estimate of uncertainty related to the different emission scenarios.

#### 4.2.1 CMIP3 and CMIP5 model projections

##### Present climate

Before analyzing the climate change projections, a spatial analysis of the CMIP3 and CMIP5 GCM (General Circulation Models) ensemble means representation of the present-time seasonal climatology (1961-1990) was performed for the surface air temperature and precipitation. Additionally, all GCMs historical simulations for the twentieth century were compared against the observed surface air temperature and precipitation from the CRU TS 3.0 dataset (Mitchell and Jones 2005) produced by the University of East Anglia Climate Research Unit (UEA/CRU). In general, the CMIP3 ensemble mean well-represents the SA monsoon system and the associated South Atlantic Convergence Zone (SACZ), characterized by the northwest/southeast migration of the maximum rainfall amounts from the Amazon basin to the southeast Atlantic (Figure 8 a-e). However, overestimation of the rainfall is observed for almost all seasons (except for JJA) over the central Andes (with values larger than 4 mm day<sup>-1</sup> in the DJF and the SON) and in the DJF over Northeast Brazil (~ 1-4 mm day<sup>-1</sup>), and an underestimation is observed for all seasons in nearly all of the Amazon, eastern Colombia, Venezuela, Guyana, French Guyana and Suriname, and CA (~1-4 mm day<sup>-1</sup>) (Figure 8 k-o). Regarding the simulation of the surface air temperature climatology, the CMIP3 ensemble average (Figure 9 f-j) is very similar to the observed data (Fig. 4.2.2 a-e), in which the temperature bias does not exceed 1°C over nearly the entire continent (Figure 9 k-o). Nevertheless, colder than observed temperatures are identified over the Northeast and Center West Brazil (except for the SON) and the Andes and Mexico, and higher temperatures are observed over Northeast Argentina (except for JJA) and over the Amazon Basin in the SON (Fig. 4.2.2 k-o).

Figure 8 – Observed (a-e) and CMIP3 ensemble mean (f-j) patterns of seasonal precipitation and bias (k-o) for 1961-1990. Bias was calculated as the difference between simulation (ensemble mean) and observation (CRU-TS 3.0). Symbols DJF, MAM, JJA, SON, and ANO, represent the periods from December to February, March to May, June to August, September to November, and annual mean, respectively. Units are in millimeters per day.



Poor representation of the current climate conditions over the Andes can be related to, among other things, the coarse model resolution that does not allow a good representation of the complex topography of this region. Furthermore, as shown by Seth et al (2010), the ensemble mean exhibits a weaker moisture transport to the east of the Andes, which can be one of the factors inducing an underestimation of the rainfall over the La Plata basin, especially during the austral winter (Figure 8 m). In fact, over the Amazon basin, the systematic rainfall underestimation by the models can be related to many factors, such as the poor representation of cumulus convection, the biosphere-atmosphere interactions in the rainforest, soil moisture and land surface processes. On the other hand, there is poor data observation coverage in some portions of SA, mainly in the Amazon basin, in which few meteorological stations are available, which slightly influences the magnitude and location of the bias patterns (mainly for precipitation).

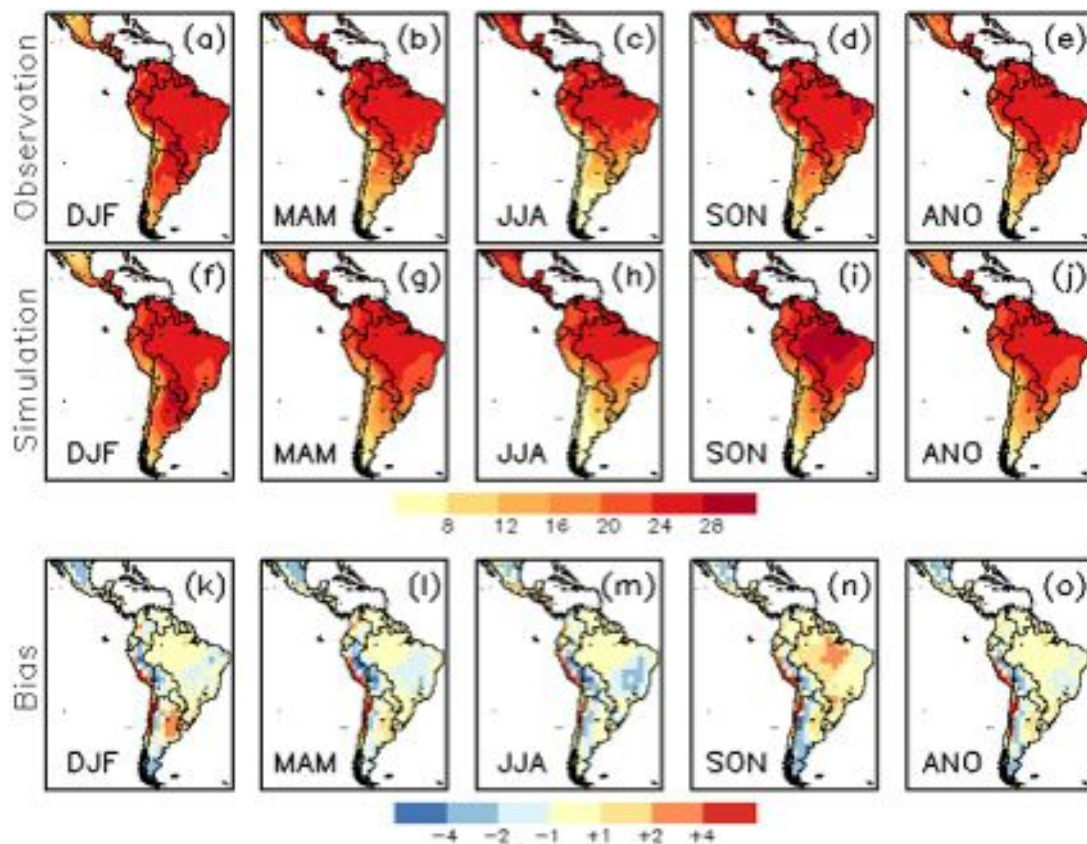


Figure 9 – The same as in Figure 8, but for seasonal surface air temperature (in degrees Celsius).

Kim et al (2008), when analyzing the spatial and temporal variability of the global monsoon simulated by the CMIP3 models, grouped the models into three sets according to their spatial resolution (low, medium, and high resolution group, corresponding to a horizontal resolution of 4o-5o, 2o-3o and less than 2o, respectively), attempting to analyze the impact of this parameter in representing the global monsoon climate. Those authors concluded that, although the higher resolution models provided a slight improvement of the rainfall simulation over high topography, any set performed better in representing the current climate conditions as a whole. Even those sets with coarser resolution exhibited results comparable to those with higher resolution. Therefore, it was decided to use all of the available models in our analysis, instead of using only those with higher resolution.



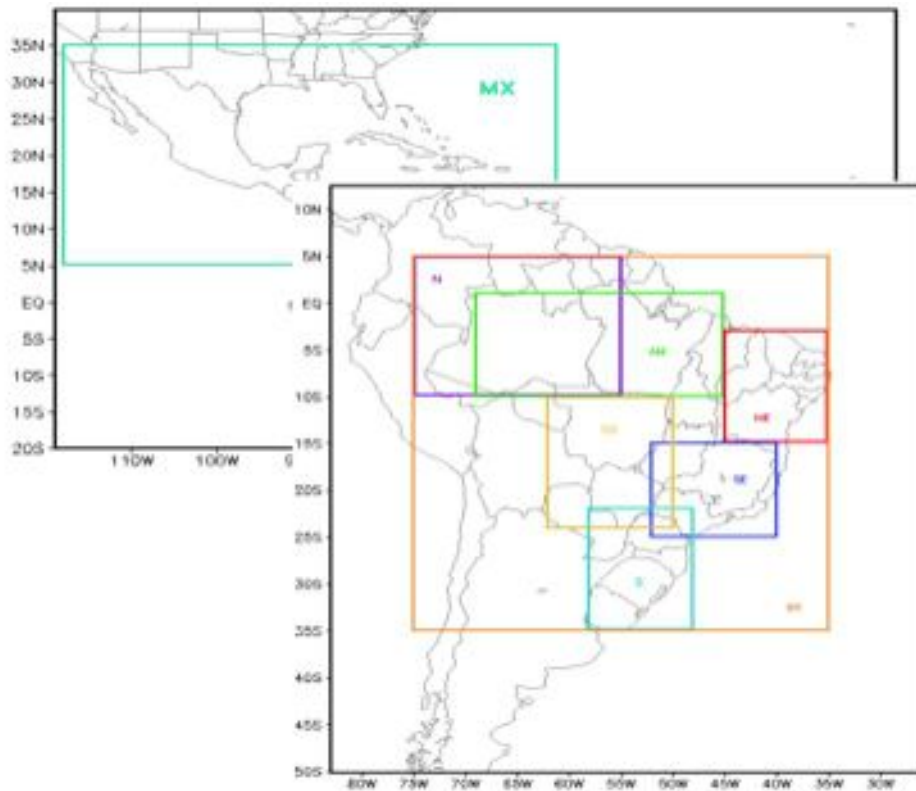


Figure 10 – Study domain. Rectangles indicate some sub-regions of interested: Mexico and Central America (MX), North-western South America (N), Amazon Basin (AM), Northeast Brazil (NE), Central-Western South America (CO), south-eastern and southern Brazil (SE and S, respectively), and a rectangle containing the full extent of the Brazilian territory (BR).

Figure 11 shows the annual cycle of observed precipitation and the annual cycle of historical simulations generated by 24 GCMs from the CMIP3 dataset averaged over the eight sub-regions described in Figure 10 for 1961-1990. It can be seen that the precipitation annual cycle is reasonably well represented by the ensemble mean (black bold line in Figure 11) for all sub-regions evaluated. However, some deficiencies can be easily observed, such as the dry bias displayed over all sub-regions, except for the Northeast Brazil during the months from November to March. Among the sub-regions analyzed, the North-western South America (N) and Amazon Basin (AM) are the regions in which the GCMs showed the worst performance, indicated by the mean GCMs root mean square error (RMSE). Additionally, over the N e AM regions there was a large underestimation of the rainy period, as well as a shift (~ 1 month) in the rainy and dry season, respectively. Another remarkable deficiency is the one month shift in the simulated rainy season over the NE region.

Regarding to the annual cycle of temperature (Figure 12), the CMIP3 ensemble mean provides a good representation of the observed patterns, and a reasonable agreement among all models analyzed. Nevertheless, the ensemble mean shows unrealistic amplitude of oscillation in the annual cycle of temperature over the N and AM regions. Additionally, for this climate variable, the sub-regions of larger discrepancies among the ensemble members are the Central-Western South America (CO), N, and AM region.

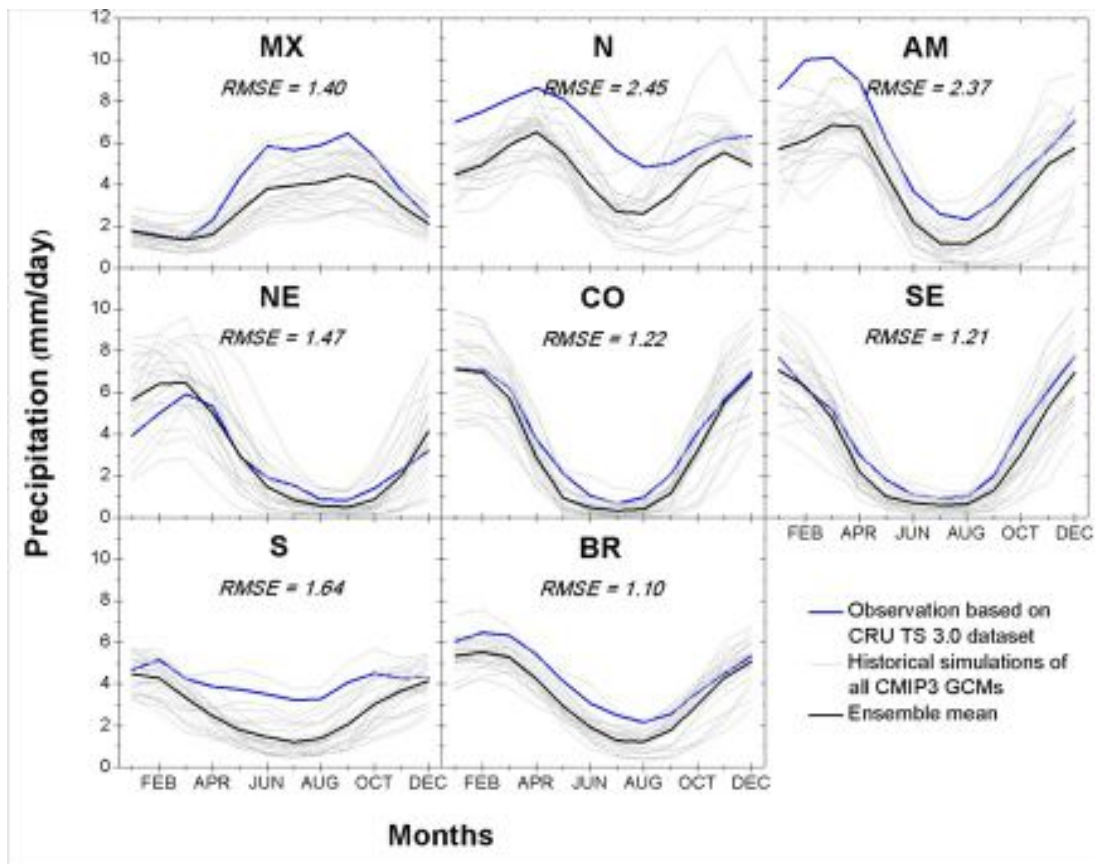


Figure 11 – Annual cycle of observed precipitation (blue) and historical simulations (gray) of 24 GCMs from the CMIP3 dataset averaged over the sub-regions described in Figure 10 for 1961-1990. The black bold line represents the CMIP3 GCMs ensemble mean. The mean GCMs root mean square error ((RMSE)) is indicated below each region acronym. Units are in mm day<sup>-1</sup>.

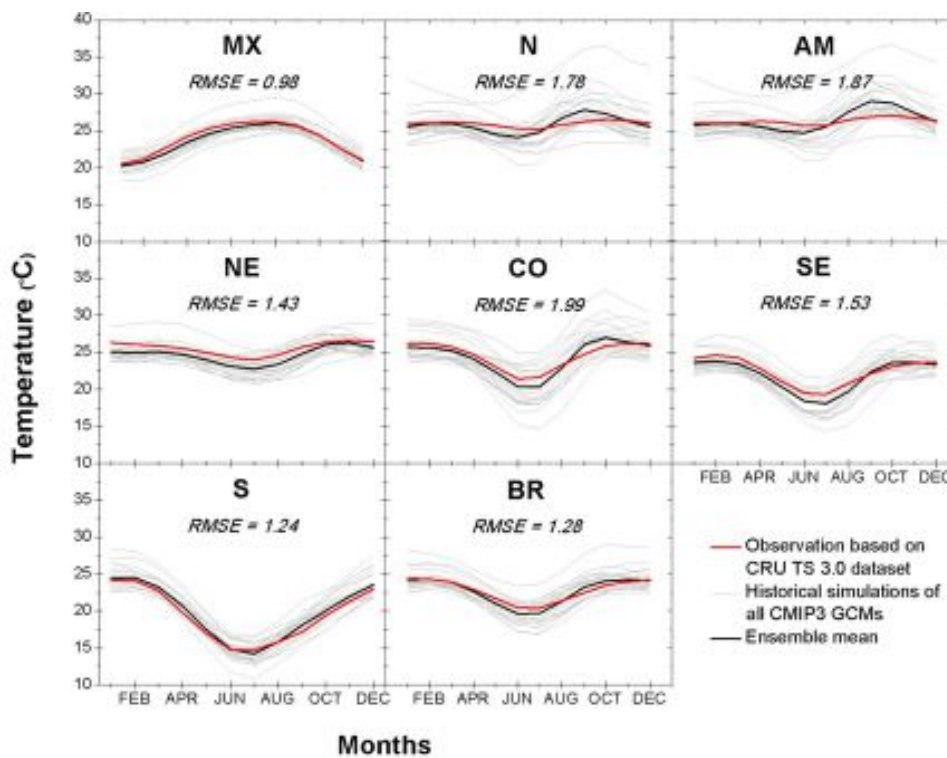


Figure 12 – The same as in Figure 11, but for seasonal surface air temperature (in degrees Celsius).

The observed seasonal precipitation and the CMIP5 ensemble mean patterns of seasonal precipitation and bias for 1961-1990 are shown in Figure 13. Comparing the climatologies generated from the CMIP5 models (Figure 13) with that from the CMIP3 dataset, we note a strong similarity among them. On the other hand, a considerable reduction in the dry bias can be seen in the northwest / northern South America and in the Amazon region in the newest dataset (CMIP5). However, although the CMIP5 GCMs have a higher horizontal resolution compared to that from the CMIP3 dataset, no improvement is noticeable in the Andes region / western South America (regions of complex topography).

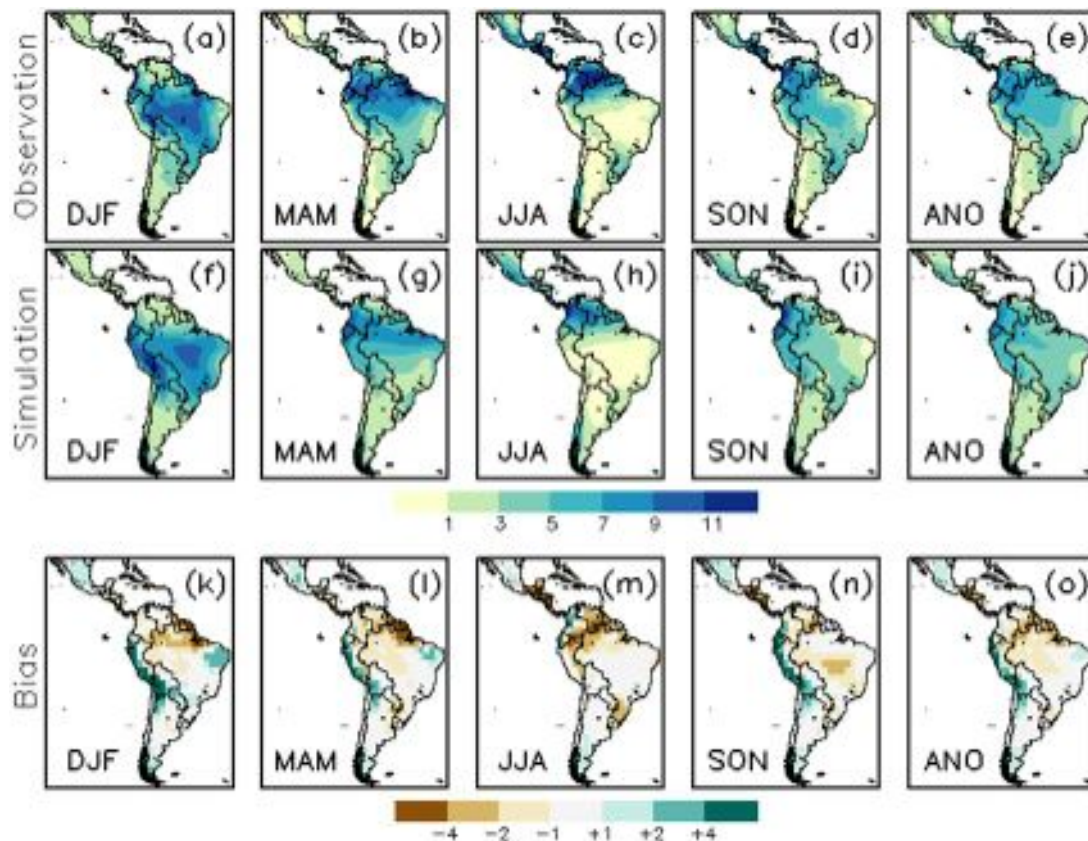
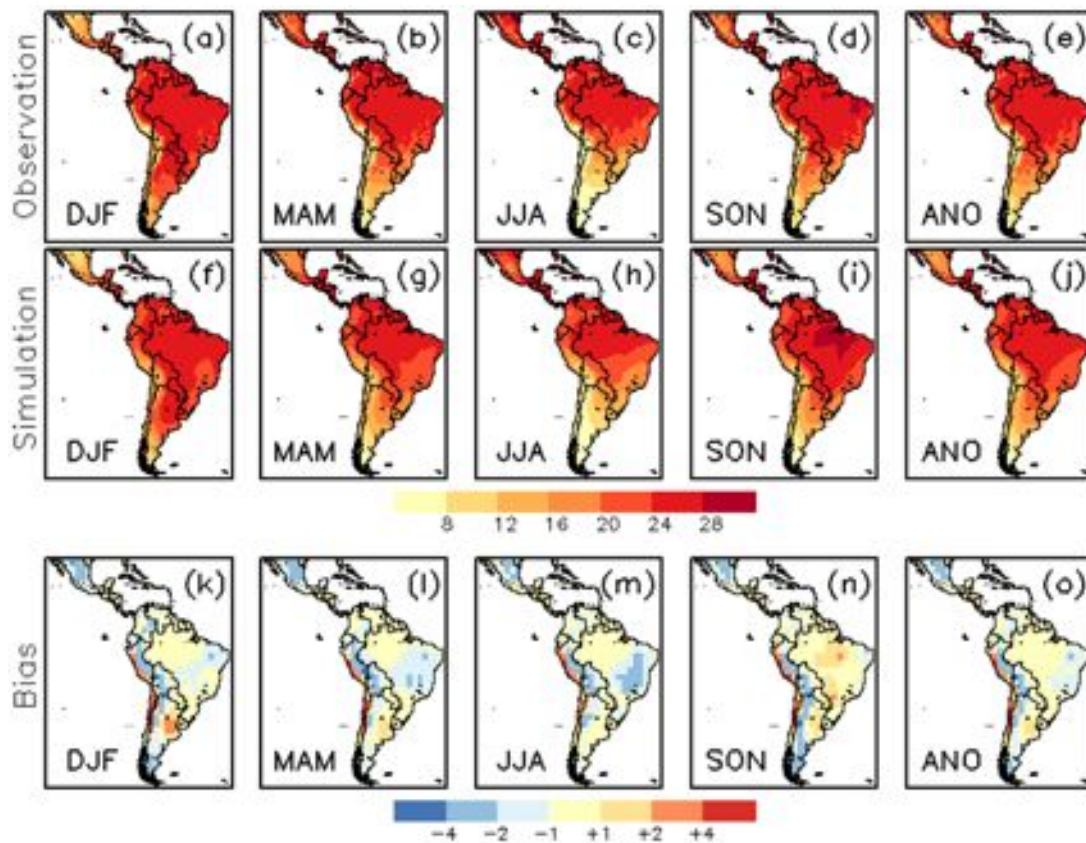


Figure 13 – Observed (a-e) and CMIP5 ensemble mean (f-j) patterns of seasonal precipitation and bias (k-o) for 1961-1990. Bias was calculated as the difference between simulation (ensemble mean) and observation (CRU-TS 3.0). Symbols DJF, MAM, JJA, SON, and ANO, represent the periods from December to February, March to May, June to August, September to November, and annual mean, respectively. Units are in millimeters per day.

Regarding temperature, it is also possible to notice a strong similarity between the CMIP3 and CMIP5 (Figure 14) biases. However, the warm bias over the eastern Amazon in SON was considerably reduced, and a slight reduction in bias over the Andes / west of the South American continent can be seen in the new version of GCMs.

Analyzing the annual cycle of precipitation and temperature simulated by the CMIP5 GCMs (Figures 15 and 16, respectively), it is possible to identify several improvements compared to CMIP3. First of all, except for precipitation over Northeast Brazil and Central-Western South America (Figure 15), and for temperature over North-western South America (Figure 16), the mean GCMs root mean square error decreased in all sub-regions and variables evaluated, as well as the spread of the ensemble members.

Figure 14– The same as in Figure 13, but for seasonal surface air temperature (in degrees Celsius).



With respect to CMIP5 precipitation (Figure 15), the dry bias of the GCMs ensemble mean has been reduced considerably in the North-western South America and Amazon Basin in all months of the year, as also observed by Joetzjer et al (2013). Over Northeast Brazil, the overestimation of precipitation from January to April increased in CMIP5, compared to CMIP3 dataset, which explains the increase in the mean GCMs root mean square error. However, the lag of about 1 month of the rainy season in Northeast Brazil simulated by the CMIP3 ensemble was corrected in the CMIP5 ensemble.

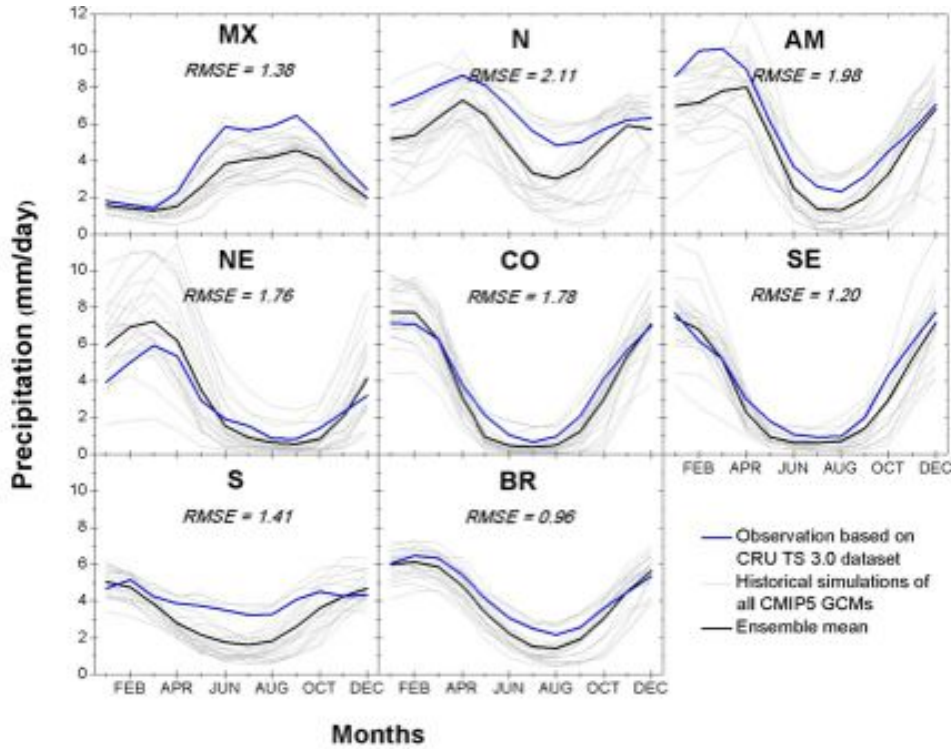


Figure 15 – Annual cycle of observed precipitation (blue) and historical simulations (gray) of 24 GCMs from the CMIP5 dataset averaged over the sub-regions described in Fig. 4.2.3 for 1961-1990. The black bold line represents the CMIP5 GCMs ensemble mean. The mean GCMs root mean square error ((RMSE)) is indicated below each region acronym. Units are in mm day<sup>-1</sup>.

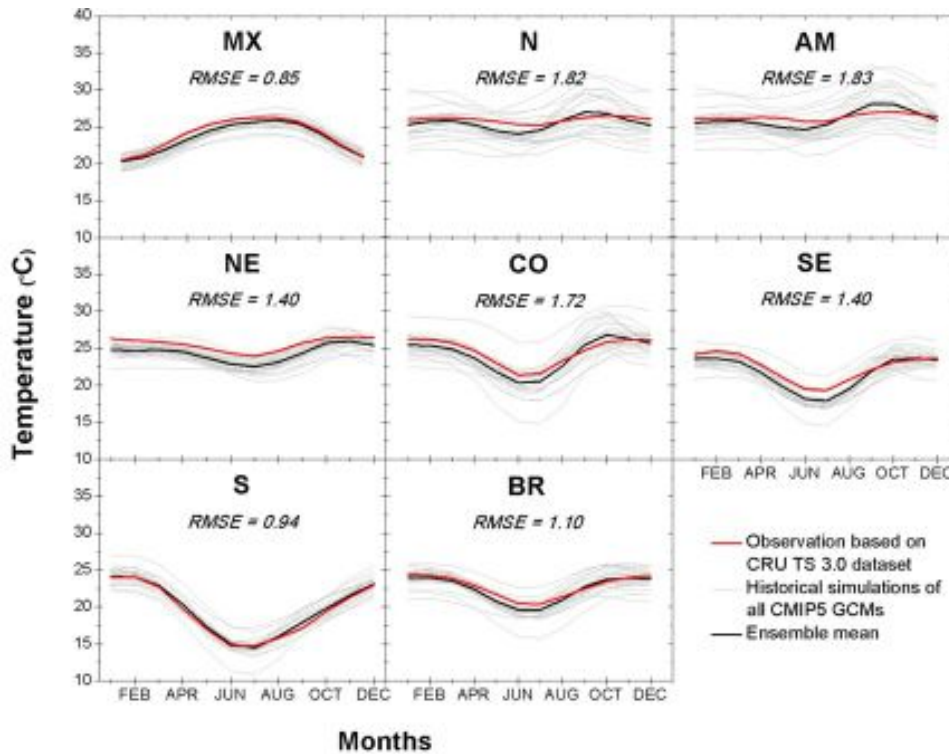


Figure 16 – The same as in Figure 15, but for seasonal surface air temperature (in degrees Celsius).

### Future climates from CMIP3 and CMIP5 projections

Figures 17 and 18 show the projected changes in temperature and rainfall extremes for Central and South America, based on the IPCC AR4 models, for the SRES A1B Scenario, for 2081-2100 relative a 1980-1999. Figure 17 shows a pattern that is consistent with a general warming in the region: and increase in the fraction of warm days and nights and decrease in the fraction of cold days and nights. These changes are more intense in Northwestern and Southeastern South America. Increases in extreme rainfall are particularly strong in western Amazonia and the west coast of Peru and Ecuador and in Southeastern South America, while in CA this is a slight tendency for reduction on the number of days with precipitation above 10 mm.

The intensity of dry spells and soil moisture availability for the mid (2041-65) and long (2081-2100) term shows for the SRES A2 scenario increase in the frequency and duration of dry spells in eastern Amazonia, Northeast Brazil, central and southern Chile and in central America in Mexico, while reductions are projected for the Northern Peru and Ecuador region, consistent with positive rainfall anomalies on those regions (Figure 19). This is perhaps better detected on the soil moisture anomaly maps, where negative anomalies are found over most of Tropical South America, particularly northern South America, Bolivia, Chile and Mexico, this last consistent with a possible reduction on the intensity and extension of the NAMS.

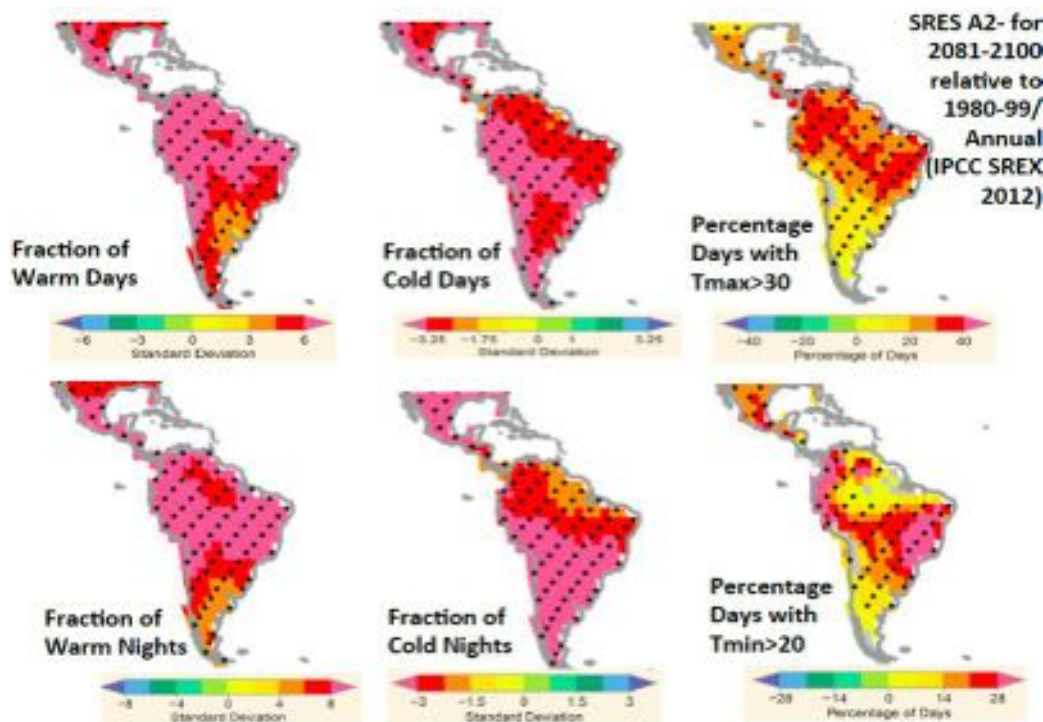


Figure 17. Projected annual changes in some indices for daily Tmin for 2081-2100 with respect to 1980-1999, based on 14 GCMs contributing to the CMIP3: fraction of warm days (days in which Tmax exceeds the 90th percentile of that day of the year, calculated from the 1961-1990 reference period); fraction of cold days (days in which Tmax is lower than the 10th percentile of that day of the year, calculated from the 1961-1990 reference period); percentage of days with Tmax > 30°C; fraction of warm nights (days at which Tmin exceeds the 90th percentile of that day of the year, calculated from the 1961-1990 reference period); fraction of cold nights (days at which Tmin is lower than the 10th percentile of that day of the year, calculated from the 1961-1990 reference period); percentage of days with Tmin > 20°C. The changes are computed for the annual time scale, as the fractions/percentages in the 2081-2100 period (based on simulations under emission scenario SRES A2) minus the fractions/percentages of the 1980-1999 period (from corresponding simulations for the 20th century). Warm night and cold night changes are expressed in units of standard deviations, derived from detrended per year

annual or seasonal estimates, respectively, from the three 20-year periods 1980-1999, 2046-2065, and 2081-2100 pooled together.  $T_{min} > 20^{\circ}\text{C}$  changes are given directly as differences of percentage points. Color shading is only applied for areas where at least 66% (i.e., 10 out of 14) of the GCMs agree in the sign of the change; stippling is applied for regions where at least 90% (i.e., 13 out of 14) of the GCMs agree in the sign of the change (IPCC SREX 2012).

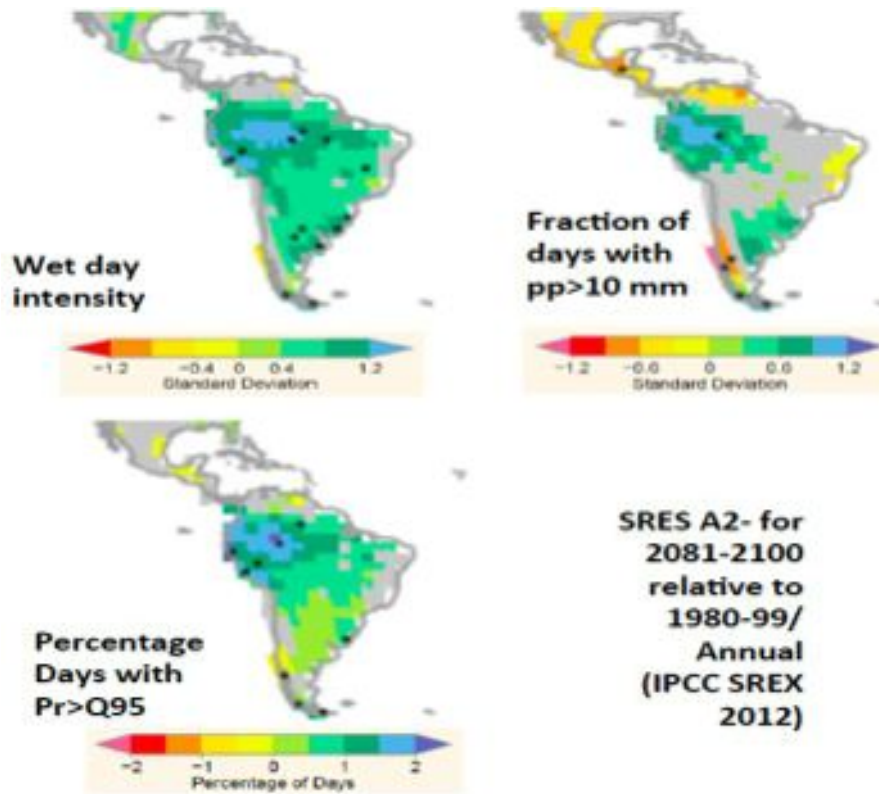
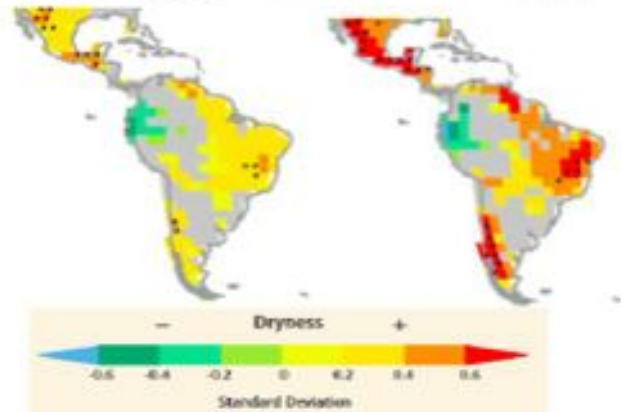


Figure 18. Projected annual and seasonal changes in three indices for daily precipitation for 2081-2100 with respect to 1980-1999, based on 17 GCMs contributing to the CMIP3: wet-day intensity, percentage of days with precipitation above the 95% quantile of daily wet day precipitation for that day of the year, calculated from the 1961-1990 reference period; right column: fraction of days with precipitation higher than 10 mm. The changes are computed for the annual time scale as the fractions/percentages in the 2081-2100 period (based on simulations under emission scenario SRES A2) minus the fractions/percentages of the 1980-1999 period (from corresponding simulations for the 20th century). Changes in wet-day intensity and in the fraction of days with  $Pr > 10$  mm are expressed in units of standard deviations, derived from detrended per year annual or seasonal estimates, respectively, from the 2081-2100 pooled together. Changes in percentages of days with precipitation above the 95% quantile are given directly as differences in percentage points. Color shading is only applied for areas where at least 66% (i.e., 12 out of 17) of the GCMs agree on the sign of the change; stippling is applied for regions where at least 90% (i.e., 16 out of 17) of the GCMs agree on the sign of the change (IPCC SREX 2012).

**A2-Change in consecutive dry days  
(CDD) 2046 - 2065 2081 - 2100**



**A2-Soil moisture anomalies (SMA)  
2046 - 2065 2081 - 2100**

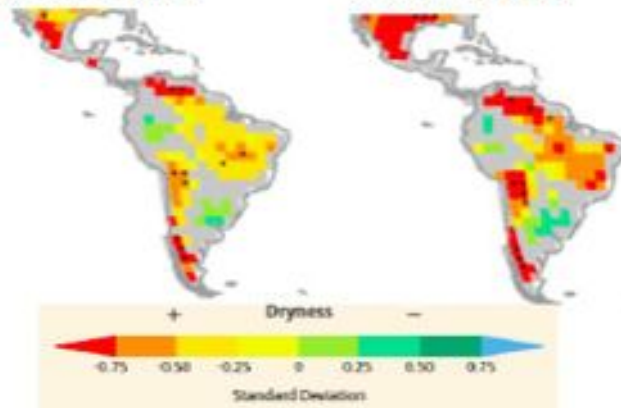


Figure 19. Projected annual changes in dryness assessed from two indices. Upper panels: Change in annual maximum number of consecutive dry days (CDD: days with precipitation <1 mm); lower panel: Changes in soil moisture (soil moisture anomalies, SMA). Increased dryness is indicated with yellow to red colors; decreased dryness with green to blue. Projected changes are expressed in units of standard deviation of the interannual variability in the three 20-year periods 1980–1999, 2046–2065, and 2081–2100. The figures show changes for two time horizons, 2046–2065 and 2081–2100, as compared to late 20th-century values (1980–1999), based on GCM simulations under emissions scenario SRES A2 relative to corresponding simulations for the late 20th century. Results are based on 17 (CDD) and 15 (SMA) GCMs contributing to the CMIP3. Colored shading is applied for areas where at least 66% (12 out of 17 for CDD, 10 out of 15 for SMA) of the models agree on the sign of the change; stippling is added for regions where at least 90% (16 out of 17 for CDD, 14 out of 15 for SMA) of all models agree on the sign of the change. Grey shading indicates where there is insufficient model agreement (<66%). (IPCC SREX 2012)

Based on CMIP3 model analyses, Table 5 shows some tendencies on observed and projected changes in monsoons, El Nino, and tropical and extratropical cyclones. There is low confidence in observed projected trends in the monsoon regions in northern and South America because of insufficient evidence, but negative rainfall trends in the North American Monsoon have been detected (in few studies only). Concerning El Nino observed and projected changes, while there is medium confidence on observed changes in El Nino, projections show lower confidence in changes, because there is low agreement between models on any change in SST anomalies in the equatorial Pacific. With regard to tropical cyclones and hurricanes, there is low confidence on observed trends, while projections show a decrease in the total number of cyclones and exhibit a tendency for an increase in the frequency of



intense hurricanes, where the confidence is still low. This would determine increases in the frequency of intense rain in CA. As a consequence of rainfall changes, the CA region shows a consistent future runoff reduction. Maurer et al (2009) studied climate change projections for the Lempa River basin, one of the largest basins in CA, covering portions of Guatemala, Honduras and El Salvador. They showed that future climate projections (increase in evaporation and reduction in precipitation) imply a reduction of 20% in inflows to major reservoirs in this system. Imbach et al (2012) found similar results using a modeling approach that also considered potential changes in vegetation.

In SA, few studies show a tendency for a poleward shift of extratropical cyclones affecting rainfall on the region, and projections suggest changes in storm activity with medium to low confidence.

#### 4.2.2. CMIP5 model projections

Each one of the 23 CMIP5 models suggest warming for both seasons DJF and JJA for 2071-2100 (relative to 1961-90), with some models warmer than others, particularly in tropical and subtropical SA and in CA. The most intense warming is shown in the GFDL, ACCESS, IPSL and HadGEM2 ES, and less warming is noted in the CCSM4, INMCM4, NASA GISS and GFDL-2M. In SA, some models suggest a more intense warming during austral winter JJA (Figure 20).

Table 5. Overview of considered extremes and summary of observed and projected changes on global scale (CDKN 2013)

	Observed changes (since 1950)	Attribution of observed changes	Projected changes (up to 2100) with respect to late 20th century	
Phenomena related to weather and climate extremes	<b>Monsoons</b>	Low confidence in trends because of insufficient evidence.	Low confidence due to insufficient evidence.	Low confidence in projected changes of monsoons, because of insufficient agreement between climate models.
	<b>El Niño and other modes of variability</b>	Medium confidence of past trends towards more frequent central equatorial Pacific El Niño Southern Oscillation (ENSO) events. Insufficient evidence for more specific statements on ENSO trends. Likely trends in Southern Annular Mode.	Likely anthropogenic influences on identified trends in Southern Annular Mode. <sup>20</sup> Anthropogenic influence on trends in NAO are as likely as not. No attribution of changes in ENSO.	Low confidence in projections of changes in behaviour of ENSO and other modes of variability because of insufficient agreement of model projections.
	<b>Tropical cyclones</b>	Low confidence that any observed long-term (i.e. 40 years old or more) increases in tropical cyclone activity are robust, after accounting for past changes in observing capabilities.	Low confidence in attribution of changes in tropical cyclone activity to anthropogenic influences (insufficient data quality and physical understanding).	Likely decrease or no change in frequency of tropical cyclones. Likely increase in mean maximum wind speed, but possibly not in all basins. Likely increase in heavy rainfall associated with tropical cyclones.
	<b>Extratropical cyclones</b>	Likely poleward shift in extratropical cyclones. Low confidence in regional changes in intensity.	Medium confidence in anthropogenic influence on poleward shift.	Likely impacts on regional cyclone activity but low confidence in detailed regional projections due to only partial representation of relevant processes in current models. Medium confidence in a reduction in the numbers of mid-latitude storms. Medium confidence in projected poleward shift of mid-latitude storm tracks.

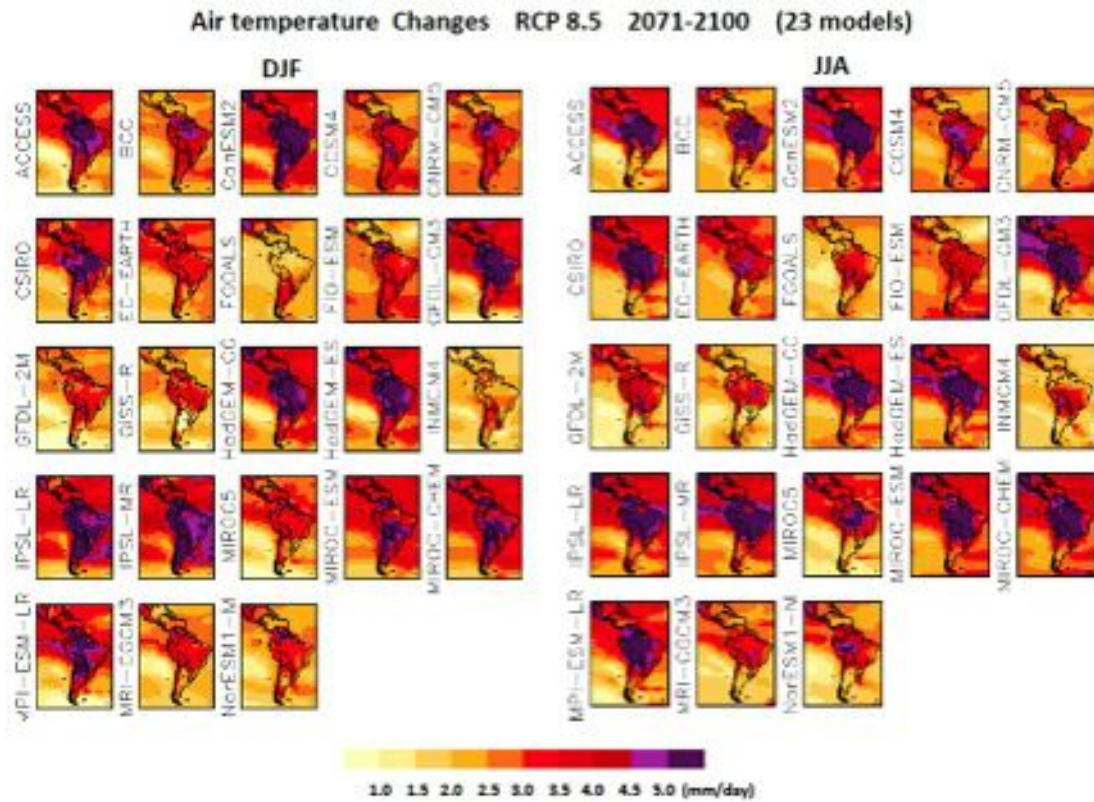


Figure 20. Seasonal (DJF and JJA) air temperature anomalies from 23 CMIP5 models for CA and SA for the RCP8.5 scenario. Units are in °C, and color scale is shown on the lower side of the panel. Name of the model is shown at the left side of each map. Projections are for 2071-2100 relative to 1961-90.

Figure 21 shows that there is some consensus on changes in rainfall for the RCP8.5 scenario, with rainfall increase in Southeastern South America, Northwest Coast of Peru and Ecuador and rainfall reductions over Southern Chile and over the Central American-Caribbean region, suggesting a weakening of North American monsoon systems. There is a large model spread among projected rainfall reductions suggesting less confidence on those changes over such tropical regions, including the SA monsoon region, eastern Amazonia-Northeast Brazil and the central South American region. The intermodel differences are large among most of the models, where the FGOALS models shows a wet Amazonia and the CanESM2 shows a drier Amazonia during austral summer, while during boreal summer most of the models shows rainfall decrease in central America while GFDL and the GIS models show rainfall increase on those areas.



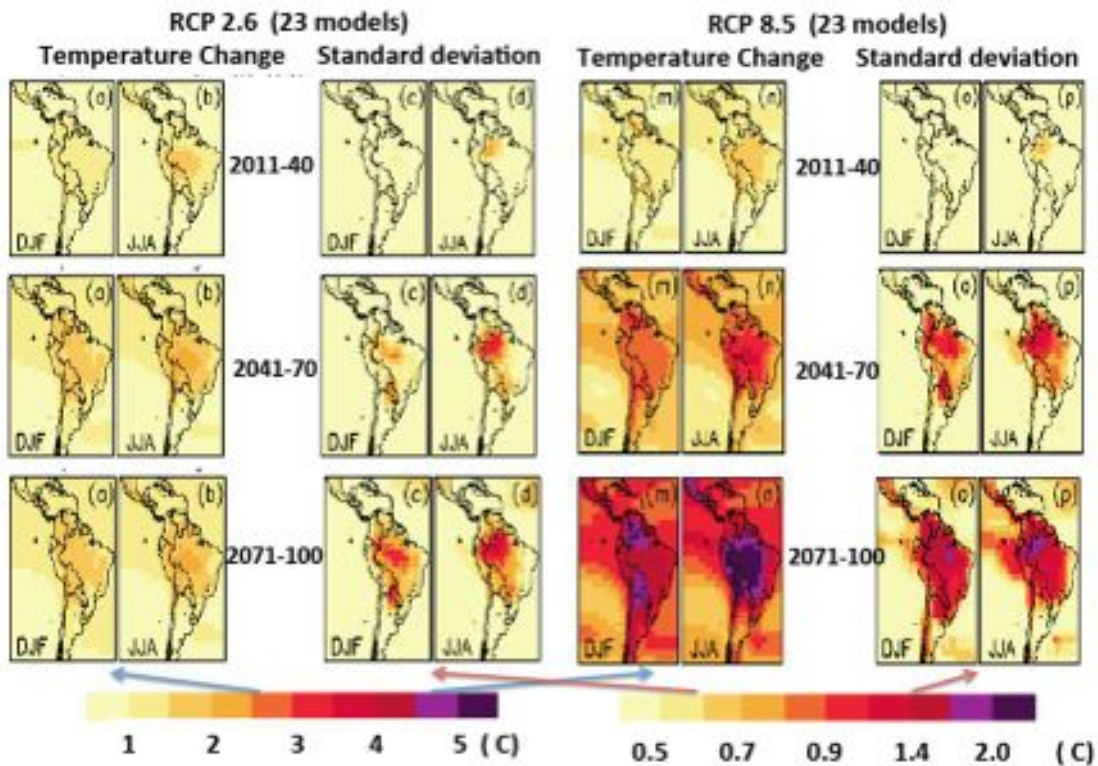
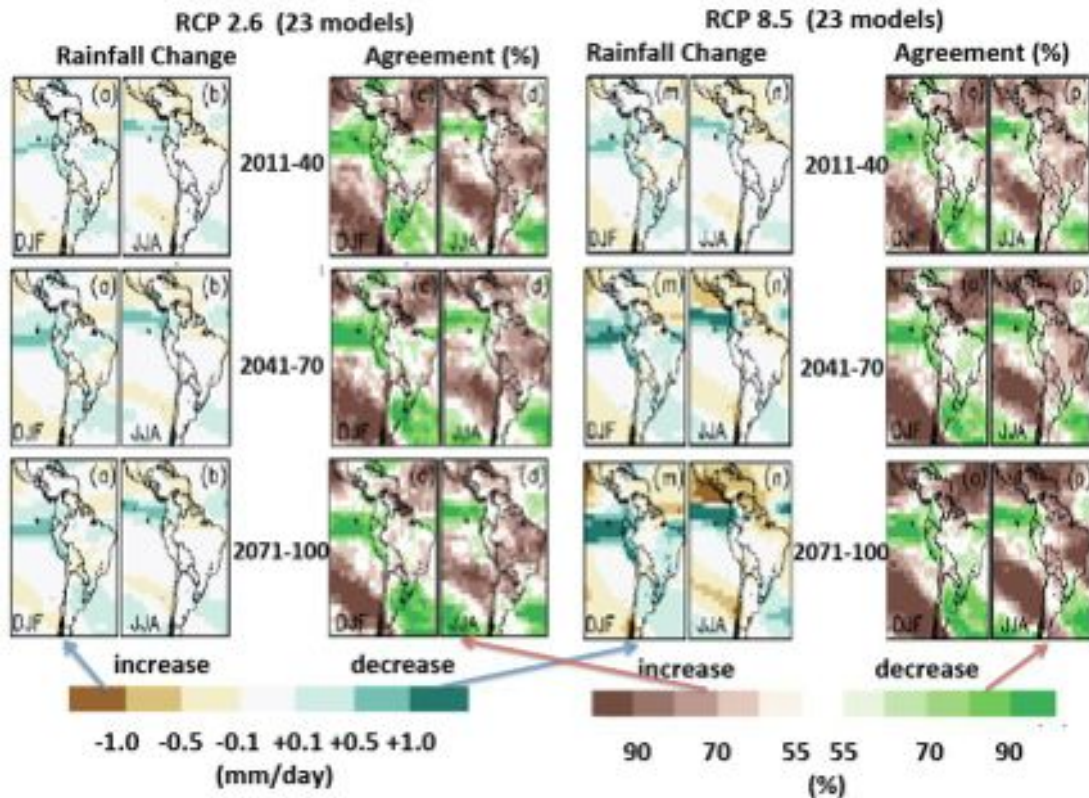


Figure 22. Seasonal (DJF and JJA) air temperature anomalies from the mean of 23 CMIP5 models for CA and SA for the RCP8.5 scenario for the short (2010-40), medium (2041-70) and long term (2071-2110) relative to 1961-90 (first and third columns). Maps of standard deviation are shown in second and fourth columns Units are in °C, and color scale is shown on the lower side of the panels. Arrows indicate the correspondence between the maps and the color for means and standard deviation.

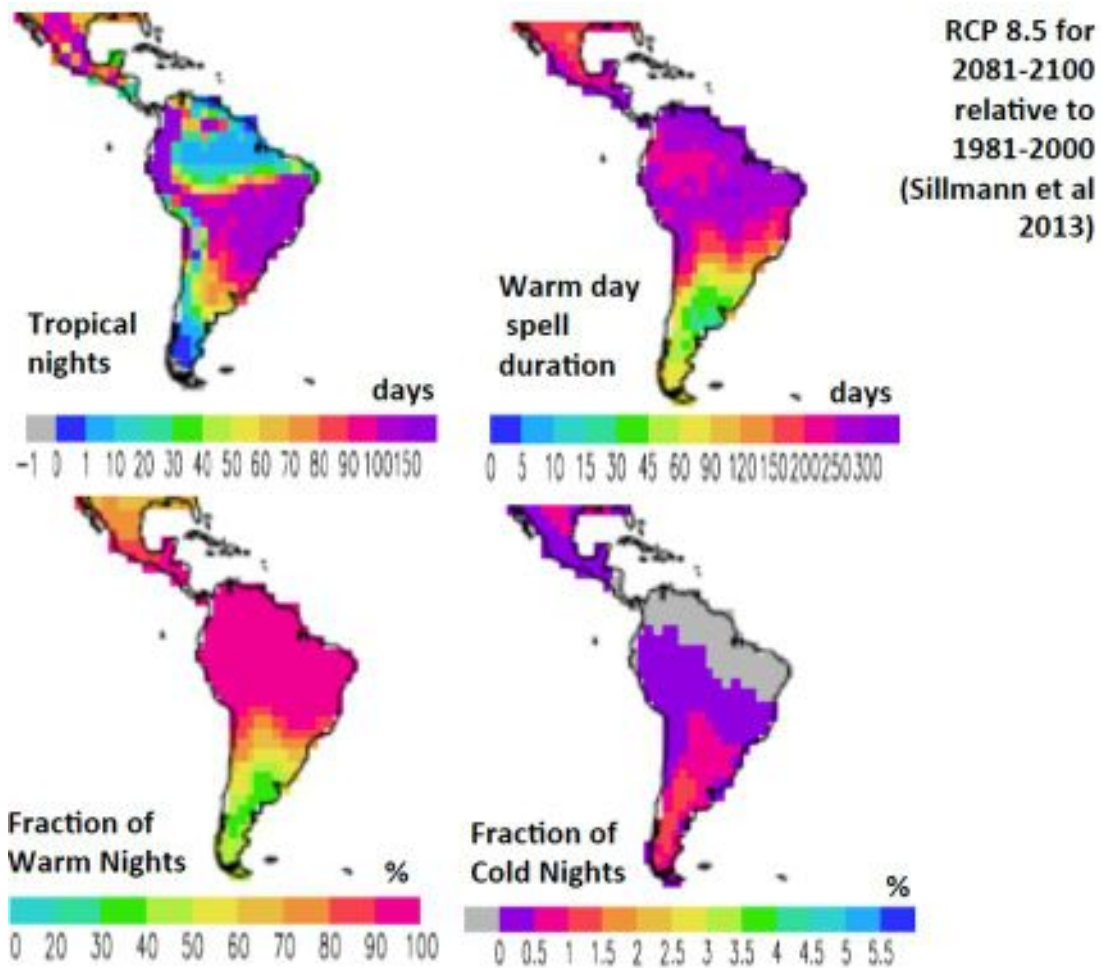
For rainfall changes (Figure 23) rainfall increases are indicated in southeastern South America and the Northwest coast of Peru and Ecuador, being more intense by 2071-2100 on the RCP8.5 for austral summer, and more than 80% of the models agree in those changes. On rainfall reduction during austral summer, 80% of the models agree with reduction in Southern Chile. In boreal summer, more than 80% of the models agree with rainfall reductions in CA and northern South America, and also over Amazonia and Northeast Brazil. This is relevant in Southern Amazonia since this implies the possibility of a late on set of the rainy season in that region. Regions such as parts of tropical and subtropical South America show uncertainties since less than 50% of the models agree on rainfall change from one direction to another.

Figure 23. Seasonal (DJF and JJA) rainfall anomalies from the mean of 23 CMIP5 models for CA and SA for the RCP8.5 scenario for the short (2010-40), medium (2041-70) and long term (2071-2110) relative to 1961-90 (first and third columns). Maps of agreement between models for increase or decrease of precipitation. Units are in mm/day for rainfall and in n% for the model agreement. Color scale is shown on the lower side of the panels. Arrows indicate the correspondence between the maps and the color for means and model agreements.



As in the case of CMIP3 models, some indices of extreme precipitation and temperature have been calculated and show in Figures 24 and 25 for 2081-2100 for the RCP8.5. The ensemble of CMIP5 model, as shown by Sillmann et al (2013), suggest an increase in the number of tropical nights in Southern Amazonia, Southeastern South America, and also over CA, and to a lesser degree in central Amazonia and Southern Chile. The duration of warm spells and the fraction of warm nights are projected to increase largely in CA and tropical SA and in to a lesser degree in Southeastern South America. The fraction of cold nights is projected to increase at a very low rate over subtropical SA and CA.

Figure 24. The multimodel median of temporally averaged changes in tropical nights (days), fraction of warm nights (%), warm day spell duration (days), and fraction of cold nights (%), over the period 2081– 2100 relative to 1981-2000, for RCP8.5. All changes are significant at the 5% significance level. Stippling indicates grid points with changes that are not significant at the 5% significance level (modified from Sillman et al. 2013).



Projections for extremes of precipitation show an increase in the frequency of dry days, particularly over Eastern Amazonia-Northeast Brazil and over the South American monsoon region, and also in CA and the North American monsoon region. The most significant changes are detected over western Amazonia (reduction) and Southeastern South America (increase). In all of Central and South America there is a projected tendency for increases of very high precipitation on the 95th percentile, while the frequency of total wet day precipitation and the fraction of days with precipitation above 10 mm/day shows a slight decrease.

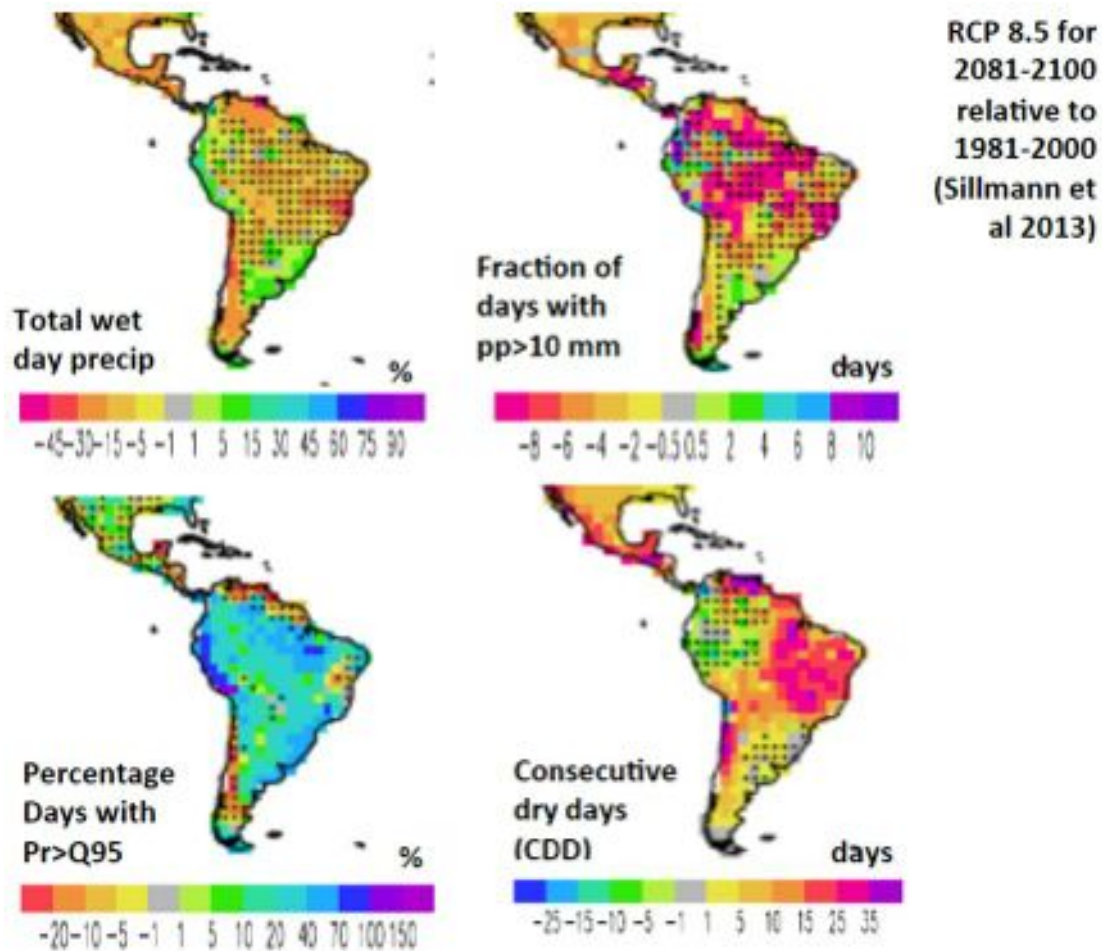


Figure 25. Same as Figure 24, but for total wet day precipitation (%), fraction of days with  $pp > 10$  mm (days), percentage of days with  $Pr > PQ85$  and consecutive dry days. All changes are significant at the 5% significance level. Stippling indicates grid points with changes that are not significant at the 5% significance level (modified from Sillman et al. 2013).

Figures 21 and 23 suggest that in regions such as CA increases in consecutive dry days coincide with decreases in heavy precipitation days and maximum consecutive 5-day precipitation, which indicates future intensification of dry conditions. Particularly for the precipitation-based indices, there can be a wide disagreement about the sign of change between the models in some regions. Changes in temperature and precipitation indices are most pronounced under RCP8.5, with projected changes exceeding those discussed in previous studies based on SRES scenarios from the CMIP3 models.

None of the SRES simulations considered in this study or previous studies (i.e., B1, A1B, and A2) project changes in temperature and precipitation extremes as pronounced as in RCP8.5, which has the largest radiative forcing amongst the scenarios we considered. If greenhouse gas emissions continue to rise at the current pace or even accelerate, very large changes in extremes are to be expected as projected in RCP8.5 projections.

## 5. High-resolution climate change projections for CA and SA: Downscaling of the HAdGEM2 ES using the Eta regional model

In the following we describe the global and regional models, scenarios used and other details for the generation of high-resolution future climate change scenarios for CA and SA.

### 5.1 Models used for the climate downscaling (HadGEM2 ES and Eta)

#### 5.1.1 HadGEM2 ES global model

The HadGEM2 physical model includes improvements designed to address specific systematic errors encountered in the previous climate configuration, HadGEM1. The HadGEM2 family of model configurations includes atmosphere, ocean, and sea-ice components, with and without a vertical extension in the atmosphere model to include a well-resolved stratosphere, and Earth System (ES) components including the terrestrial and oceanic carbon cycle and atmospheric chemistry. Specific systematic errors encountered in HadGEM1 include Northern Hemisphere continental temperature biases, tropical sea surface temperature biases, and poor variability. Targeting these biases was crucial for the Earth System configuration to represent important biogeochemical climate feedbacks.

Much of the work done to improve the atmosphere and ocean components of this HadGEM2 focused on addressing systematic errors in HadGEM1 (Martin et al 2011; Johns et al 2006) that would otherwise lead to unrealistic simulations of Earth-system feedbacks (e.g. regional errors in land surface temperature and humidity that would have led to biases in modelled vegetation and unrealistic representation of the carbon cycle). Another area of interest was the representation of aerosols. Aerosol optical depths are underestimated globally in HadGEM1 compared with satellite observations and surface measurements (Collins et al 2008) and the error in clear sky radiative fluxes is largely due to the lack of representation of natural (biogenic) continental aerosols and mineral dust aerosols in HadGEM1 (Bodas-Salcedo et al 2008).

The HadGEM2 ES model family comprises of configurations made by combining model components, which facilitate the representation of many different processes within the climate system, as illustrated in Martin et al (2011). These combinations have different levels of complexity for application to a wide range of science questions, although clearly many of the processes are interdependent.

The HadGEM2-ES is a coupled AOGCM developed by the UK Met Office (Collins et al 2011, Jones et al 2011), with an atmospheric resolution of N96 ( $1.875^\circ \times 1.25^\circ$ ) with 38 vertical levels and an ocean resolution of  $1^\circ$  (increasing to  $1/3^\circ$  at the equator) and 40 vertical levels. HadGEM2-ES also represents interactive land and ocean carbon cycles and dynamic vegetation with an option to prescribe either atmospheric CO<sub>2</sub> concentrations or to prescribe anthropogenic CO<sub>2</sub> emissions and simulate CO<sub>2</sub> concentrations. An interactive tropospheric chemistry scheme is also included, which simulates the evolution of atmospheric composition and interactions with atmospheric aerosols. The model time step is 30 min (atmosphere and land) and 1 h (ocean). For our purposes the HadGEM2-ES was run as the “emission-driven” RCP experiments used for CMIP5. The RCP used was the RCP4.5 (Clarke et al 2007; Smith and Wigley 2006), corresponding to a medium emission scenario, comparable to CMIP3 A1B emission scenario. This prescribed CO<sub>2</sub> concentration is then passed to



the model's radiation scheme, and constitutes a boundary condition for the terrestrial and ocean carbon cycle. The oceanic partial pressure of CO<sub>2</sub>, pCO<sub>2</sub>, is always simulated prognostically from this, i.e. it is not itself prescribed. The CO<sub>2</sub> concentrations used were taken from the CMIP5 dataset. See details in Jones et al (2011) and Martin et al (2011). For the downscaling of the HadGEM2 ES we used the RCP 4.5, for the present (1961-90) and the future (2010-2100), for one model realization.

### 5.1.2 Eta regional model

The Brazilian Center for Weather Forecasts and Climate Studies (CPTEC) has used the Eta Model operationally since 1996 to provide weather forecasts over South America. Due to the characteristics of the vertical coordinate, the Eta- model is appropriate in regions containing steep orography such as the Andes Cordillera. Chou et al (2000) did one of the first experiments with long-term climate prediction for South America, with 1 month of continuous integration of the Eta regional model. Chou et al (2000) tested the Eta Model with different lateral boundary conditions, initial conditions and lower boundary conditions, through sea surface temperature, and showed that the lateral boundary conditions exerted the major control on the simulations. This regional model has been used to investigate the predictability of precipitation at different time scales—seasonal, monthly and weekly over South America (Chou et al 2005). Comparison of the Eta seasonal forecasts with the CPTEC GCM and observed climatologies shows that dynamical downscaling through the regional model provides considerable improvement and additional useful information over the driver model.

Various papers have assessed simulations of present time climatology (1961–90) of SA from Eta regional model projections (Pisnichenko and Tarasova 2009, Pesquero et al 2009). Dynamical downscaling experiments for the purpose of constructing climate change scenarios in SA have started to become available for various emission scenarios and time-slices until the end of the 21st Century. These examples have used various regional models forced with the global future climate change scenarios as boundary conditions from various global climate models (Marengo et al 2009a, b; Nunez et al 2006; Alves and Marengo 2009, Solman et al 2007, Garreaud and Falvey 2008, Cabre et al 2010, Urrutia and Vuille 2009, Pesquero et al 2009).

Pisnichenko and Tarasova (2009) used a version of the Eta model for climate change studies (the so-called Eta-CCS) driven by the HadAM3P global model. Their results show precipitation fields with strong negative bias over a large part of South America during summer for present-climate simulations and weak precipitation activity along the Atlantic Intertropical Convergence Zone (ITCZ). Another version of the Eta model for decadal runs was developed by Pesquero et al (2009) and shows a considerable improvement in the representation of precipitation patterns in austral summer and winter. These results indicate that the Eta model provides added value in comparison to the HadAM3P (A2 and B2 scenarios) or HadCM3 global model (A1B scenario). Other articles on SA regional simulation of present climate include Rauscher et al (2006, 2007), Seth et al (2007), Solman et al (2007, 2013), Alves and Marengo (2009, 2011, 2013), Menendez et al (2010) and references quoted therein.

The regional climate will be simulated using the Eta regional model, which is derived from the Eta Model (Mesinger et al 1988) developed at Belgrade University and operationally implemented by the National Centers for Environmental Prediction (Black 1994). The Eta model was chosen because there are few existing investigations using the Eta Model for long integrations over SA and because the vertical coordinate system used in this model is recommended for use over SA due to the presence of the Andes range.

This model has been used in studies of seasonal forecasts over SA where the forecasts were improved with respect to the driver global model, which had a resolution of T62. The model is established with 38 vertical levels with the top of the model at 25 hPa and uses the eta vertical coordinate (Mesinger 1984). The treatment of turbulence is based on the Mellor–Yamada level 2.5 procedure. The radiation package was developed by the Geophysical Fluid Dynamics Laboratory, with long wave and solar radiation parameterized according to Fels and Schwarzkopf (1975) and Lacis and Hansen (1974), respectively.

The Eta Model uses the Betts–Miller scheme modified by Janjic (Janjic 1994) to parameterize deep and shallow cumulus convection and cloud microphysics are parameterized using the Zhao scheme (Zhao et al 1997). The land-surface transfer processes are parameterized by the NOAH scheme (Ek et al 2003). A more detailed description of model dynamics can be found in Janjic (1979) and Mesinger et al (1988).

Some modifications were made to the Eta model adapting it for climate change runs by using SST derived from monthly means from the HadGEM2 ES. The model updates daily SST by means of linear interpolation. The major modification is the 360-day calendar year, which is necessary in order to use lateral boundary conditions from HadCM3. The inclusion of CO<sub>2</sub> in the Eta model was made possible through the work by Schwarzkopf (2005), who developed new vertical profiles of temperature compatible with 2×CO<sub>2</sub> and 4×CO<sub>2</sub>. Alterations in the Eta original code were made so the CO<sub>2</sub> concentration from the RCP4.5 scenario could vary in accordance with the HadGEM2 ES. At decadal time scales a linear interpolation was performed so annual values of CO<sub>2</sub> were generated avoiding sudden jumps. SST comes from HadGEM2-ES simulations.

## **5.2 Climate change projections for CA and SA derived from the Eta-HadGEM2-ES**

Before analysing the projections for the future derived from the Eta-HadGEM 2 ES for than RC4.5 scenario, we discuss the simulation of the present climate, comparing it with observations (from CRU) for the various regions shown in Figure 10.

### **5.2.1 Present climates**

Figure 26 shows the observed and simulated rainfall annual cycle for the various regions indicated in Figure 10. In all of them, the HadGEM2 ES global model and the Eta-HadGEM2 ES simulations show that the model captures the observed annual cycle, with some under or over estimation. Over northern Brazil and Amazonia the models underestimate rainfall during the peak of the rainy season in austral summer, while in the other regions the HadGEM2 ES model overestimates summertime rainfall. In all regions the Eta–HadGEM2 ES show values that are closer to the observations suggesting that the Eta models could correct the global model simulations.

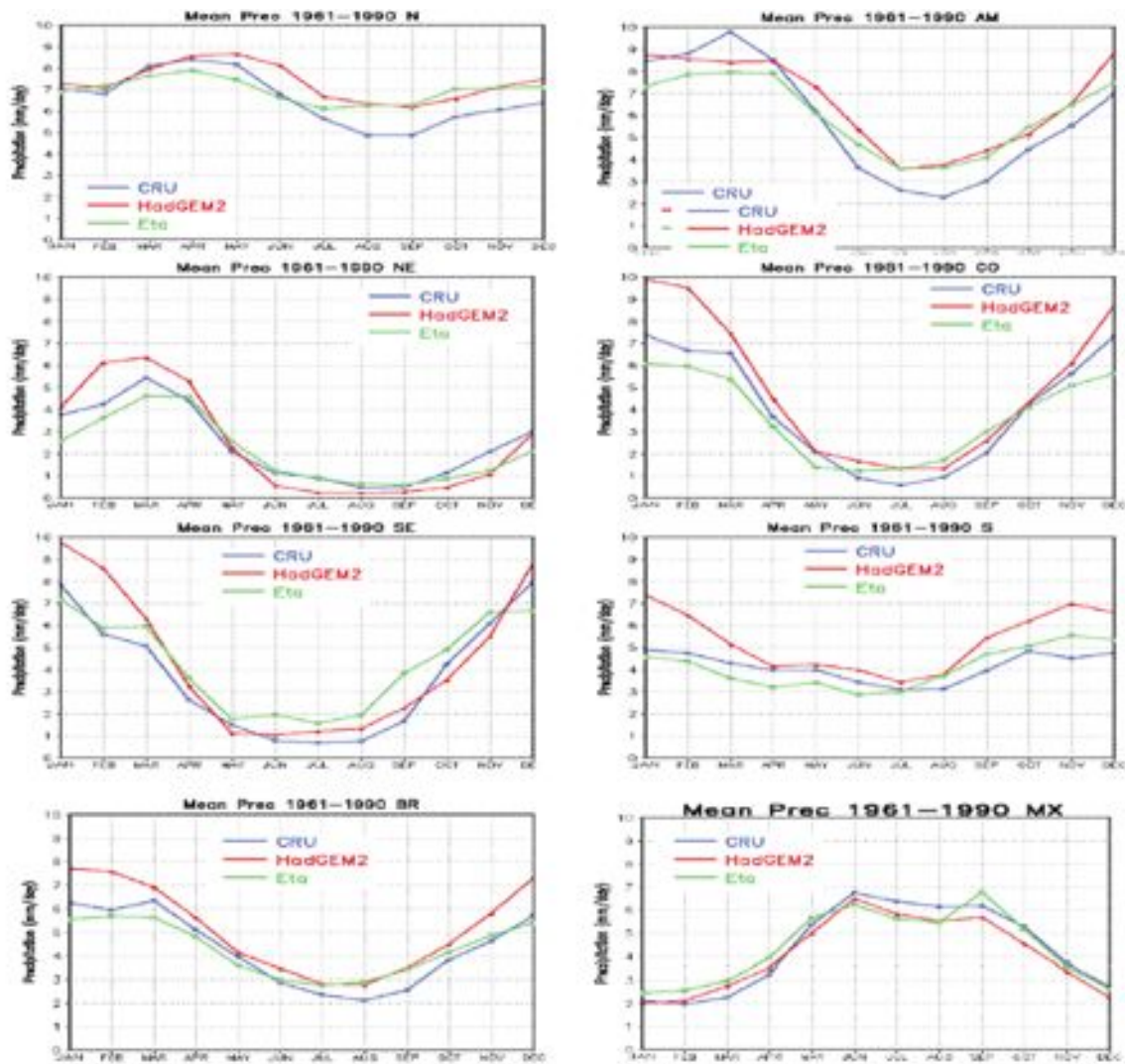


Figure 26. Comparisons between observed CRU rainfall and simulated rainfall from the Global HadGEM2 ES and from the downscaling of the HadGEM2 ES using the Eta regional model. Regions are shown in Figure 10.

As for air temperatures, Figure 27 shows the observed and simulated annual cycle for the various regions indicated in Figure 27. In all of them, the models underestimate the observed values, and the underestimation seems larger with the Eta regional model in northern Brazil and Amazonia (about 1oC lower than observed). In Northeast, West Central, Southern and Southeastern Brazil, the HadGEM2 underestimates temperature all year long, between 2-4oC. What is important to notice is that the model captures the timing of the observed annual cycle for both CA and SA.

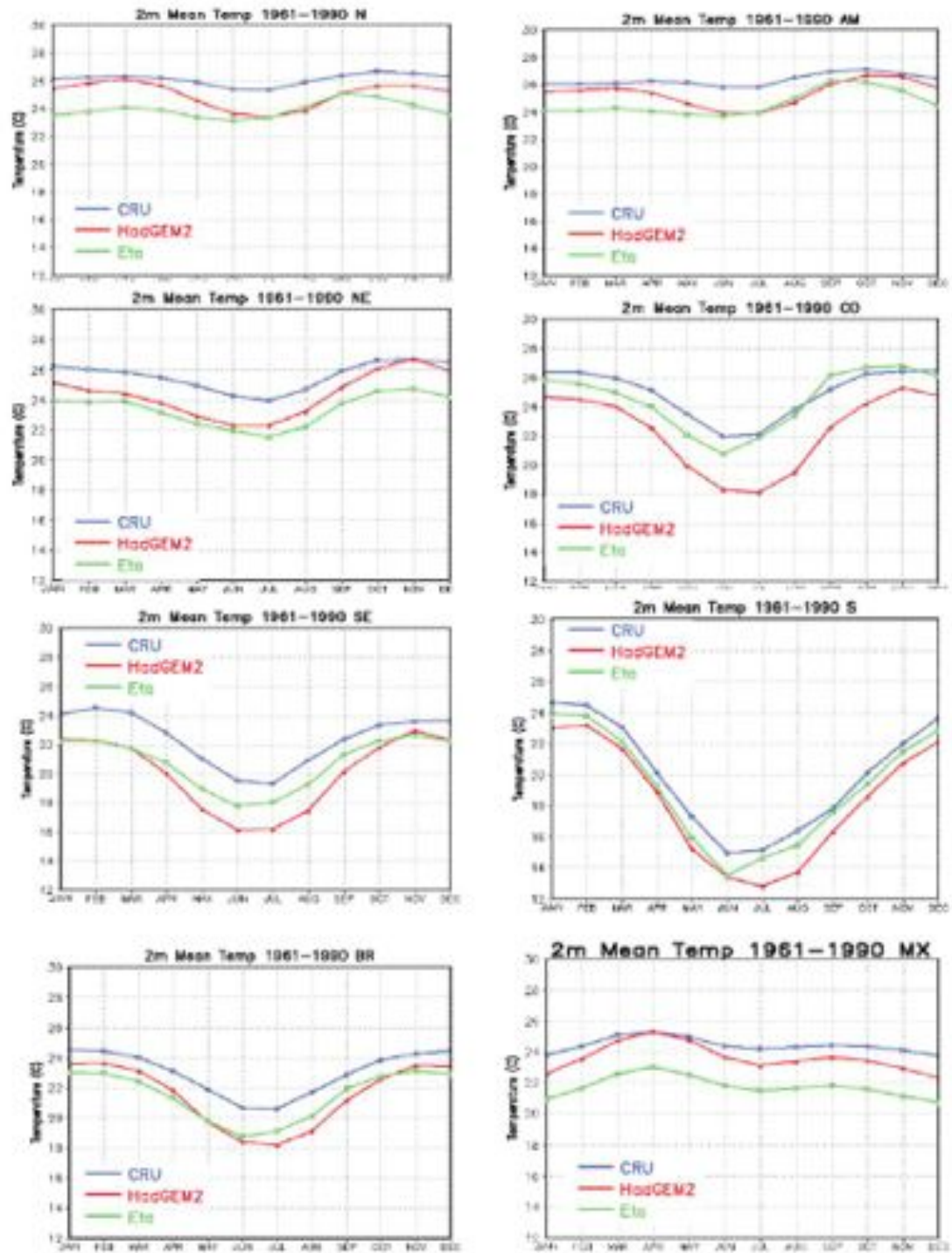


Figure 27. Comparisons between present time (1961-90) CRU and future (2011-2040, 2041-870 and 2071-2100) annual cycle of rainfall and simulated rainfall from the Global HadGEM2 ES and from the downscaling of the HadGEM2 ES using the Eta regional models. Regions are shown in Figure 10.

On rainfall distribution, the observations show the peak of the rainy season in SA and the winter time dry season in CA. For austral summer Figure 28 shows that in SA the presence of maximum rainfall over southeastern SA due to the presence of the South Atlantic Convergence Zone SACZ on the South American Monsoon region (SAMS), and the upward lifting of the Bolivian Andes of the moist winds coming from the Amazon region transported by the south American Low Level Jet East of the Andes (SALLJ). Both the HadGEM2 ES global model and the Eta-HadGEM2 ES simulations depict the dry season accurately in CA, as well as the Intertropical Convergence ITCZ in the tropical Pacific and Atlantic oceans. While both models depict observed rainfall well over western Amazonia, they underestimate rainfall along the SACZ, and the HadGEM2 ES shows a dry corridor in the coast of Northeast Brazil that seems to be corrected by the Eta-HadGEM ES.

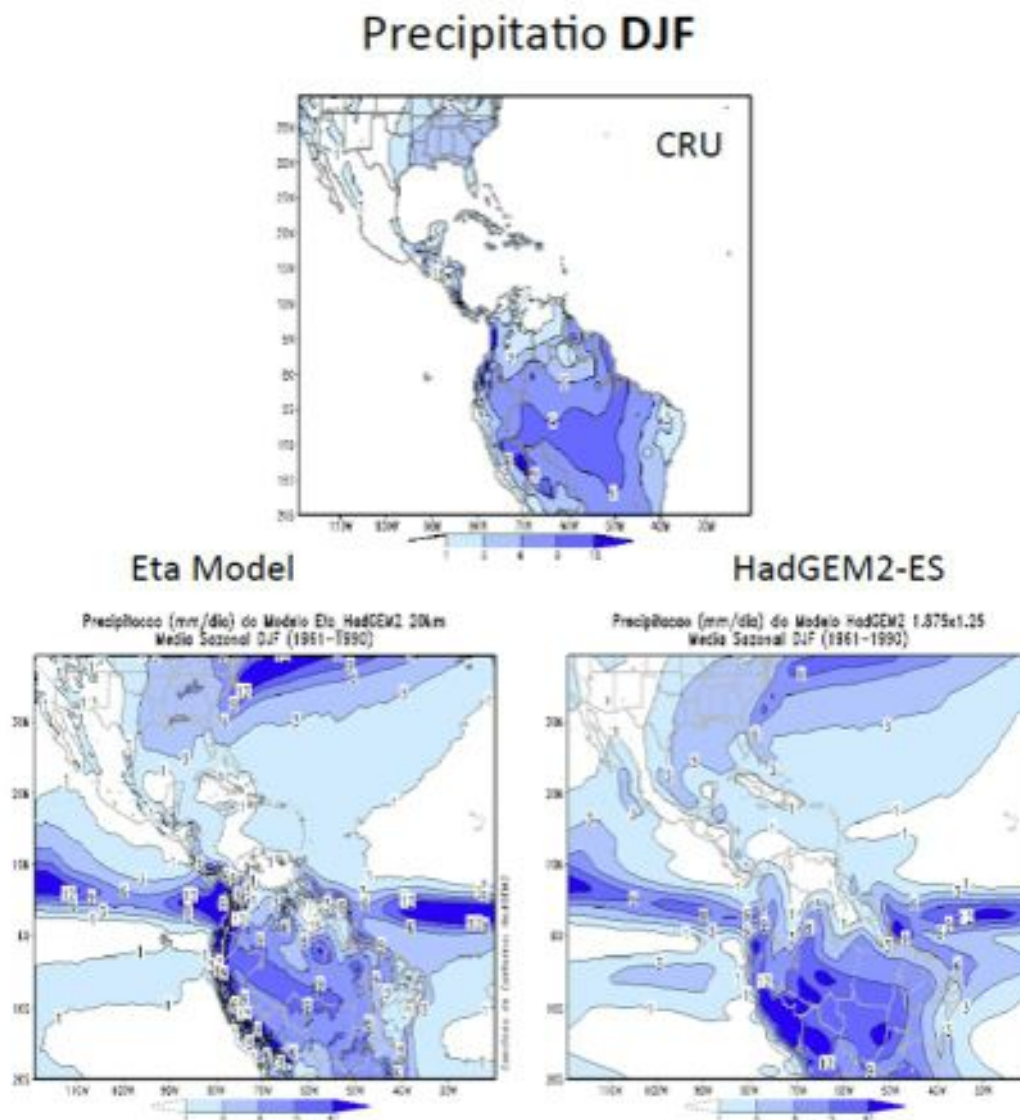


Figure 28. Comparisons between observed CRU rainfall and simulated rainfall from the Global HadGEM2 ES and from the downscaling of the HadGEM2 ES using the Eta regional models for both CA and SA, during austral summer DJF.

For austral winter (Figure 29) shows the dry season in most of SA South of the equator, and the wet season in Northern SA and CA, where the NAMS is active. Both the Eta-HadGEM2 ES and the HadGEM2 ES accurately depict maximum rainfall over northern SA and over CA, and the Eta-HadGEM2 ES improved the rainfall amount over CA. In both the ITC shows its northward position during austral winter.

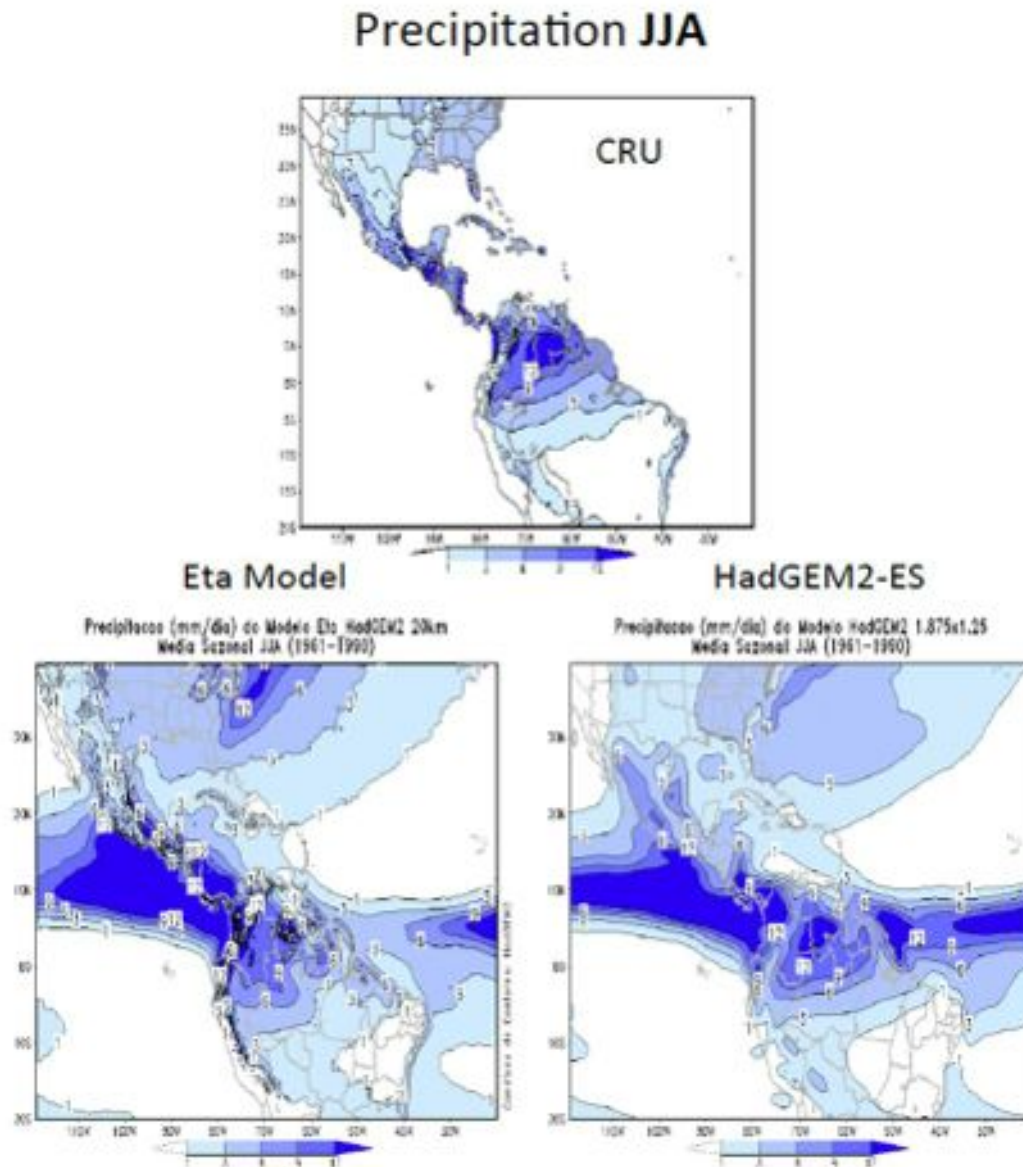


Figure 29. Comparisons between observed CRU rainfall and simulated rainfall from the Global HadGEM2 ES and from the downscaling of the HadGEM2 ES using the Eta regional models for both CA and SA, during austral winter (boreal summer) JJA.

For the summer time air temperature fields, Figure 30 shows the observed mean around 26oC along tropical SA, and colder temperatures around 18-21oC along the west coast of SA. Both model simulations show the cold bias around 1-2oC over tropical SA.

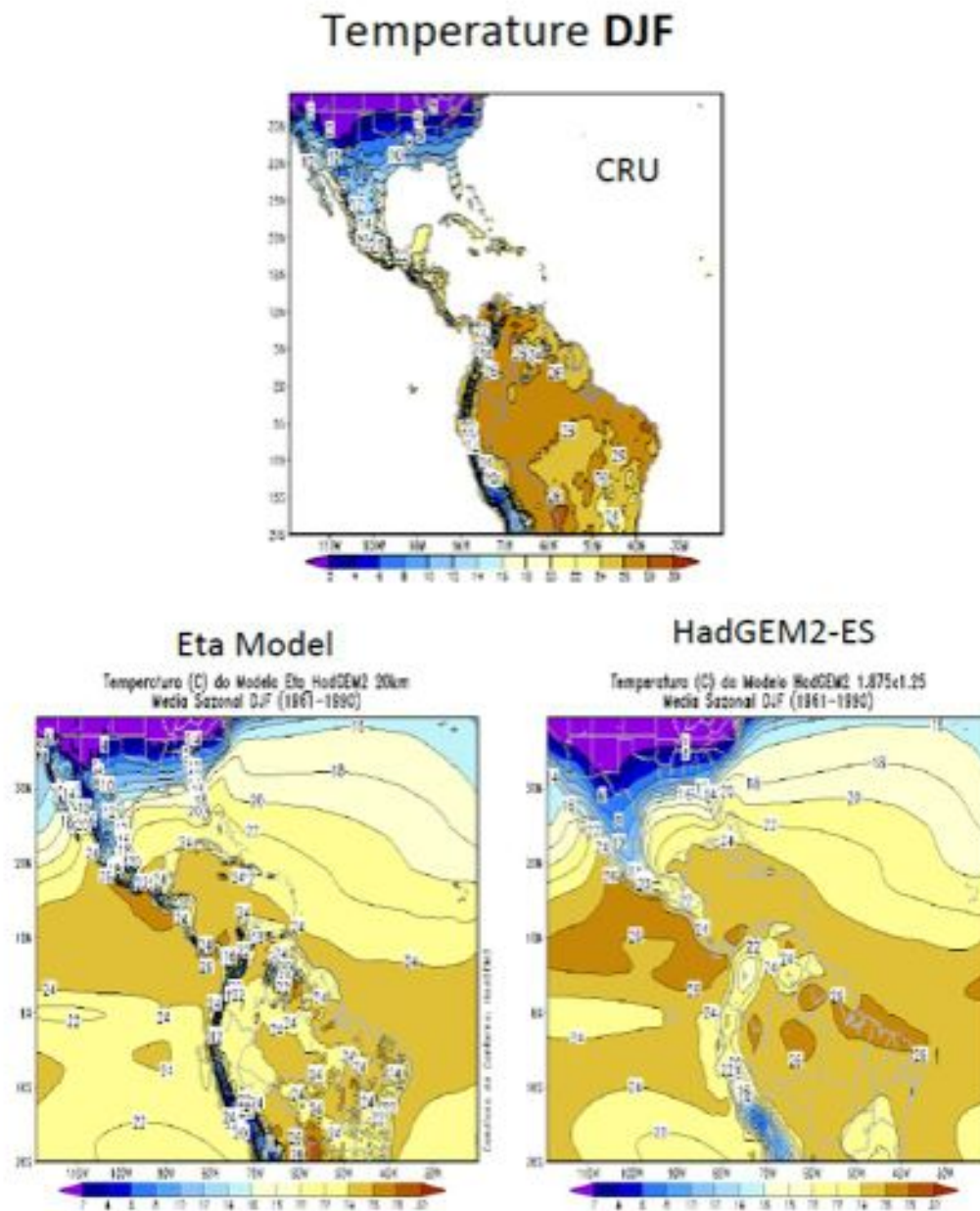


Figure 30. Comparisons between observed CRU temperature and simulated temperature from the Global HadGEM2 ES and from the downscaling of the HadGEM2 ES using the Eta regional models for both CA and SA, during austral summer DJF.

During austral winter (Figure 31) the temperature underestimation remains for tropical SA while the Eta-HadGEM2 ES simulated a more accurate temperature for CA and the Andes, as compared to the HadGEM2 ES.

## Temperature JJA

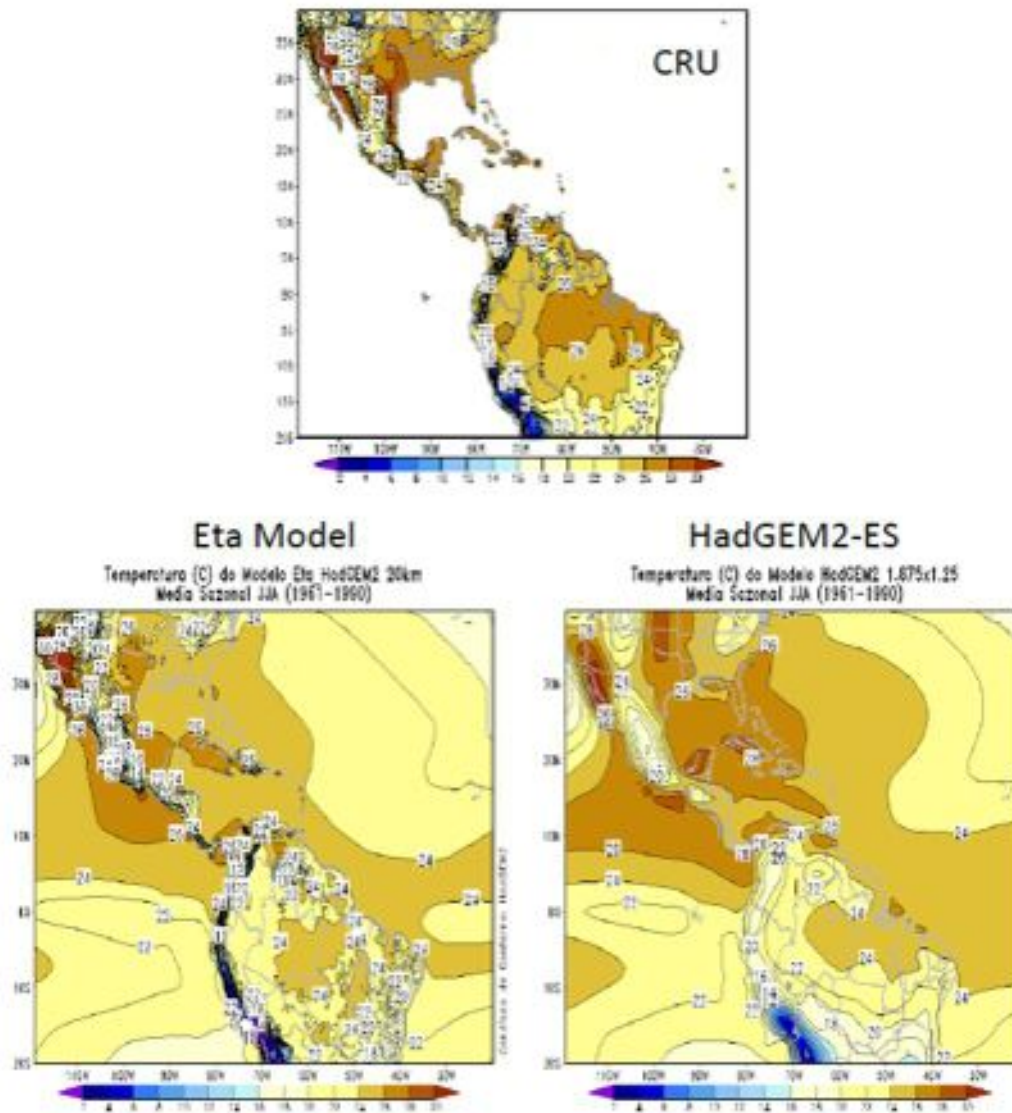


Figure 31. Comparisons between observed CRU temperature and simulated rainfall from the Global HadGEM2 ES and from the downscaling of the HadGEM2 ES using the Eta regional models for both CA and SA, during austral winter JJA.

### 5.2.2 Future climates

For some regions in Central and South America, the annual cycle of rainfall and temperature are shown in Figures 32 and 33. The present (1961-90) and three time slices in the future: 2010-40, 2041-70 and 2071-2100, are shown for rainfall (Figure 32) and mean temperature (Figure 32). In Mexico and CA, the projections show a reduction in rainfall at the peak of the rainy season, from May to October, with a possible extension of the dry season. These reductions are higher by the end of the century. For the Amazon region, Northeast Brazil and Northern South America, the models project rainfall reductions all year long, both during the summer and also in the winter season. Larger reductions are detected by the end of the century.



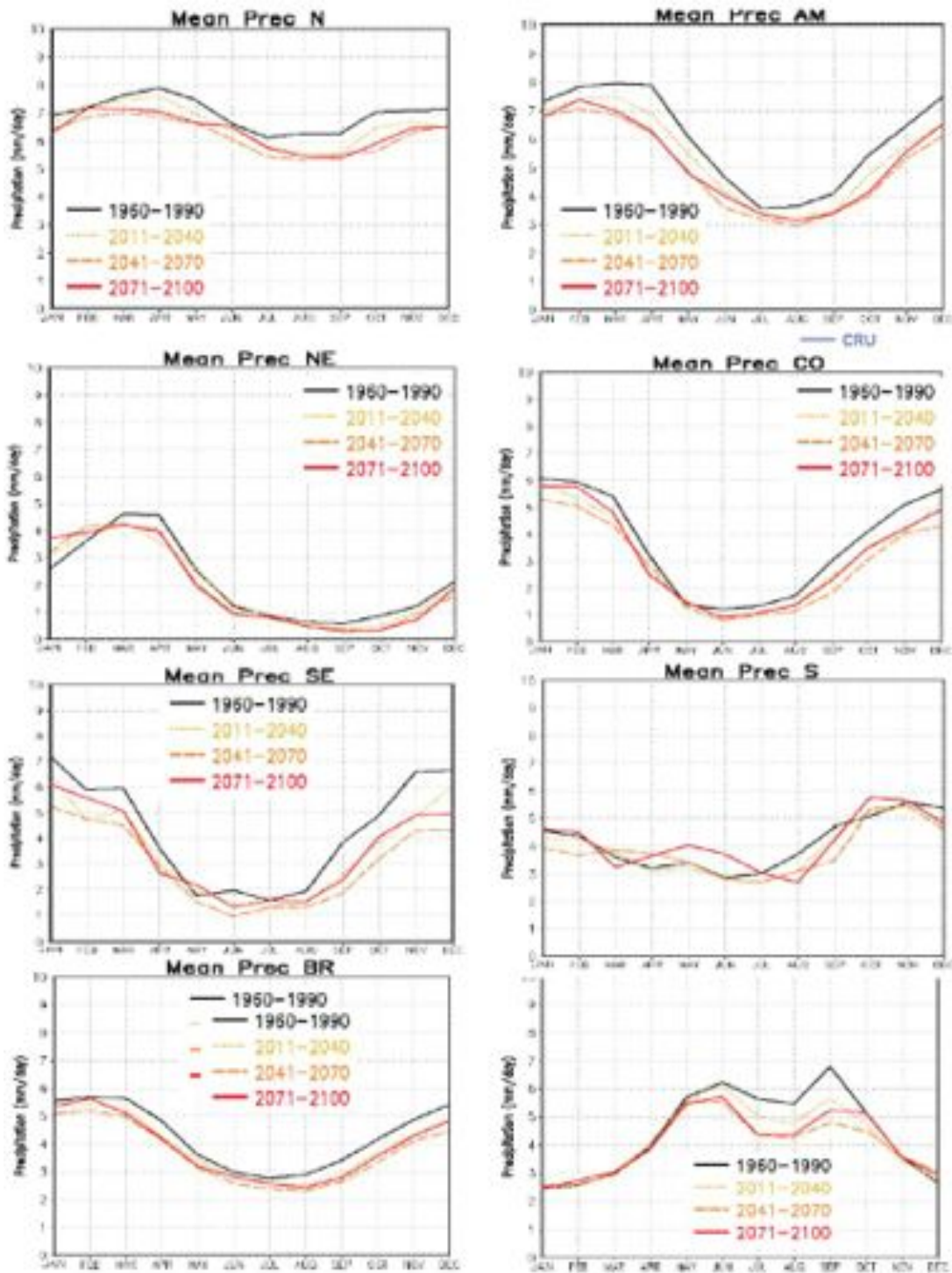


Figure 32. Comparisons between present time 1961-90 CRU rainfall and projections from the downscaling of the HadGEM2 ES using the Eta regional models for 2011-40, 2041-70 and 2071-2100, for the RCP4.5 scenario. Regions are shown in Figure 10.

Air temperature, for all regions, is predicted to increase all year long, reaching up to 1-2oC by 2010-40 and up to 2-4oC by 2100 in SA. The combination of higher air temperatures and longer dry seasons suggests strong impacts on the North and South American monsoon systems; pointing to

water availability problems in regions such as Amazonia and Northeast Brazil, which would increase the risk of desertification in semiarid lands, particularly in the second half of the XXI Century.

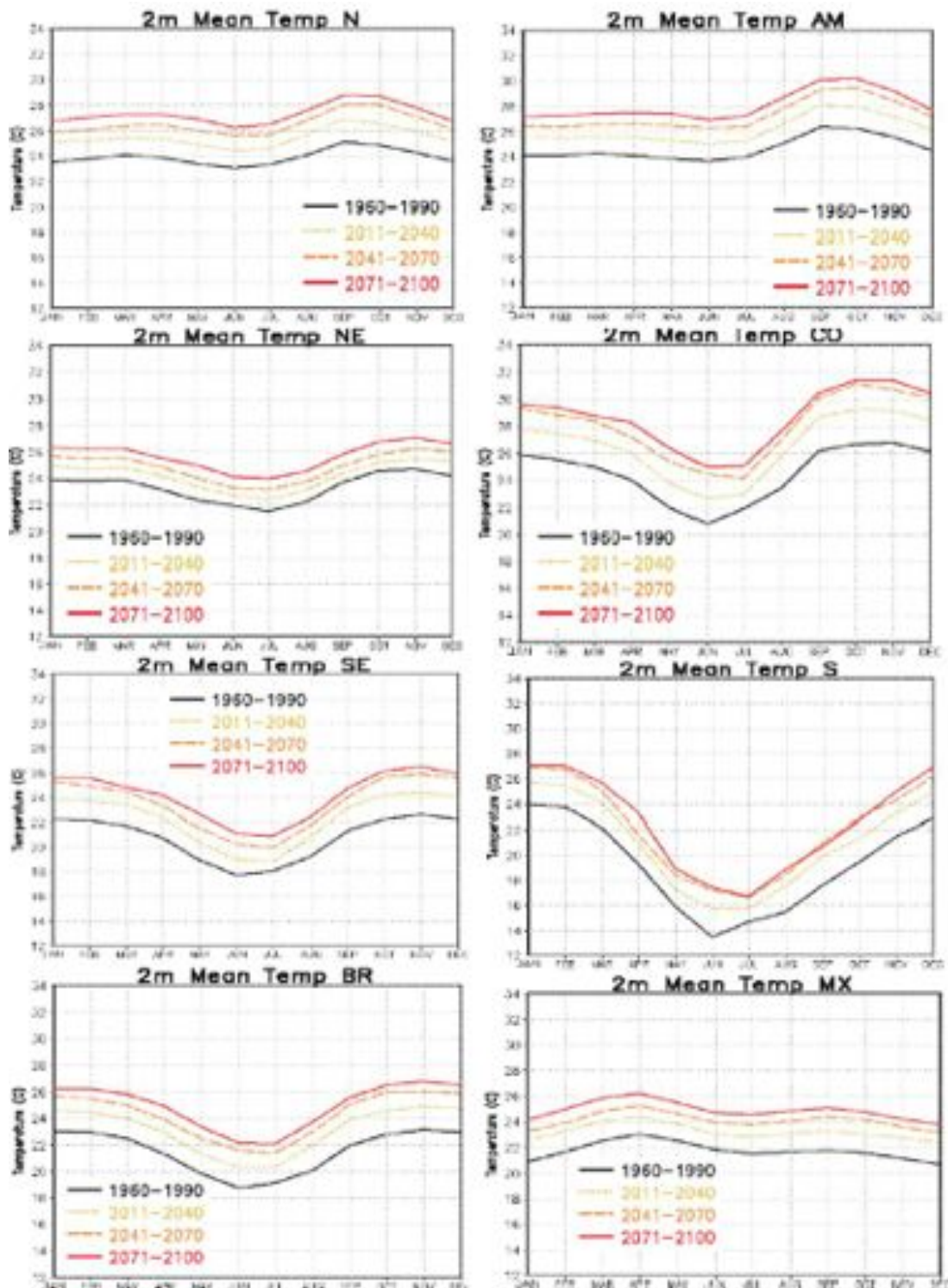


Figure 33. Comparisons between present time 1961-90 CRU temperature and projections from the from the downscaling of the HadGEM2 ES using the Eta regional models for 2011-40, 2041-70 and 2071-2100, for the RCP4.5 scenario. Regions are shown in Figure 10.

Figures 34, 35, and 36 show rainfall projections from the Eta-HadGEM2 ES for the RCP4.5 scenario at annual, summer, and winter seasons until 2100. At annual time scales, rainfall reductions are projected for CA, southern and eastern Amazonia and the coast of Northern South America, while rainfall increases are projected for the equatorial Pacific region as well as over the northern coast of Peru and Ecuador. The changes are more intense by 2071-2100. In DJF, during austral summer, rainfall reductions are projected in southern and eastern Amazonia, Pantanal and on the northern coast of South America, particularly in 2041-70, and increases in the northwest coast Peru and Ecuador and on the northern coast of Northeast Brazil. In JJA, the boreal summer, large reductions of rainfall are projected for all of CA and central-South of Mexico and on the Caribbean coast of SA.

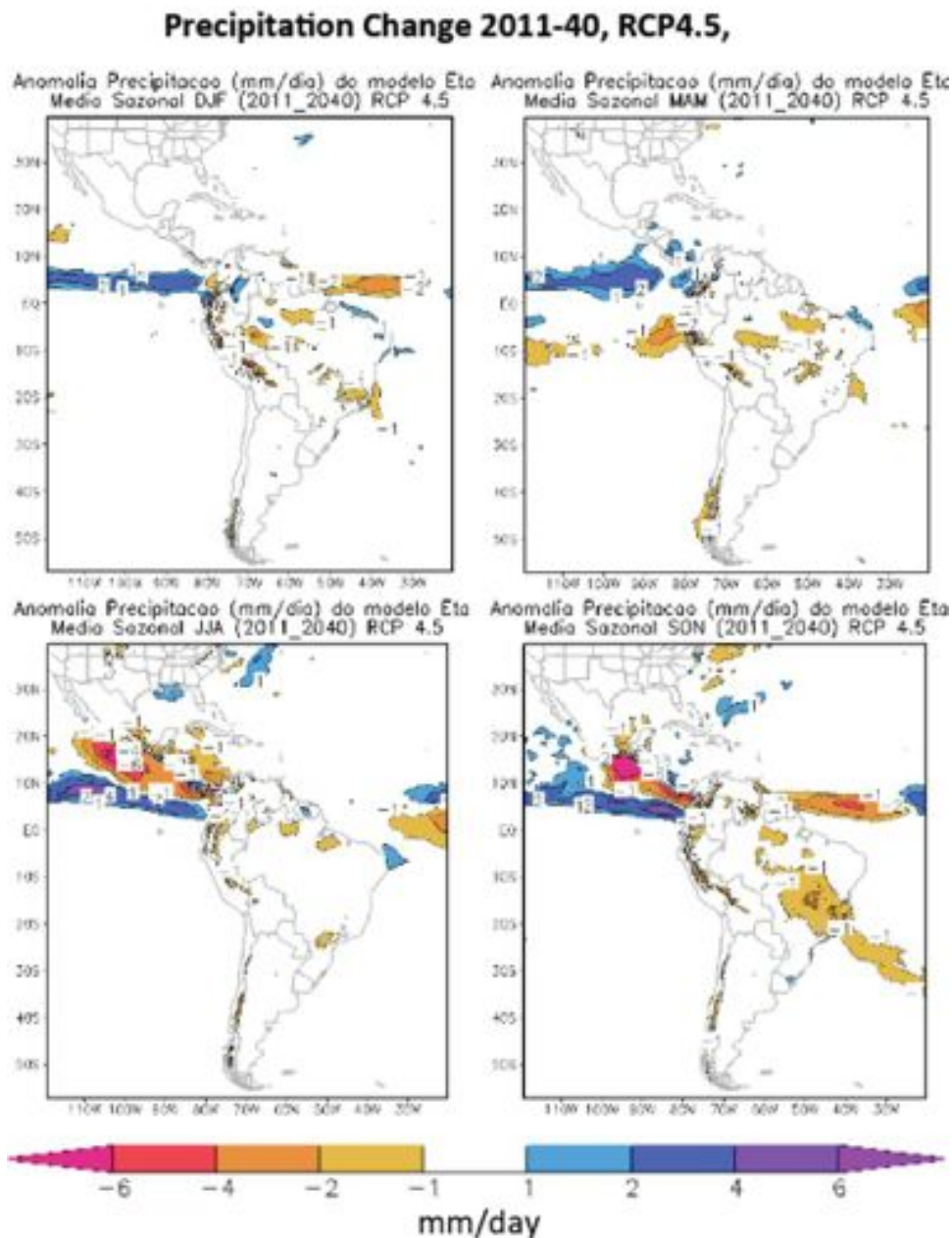


Figure 34. Seasonal rainfall anomalies for DJF, MAM, JJA and SON for 2011-40 relative to 1961-90, for the RCP8.5 derived from the downscaling of the HadGEM2 ES using the Eta regional models for both CA and SA. Units are in mm/day.

## Precipitation Change 2041-70, RCP4.5,

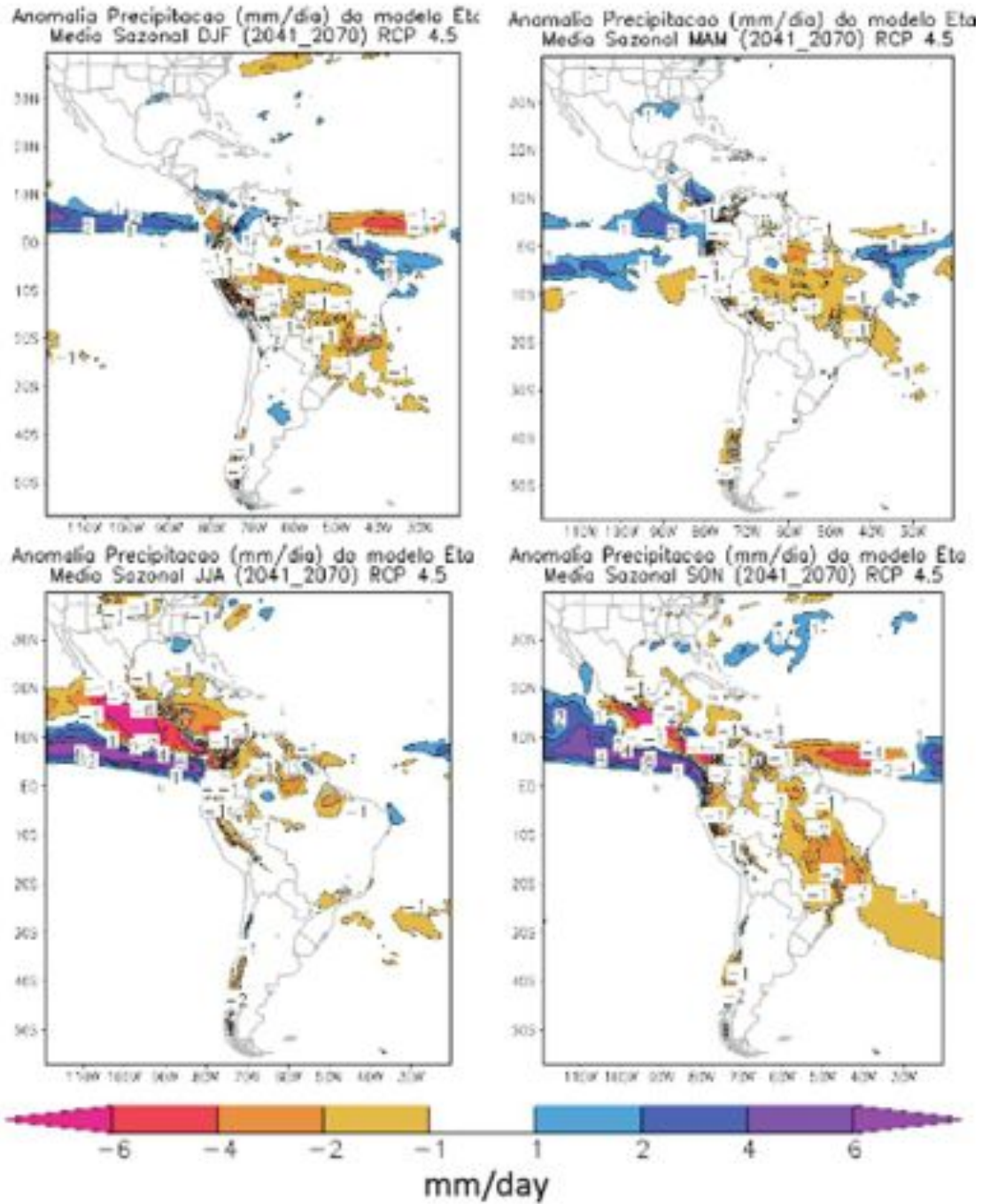


Figure 35. Seasonal rainfall anomalies for DJF, MAM, JJA and SON for 2041-70 relative to 1961-90, for the RCP8.5 derived from the downscaling of the HadGEM2 ES using the Eta regional models for both CA and SA. Units are in mm/day.

## Precipitation Change 2071-2100, RCP4.5,

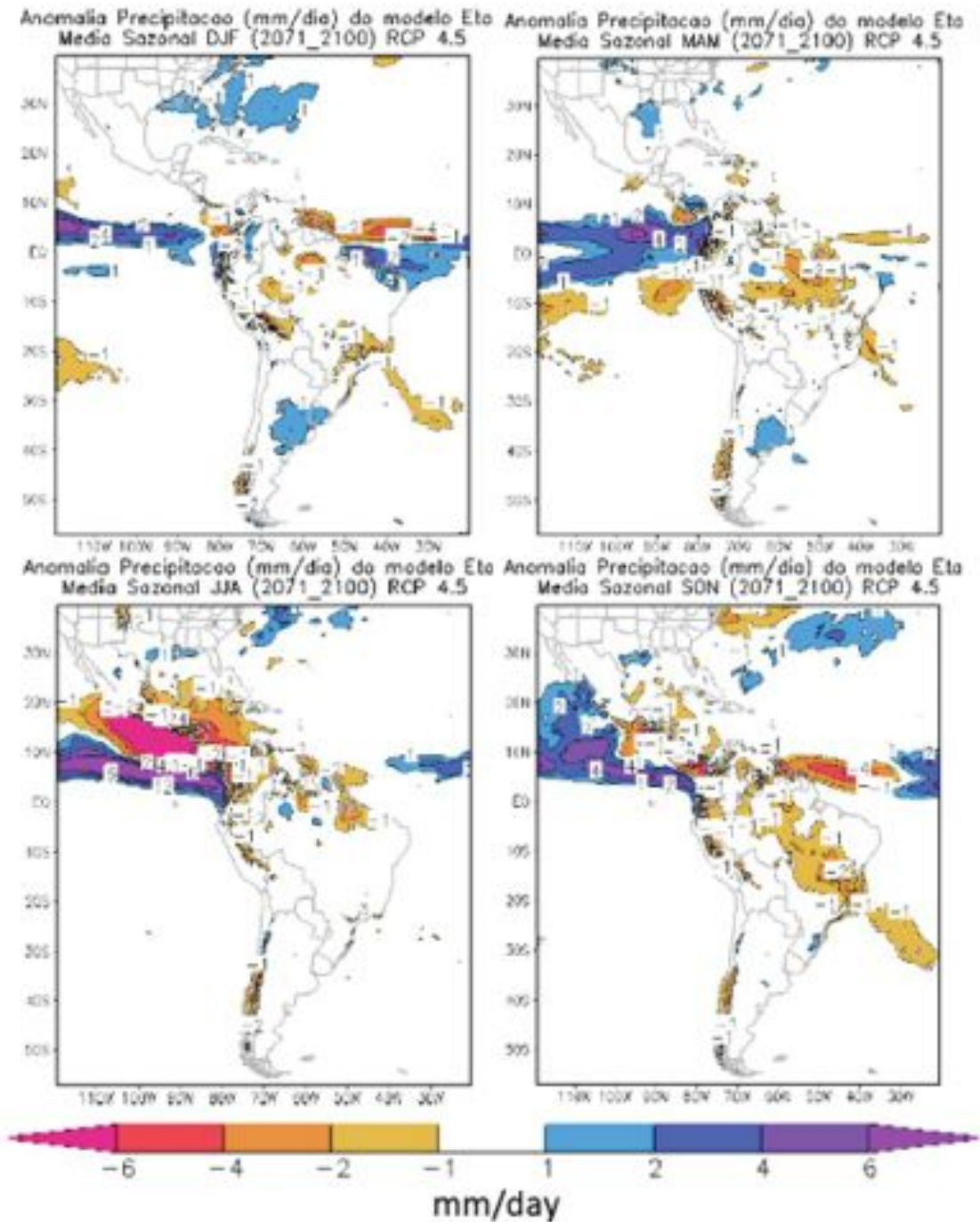


Figure 36. Seasonal rainfall anomalies for DJF, MAM, JJA and SON for 2071-2100 relative to 1961-90, for the RCP8.5 derived from the downscaling of the HadGEM2 ES using the Eta regional models for both CA and SA. Units are in mm/day.

Annual air temperature changes in 2010-40 show increases of 2oC in southern Amazonia a small warming of 1oC in all Central and South America (Figures 37, 38, 39). By 2041-70 the warming in southern Amazonia reaches 3-4oC and 2oC in the rest of the region, and by 2071-2100 warming in tropical SA reaches about 3-4oC and between 2-3oC in CA. The combination of higher temperatures and rainfall reductions in southern Amazonia and the SAMS region may imply an increase in water deficit in those regions. We have to remember that this region is extremely important because of soybean cultivation for agroindustry purposes, and the prospect of a longer dry season may have strong impacts on the regional economy, and in the long term on the GDP of the region and of Brazil. For CA, the rainfall reduction may be related to a decrease in the number of hurricanes in the future, but the uncertainties of such scenario are high. What can be said with lower confidence is a tendency for a weakening of the North American monsoon system may be seen in the future.

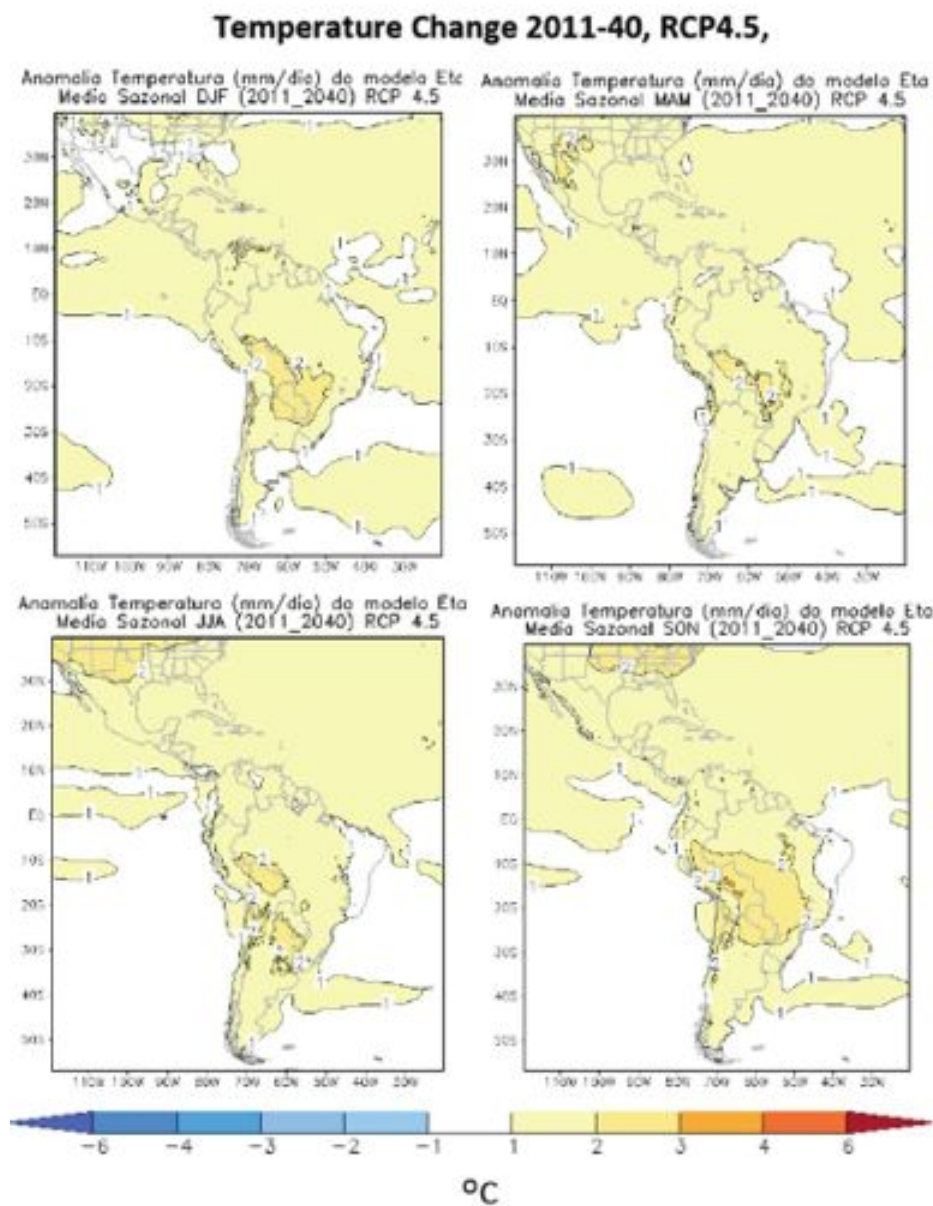


Figure 37. Seasonal temperature anomalies for DJF, MAM, JJA and SON for 2011-2040 relative to 1961-90, for the RCP8.5 derived from the downscaling of the HadGEM2 ES using the Eta regional models for both CA and SA. Units are in °C.

## Temperature Change 2041-70, RCP4.5,

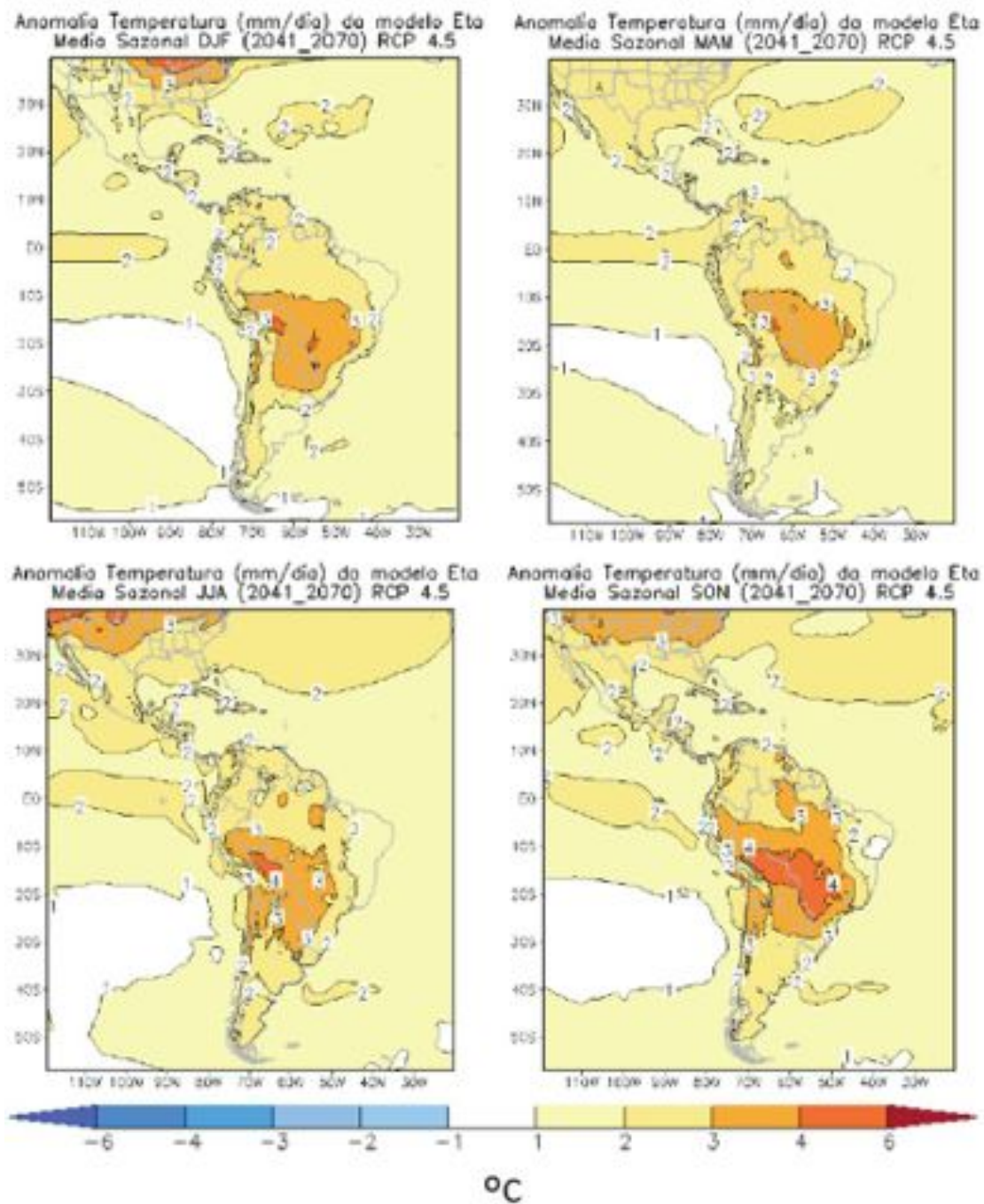


Figure 38. Seasonal temperature anomalies for DJF, MAM, JJA and SON for 2041-2070 relative to 1961-90, for the RCP8.5 derived from the downscaling of the HadGEM2 ES using the Eta regional models for both CA and SA. Units are in °C.

## Temperature Change 2071-2100, RCP4.5,

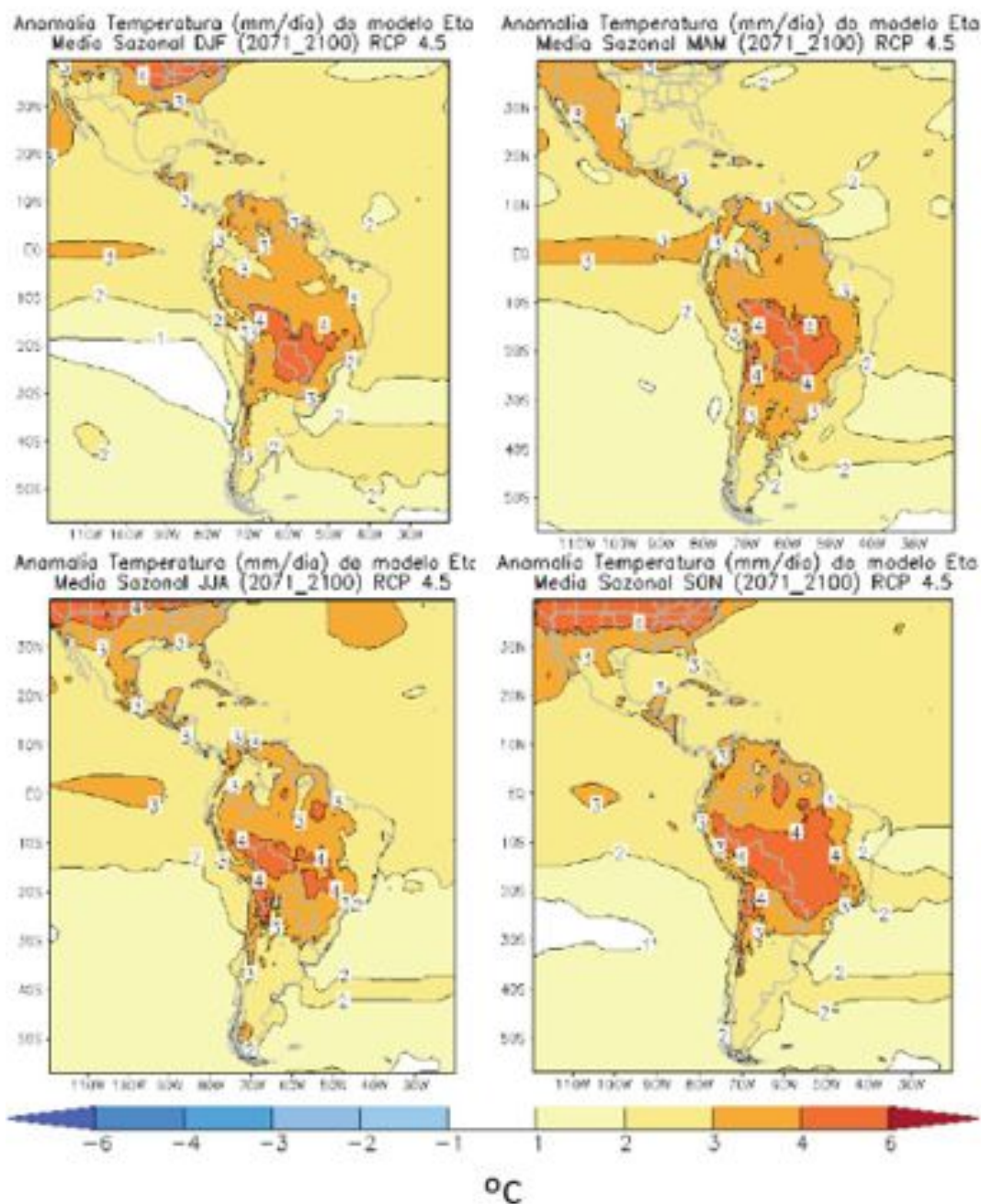


Figure 39. Seasonal temperature anomalies for DJF, MAM, JJA and SON for 2071-2100 relative to 1961-90, for the RCP4.5 derived from the downscaling of the HadGEM2 ES using the Eta regional models for both CA and SA. Units are in °C.

As shown in this section, and as summarized in Magrin et al (2014), analyses from global and regional models in tropical and subtropical SA show common patterns of projected climate in some sectors of the continent. Projections from CMIP3 regional and high resolution global models show by the end of the 21st century for the A2 emission scenario, a consistent pattern of increase of precipitation in SESA, Northwest of Peru and Ecuador and western Amazonia, while projecting decreases for northern SA, Eastern Amazonia, central eastern Brazil, NEB, the Altiplano and southern



Chile. For some regions, projections show mixed results in rainfall for the Amazonia and the SAMS region, suggesting a high level of uncertainty in the projections.

As for extremes, CMIP3 models and downscaling experiments project increases in dry spells for Eastern Amazonia and NEB, while rainfall extremes are projected to increase in SESA, in western Amazonia, Northwest Peru and Ecuador. Over southern Amazonia, northeastern Brazil, and eastern Amazonia, the maximum number of consecutive dry days tends to augment, suggesting a longer dry season. Increases in warm nights throughout SA are also projected by the end of the 21st century (Magrin et al 2014 and references quoted in). Shiogama et al (2011) suggest that although the CMIP3 ensemble mean assessment suggested wetting across most of SA, the observational constraints indicate a higher probability of drying in the eastern Amazon basin. The CMIP5 models project an even larger expansion of the monsoon regions in NAMS in future scenarios (Jones and Carvalho 2013; Kitoh et al 2013). A comparison from eight models from CMIP3 and CMIP5 identifies some improvements in the new generation models. For example, CMIP5 inter-model variability of temperature in summer was lower over northeastern Argentina, Paraguay and northern Brazil in the last decades of the 21st century, as compared to CMIP3. Although no major differences were observed in both precipitation datasets, CMIP5 intermodel variability was lower over northern and eastern Brazil in summer by 2100 (Blázquez and Nuñez 2013; Jones and Carvalho 2013).

The projections from the CMIP5 models at regional level for CA and SA (using the same regions from the IPCC SREX (IPCC SREX 2012) are shown in Figure 40, and update some of these previous projections based on SRES A2 and B2 emission scenarios from CMIP3. Figure 40 shows that in relation to the baseline period 1986-2005, for CA and northern South America-Amazonia, temperatures are projected to increase approximately by 0.6°C and 2°C for the RCP2.6 scenario, and by 3.6°C and 5.2°C for the RCP8.5 scenario. For the rest of SA, increases by about 0.6°C to 2°C are projected for the RCP4.5 and by about 2.2°C to 7°C for the RCP8.5 scenario. The observed records show increases of temperature from 1900 to 1986 by about 1°C. Precipitation levels in CA and northern South America-Amazonia is projected to vary between +10% to -25% (with large spread among models). For NEB, there is a spread among models between +30 to -30% making it difficult to identify projected rainfall change. This spread is much lower on the western coast of South America and SESA, where the spread is between +20 and -10% (Magrin et al 2014). Intermodel discrepancies are indicators of the spread among simulations and underline uncertainties in future climate projections.

Trends for rainfall and extremes for the 21st century are taken from models, found in many instances to perform an inadequate simulation of the region's 20th century climate. Given this fact, and considering the short periods being analyzed in this study, conclusions as to the possible direction and magnitude of trends in extreme events must be considered provisional. The high uncertainty in future mean conditions in some regions of CA and SA compounds this uncertainty. However, where the models show strong agreement in the direction of extreme events and the change in these events is consistent under forcing or correlates with trends in the mean conditions, some confidence in the projections can be taken. In areas which experience a drier climate, as in Northeast Brazil and northern Chile, precipitation is likely to become less consistent during the rainy season with relatively greater increases in minimum and maximum temperatures. The most intense precipitation events may increase, though this is less clear. In areas which become wetter, precipitation is likely to become more consistent, with heavier precipitation events and an increase in the magnitude of extreme events.

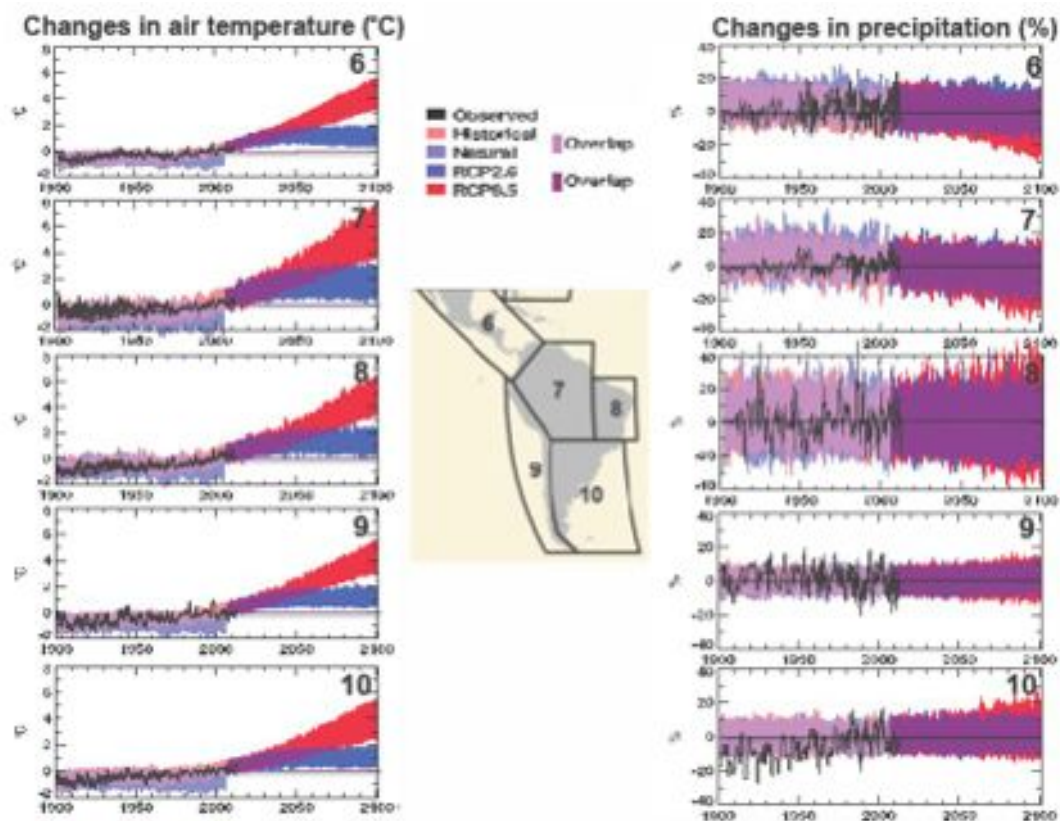


Figure 40: Observed and simulated variations in past and projected future annual average temperature over the Central and South American regions defined in IPCC (IPCC SREX 2012). Black lines show various estimates from observational measurements. Shading denotes the 5-95 percentile range of climate model simulations driven with "historical" changes in anthropogenic and natural drivers (63 simulations), historical changes in "natural" drivers only (34), the "RCP2.6" emissions scenario (63), and the "RCP8.5" (63). Data are anomalies from the 1986-2006 average of the individual observational data (for the observational time series) or of the corresponding historical all forcing simulations. Further details are given in Magrin et al (2014).

For the Amazon region, local deforestation rates or rising greenhouse gases globally drive changes in regional SA that might lead the Amazon rainforest into crossing a critical threshold at which a relatively small perturbation can qualitatively alter the state or development of a system (Cox et al 2000; Lenton et al 2008; Nobre and Borma 2009; Salazar et al 2007; Sampaio et al 2007). Various models project a risk of reduced rainfall, higher temperatures and water stress, which may lead to an abrupt and irreversible replacement of Amazon forests by savanna-like vegetation, under a high emission scenario (A2), from 2050-2060 to 2100 (Betts et al 2004; 2008; Cox et al 2004; Malhi et al 2008, 2009; Marengo et al 2011; Nobre and Borma 2009; Salazar et al 2007; Sampaio et al 2007; Sitch et al 2008). The possible 'savannization' or 'die-back' of the Amazon region would potentially have large-scale impacts on climate, biodiversity, and people in the region. The possibility of this die-back scenario occurring, however, is uncertain.

With such a high level of uncertainty, it is difficult to assess model ability to reproduce such scenarios. The spatial and temporal resolution of GCMs also means that they are unable to adequately resolve many of the most intense and short lived events. Furthermore, finding an anthropogenic "fingerprint" in patterns of change is more challenging at both a regional level and for climate extremes. To identify regional patterns in extremes and attribute them to global warming—a

necessary process if reliable projections of changes in regional extremes are to be produced—requires both of these challenges to be overcome.

This is the first time the Eta model has been extended to cover CA, and we are encouraged by the results, since projected tendencies from the Eta-HadGEM2 ES are consistent with those from the PRECIS and from the IPCC AR4 and AR5 models (Magrin et al 2014).

## 6. Impacts of climate change in agriculture in CA and SA

### 6.1 General overview

The IPCC WG2 ([www.ipcc.ch](http://www.ipcc.ch)) has summarized their major findings on impacts of climate variability and change on agriculture as:

- Climate-related impacts are already reducing crop yields in some parts of the world, a trend that is projected to continue as temperatures rise further. Crops affected include staples such as wheat, maize and rice. Climate change is projected to increase price volatility for agricultural commodities, and reduce food quality.
- Farmers can adapt to some changes, but there is a limit to what can be managed. Adaptive capacity is projected to be exceeded in regions closest to the equator if temperatures increase by 3°C or more. The agricultural industry's own interests are best served by ambitious approaches to adaptation and to cutting emissions.
- Greenhouse gas (GHG) emissions from agriculture comprised about 10–12% of man-made GHG emissions in 2010. The sector is the largest contributor of non-carbon dioxide (non-CO<sub>2</sub>) GHGs such as methane.
- Opportunities for mitigation include reducing emissions from land use change, land management and livestock management. Carbon can be captured and stored in soil and biomass. Economy-wide emissions from energy use can be reduced, under certain conditions, by replacing fossil fuels with biofuels.
- The potential for reducing GHG emissions from agriculture through changes in consumption could be substantially higher than technical mitigation options. Approaches include reducing food waste, changing diets towards less GHG-intensive food (e.g. substitution of animal products with plant-based food), and reducing overconsumption in regions where this is prevalent.

Agricultural productivity has increased in the last 50 years; nonetheless, this has not resulted in a reduction of poverty or hunger. The performance of agricultural systems is mixed in terms of production and sustainability, as well as environmental impacts.

The impacts of climate change will be numerous, affecting both food supply and demand. Droughts and water scarcity reduce overall food security and diminish dietary diversity. Infectious disease, which shares a vicious circle with malnutrition, will also increase as a result of climate change. Food systems at local levels in small farming communities will also be adversely affected, and overall, climate change could potentially slow down or reverse progress toward a world without hunger.

From production to prices, the threats climate change poses to our food supply are significant. Various studies show that climate change has already affected agriculture, such as the ongoing and historic droughts in [Brazil](#) and [California](#).

Major impacts are projected on water availability and supply, food security, and agricultural incomes, including shifts in production areas of food and non-food crops. The increasing frequency and intensity of climatic shocks will decrease poor producers' abilities to sell an agricultural surplus, meaning less reinvestment in their farms and other livelihood activities, and less ability to buy a nourishing diet. In total, research by Ericksen et al (2011) found that around 265 million people across Latin America, Southern and West Africa, Eastern China, Southeast Asia, and the northern part of south Asia are highly vulnerable to a 5% decrease in the length of the growing season and are likely to face declines in food security due to climate change over the next 40 years.

The following review has been taken from Chapter 27 on Central and South America of the IPCC AR5 WG2 (Magrin et al 2014). CA and SA agriculture is characterized by its heterogeneity and diversity of cultures and actors. Its heterogeneity is expressed by reference to agro ecological conditions, resource endowment and means of production and access to information and other services. The diversity of cultures and actors implies differences in the systems for producing, generating and using knowledge, resource management and stewardship, worldviews, survival strategies and forms of social organization. Agricultural productivity has increased in the last 50 years; nonetheless, there are 54 million people suffering malnutrition in the region, while the amount of food produced is three times the amount consumed.

Although agricultural knowledge, science and technology systems have been aimed at increasing agricultural production, factors such as lack of access to and distribution of foods and the low purchasing power of a large sector of the population have stood in the way of this translating into less hunger. Hunger and malnutrition in CA and SA are not the result of the inability to produce enough food; therefore, increasing production will not solve the problem of hunger and malnutrition in the region. To the contrary, one of the main problems in the rural sector has been food import from other countries where production is subsidized. This supply of food products drives down the price of local products and has a direct negative impact on the standard of living and the ability to make a living of the rural population.

The performance of agricultural systems is mixed in terms of production and sustainability, as well as environmental impacts. The traditional/indigenous system is characterized by diversity with variable levels of production (from high to very low). The conventional system has high levels of production and competitiveness in external markets, yet under current conditions is not sustainable or efficient in terms of energy use. The agro ecological system has high productivity and sustainability and a market niche for certified organic products, yet has been limited by the lack of governmental-institutional support and there is a debate as to whether it can satisfy the world demand for food. The development of agriculture over the last 50 years in CA and SA has caused critical environmental impacts. Among the impacts, mention should be made first of the deforestation of vast areas high in biodiversity, especially in the tropical forests of Central America and the Amazon. In addition, the use of agrochemicals and soil erosion caused by farming has had a major negative impact on terrestrial, aquatic and marine biodiversity. More diversified agricultural systems can mitigate these impacts up to a point, providing habitats and also connectivity between fragments of natural habitats.

The SESA region has shown significant increases in precipitation and wetter soil conditions during the 20th century (Giorgi 2002) that benefited summer crops and pastures productivity, and contributed to the expansion of agricultural areas (Barros 2010; Hoyos et al 2012). Wetter conditions observed during 1970-2000 (in relation to 1930-1960) led to increases in maize and soybean yields (9% to 58%) in Argentina, Uruguay and Southern Brazil (Magrin et al 2007). Even if rainfall projections estimate increases of about 25% in SESA for 2100, agricultural systems could be threatened if the climate reverts to a drier situation due to interdecadal variability. This could put viability of continuous agriculture in marginal regions of the Argentina's Pampas at risk (Podestá et al 2009). During the 1930's and 1940's, dry and windy conditions together with deforestation, At the global scale (see Chapter 7), warming since 1981 has reduced wheat, maize and barley productivity, although the impacts were small compared with the technological yield gains over the same period (Lobell and Field 2007).

In central Argentina, simulated potential wheat yield- without considering technological improvements- has been decreasing at increasing rates since 1930 (1930-2000: -28 kg/ha/year; 1970-2000: -53 kg/ha/year) in response to increases in minimum temperature during October-November (1930-2000: +0.4°C/decade; 1970-2000: +0.6°C/decade) (Magrin et al 2009). The observed changes in the growing season temperature and precipitation between 1980 and 2008 have slowed the positive yield trends due to improved genetics in Brazilian wheat, maize and soy, as well as Paraguayan soy. In contrast, rice in Brazil and soybean in Argentina have benefited from precipitation and temperature trends. In Argentina, increases in soybean yield may be associated with weather types that favor the entry of cold air from the south reducing thermal stress during flowering and pod set, and weather types that increase the probability of dry days at harvest (Bettolli et al 2009). In South Brazil, irrigated rice yield (Walter et al 2010) and bean productivity (Costa et al 2009) is expected to increase. If technological improvement is considered, the productivity of common bean and maize could increase between 40% and 90% (Costa et al 2009). Sugarcane production could benefit as warming could allow the expansion of planted areas towards the south, where low temperatures are a limiting factor (Pinto et al 2008). Increases in crop productivity could reach 6% in São Paulo state towards 2040 (Marin et al 2009). In Paraguay the yields of soybean, maize and wheat could have slight variations (-1.4% to +3.5%) until 2020 (ECLAC 2010a).

In Chile and western Argentina, yields could be reduced by water limitation. In central Chile (30°S to 42°S) temperature increases, reduction in chilling hours and water shortages may reduce productivity of winter crops, fruits, vines and radiata pine. Conversely, rising temperatures, more moderate frosts and more abundant water will very likely benefit all species towards the South (ECLAC, 2010a; Meza and Silva, 2009). In northern Patagonia (Argentina) fruit and vegetable growing could be negatively affected because of a reduction in rainfall and in average flows in the Neuquén River basin. In the north of the Mendoza basin (Argentina) increases in water demand, due to population growth, may compromise the availability of subterranean water for irrigation, pushing up irrigation costs and forcing many producers out of farming towards 2030. Also, water quality could be reduced by the worsening of existing salinization processes (ECLAC 2010a).

In CA, Northeast Brazil and parts of the Andean region, climate change could affect crop yields, local economies and food security. It is very likely that growing season temperatures in parts of tropical SA, east of the Andes and CA exceed the extreme seasonal temperatures documented from 1900 to 2006 at the end of this century (23 GCMs), affecting regional agricultural productivity and human welfare (Battisti and Naylor 2009). For Northeast Brazil, declining crop yields in subsistence crops

such as beans, corn and cassava are projected (Lobell et al 2008; Margulis et al 2010). In addition, increases in temperature could reduce the areas currently favorable to cowpea bean (Silva et al 2010). The highest warming foreseen for 2100 (5.8 °C, under SRES A2 scenario) could make the coffee crop unfeasible in Minas Gerais and São Paulo in southeastern Brazil if no adaptation action is accomplished. Thus, the coffee crop may have to be transferred to southern regions where temperatures are lower and the frost risk can be reduced (Camargo 2010). With +3°C, Arabica coffee is expected to expand in the extreme south of Brazil, the Uruguayan border and North of Argentina (Zullo et al 2011). Brazilian potato production could be restricted to a few months in currently warm areas, which today allow potato production all year (Lopes et al 2011).

In the Amazon region soybean yields would be reduced by 44% in the highest emission scenario (HadCM3 and no CO<sub>2</sub> fertilization) by 2050 (Lapola et al 2011). By 2050, according to 17GCMs under SRES A2 scenario, 80% of crops will be impacted in more than 60% of current areas of cultivation in Colombia, with severe impacts in perennial and exportable crops (Ramirez- Villegas et al 2012). Teixeira et al (2013) identified hot spots for heat stress towards 2071-2100 under the A1B scenario and suggest that rice in South East Brazil, maize in CA and SA, and soybean in Central Brazil will be the crops and zones most affected by increases in temperature.

In CA, changes projected in climate could severely affect the poorest population and especially their food security, increasing the current rate of chronic malnutrition. Currently, Guatemala is the most food insecure country by percentage of the population (30.4%) and the problem has been increasing in recent years (FAO 2012). The impact of climate variability and change is a great challenge in the region. As an example, the recent rust problem on the coffee sector of 2012/2013 has affected near to 600.000 ha (55% of the total area) (ICO 2013) and will reduce employment by 30% to 40% for the harvest 2013/2014 (FEWS NET 2013). At least 1.4 million people in Guatemala, El Salvador, Honduras and Nicaragua depend on the coffee sector, which is very susceptible to climate variations. In Panamá, the large interannual climate variability will continue to be the dominant influence on seasonal maize yield into the coming decades (Ruane et al 2013). In the future, warming conditions combined with more variable rainfall are expected to reduce maize, bean and rice productivity (ECLAC 2010c); rice and wheat yields could decrease up to 10% by 2030 (Lobell et al 2008-medium confidence). In CA, near to 90% of agricultural production destined to internal consumption is composed by maize (70%), bean (25%) and rice (6%) as shown by ECLAC (2010d).

## **6.2 Degree of vulnerability of specific crops production in CA and SA**

Considering the phenology of certain crops subject to future scenarios can indicate the degree of vulnerability of a specific crop production to climate change. Coffee is an important crop in countries such as Costa Rica, Colombia and Brazil where it is produced in large scale with superior quality for export. Rodrigues et al (2011) evaluated the frequency of occurrence of temperature above 34°C during the growing in different regions in Sao Paulo State, Brazil. Higher temperatures accelerate the cycle and, consequently, affect the productivity- especially the phenological stages of flowering and ripening.

The authors considered the Eta/CPTEC (A1B climate scenario-IPCC) model with 40km horizontal resolution. The scenario was generated by the Eta model nested into the conditions of HadCM3 model. The results showed that the frequency of days with maximum temperature above 34°C

gradually increased over the years for this A1B Scenario, which may indicate impact in the coffee yield in this condition (Figure 41).

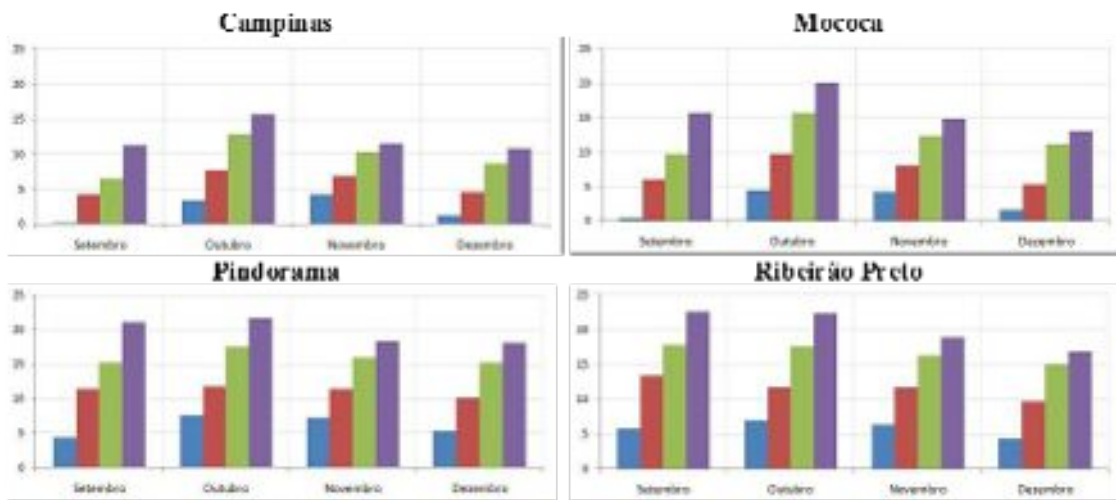


Figure 41. Number of days considering maximum temperatures above 34°C during the months of September, October, November and December (Flowering and ripening stages for coffee crop in Sao Paulo State-Brazil). Source: Rodrigues et al (2011).

In another study also conducted with the coffee crop, Resende et al (2011) estimated the effects of climate change on predicting an increase or decrease of the coffee rust disease, based on A1B Scenario simulated by Eta model 40km-resolution. The systematic errors were evaluated for each ensemble and it was observed a sensible improved in the variables estimated by the model. Figure 42 demonstrated the temperature values before and after the removal of the systematic errors for each ensemble, emphasizing the importance of this analysis presented by these authors.

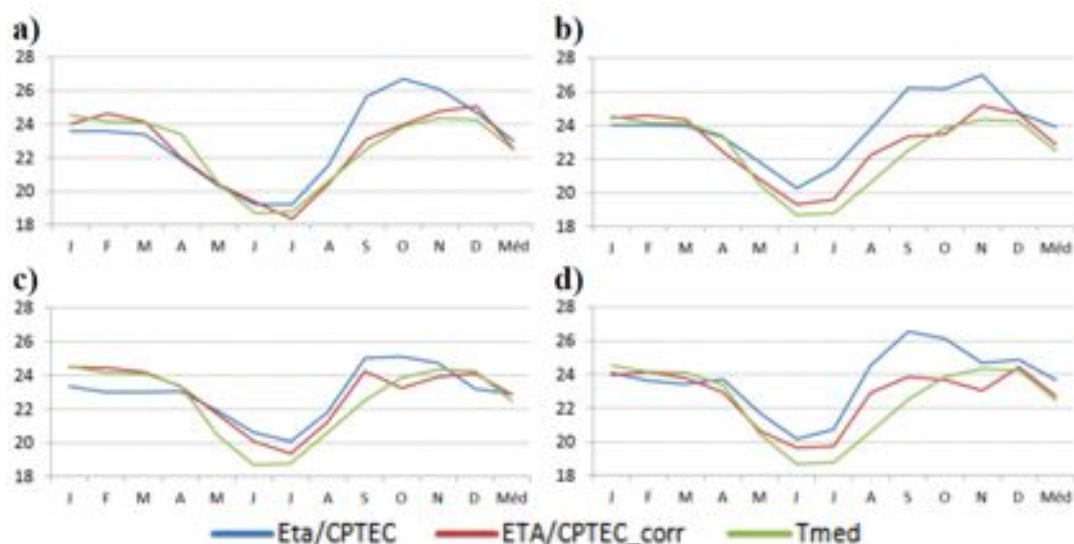


Figure 42. Air temperatures simulated by the Eta model before (blue) and after (red) removing the systematic errors when compared with temperature values extracted from meteorological stations (green) for Ribeirão Preto location, Sao Paulo-Brazil, for the period 1986-1990 and for 4 ensembles' members: a) CNTRL; b) HIGH; c) LOW and d) MIDI. Source: Resende et al (2011).

This study concluded that the optimal conditions for the occurrence of the coffee rust based on the air temperature and the precipitation for the A1B climate change scenario tends in general to decrease over the years for this study area.

Studies that involve projections of the duration of the crops life cycles can serve as an important tool to apply in modeling, since the yield depends on the all crop stages and their durations. Due to the diverse variety of soybean cultivars, there is also large variation in the seeding periods, which considers soil moisture conditions, daylight length, and means air temperature. Tavares et al (2010) evaluated the duration of the soybean life cycle (in days) for an agricultural region in the Parana State, Brazil, for the A1B-IPCC climate change scenario. The Eta model nested into the conditions of HadCM3 model for two periods generated the scenario: present climate (1961-1990) and future climate (2011-2100). The model presented good performance for the duration of soybean life cycle during the current climate, however, a reduction in the life cycle on projections for future scenarios was observed due to the increase in air temperature. The locations of Ponta Grossa and Telemaco Borba presented a reduction in soybean life cycle of 55 and 45 days in future scenarios, respectively (Figure 43).

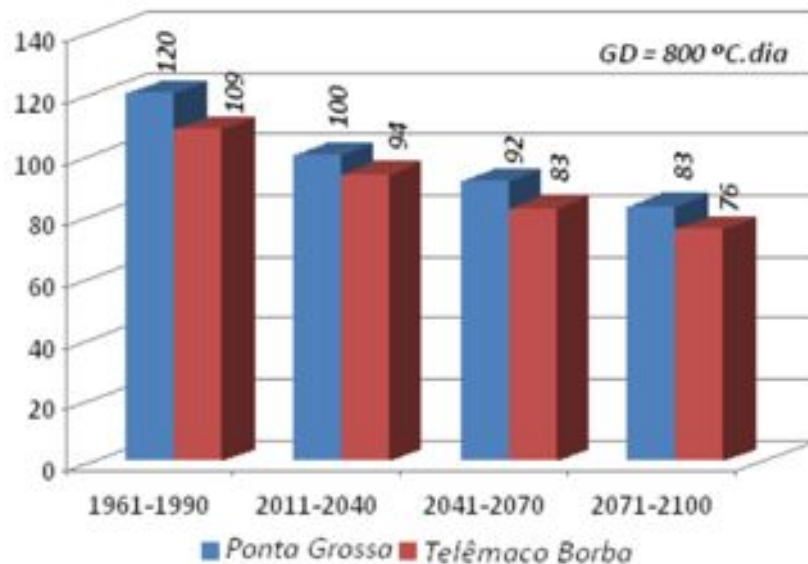


Figure 43. Duration of soybean life cycle (in days) for 2 locations in Parana State- Brazil, based on A1B Scenarios generated by Eta-HadCM3 model. Source: Tavares et al (2010).

### 6.2.1 Crops

The crops analyzed in this report are selected on the basis of the importance of the crops to regional food security for each country. Bean, coffee, maize, potato, soybean, sugarcane and wheat are among the most important crops in Latin America. A brief description of each crop follows, according to CIIAGRO (Centro Integrado de Informações Agrometeorológicas) and EMBRAPA (Empresa Brasileira de Pesquisa Agropecuária):

#### Beans

The bean crop originated in the Americas, where CA, southern Mexico, Guatemala, Honduras and Costa Rica are the main producers, followed by the high mountainous areas of Ecuador, Peru and Bolivia. Guanajuato, located in Mexico at 21°10' north and about 2.100m altitude with rainy summers and mild temperatures around 20°C, presents an ideal climatic condition to vegetation and bean



production. The bean crop can be considered one of the most demanding crops in terms of climatic conditions. However, as its cycle is very short (about three months), the choice of the period or season of the year is very favorable to cultivation. The monthly average temperature of 21°C during the growing season can be considered ideal. From sowing to maturity of the pods, it is important that beans do not encounter water stress.

### **Coffee**

The main producing countries are concentrated in SA (Brazil and Colombia), CA, and Asia (Vietnam). Coffee Arabica is native to the highlands of Ethiopia, located between latitudes 6° N and 9° N, at altitudes ranging from 1.600 to 2.000m, where the air temperature occurs between 18°C and 20 ° C and annual rainfall varies from 1.500 mm to 1.800 mm. Air temperature is one of the most important climatic elements to set for coffee crop adaptation in commercial areas (Meireles et al 2009). Arabica coffee grows very well in regions whose limits of annual average temperatures are between 18°C and 22°C. However, extremes of air temperature can influence growth physiological processes and, consequently, the yield.

### **Maize**

Due to huge diversity in types and varieties developed over time, the maize crop is cultivated in several weather conditions (Camargo 1966). Some varieties have been adapted to temperate regions with short vegetative growing, while others have been adapted to humid equatorial zones with long cycles. This crop is not cultivated in areas where the monthly average temperature falls below 19.5°C during the vegetative stage, depending on the cultivar. In relation to rainfall, the maize crop grows in regions with annual values from 250 to 5000 mm or more.

### **Potato**

The potato crop is native to tropical America where it is widely cultivated in the Andes of Peru. Normally, crops grown on mountain slopes have good productivity. This crop is essentially adapted to temperate climates, where air temperature has an important threshold: temperatures below 10°C and above 30°C inhibit the development of the tuber, while a good growth occurs when the average temperature rests between 18°C and 20°C. The most productive crops are found in regions where low temperatures prevail.

### **Soybean**

Average air temperature between 20°C and 30°C is considered ideal for soybean growth. The range of adequate soil temperature for soybean sowing varies from 20°C to 30°C, but 25°C is an ideal value for rapid and uniform emergence. Water availability is important in two periods of soybean development: germination-emergence and flowering-grain ripening. The need for water for this crop increases with plant development, reaching a maximum during flowering-grain ripening (7-8 mm/day), and then decreases afterwards.

### **Sugarcane**

Sugarcane is cultivated in areas between latitude 36.7 N and 31.0 S, from sea level to 1.000m altitude or a little more and is considered a tropical plant. Sugarcane is a crop with long cultivation, so it coexists during its life cycle with different seasons (rainy, winter, and summer). The main climatic components that control growth, yield and quality in sugarcane are air temperature, solar radiation, and moisture availability. The plant presents better development in hot and tropical areas. A total

rainfall between 1100 and 1500 mm is adequate if distribution is abundant during the vegetative growth and maturation phase. During the period of active growth, rainfall encourages a rapid growth of cane, as well as elongation and internodes formation. However, during the ripening phase, a high rainfall is not desirable as it leads to poor juice quality and encourages vegetative growth. The ideal temperature for growing varies between 32°C and 38°C.

### **Wheat**

Wheat of a good condition grows when the air temperature remains relatively low during the first part of the cycle. Air temperature of around 19°C before harvest is considered satisfactory to obtain good grain quality. Regarding precipitation, this cereal does not require large quantities of water for its development. The zones of high yield for this crop are generally characterized by low precipitation.

### **6.2.2 Climate Change and vulnerability**

Changes in crop phenology provide important evidence of the response to recent regional climate change (Rosenzweig 2007). Phenology is the study of natural phenomena that recur periodically, and how these phenomena relate to climate and seasonal changes.

Several researchers believe that agricultural production could be significantly affected by the severity and pace of climate change. If change is gradual, there may be enough time for an adjustment, but rapid climate change could harm agriculture in many countries, especially those already suffering from poor soil and climate conditions.

More favorable effects on yield tend to depend on the realization of the potentially beneficial effects of carbon dioxide on crop growth and increase of efficiency in water use. Decrease in potential yields is likely to be caused by a shortening of the growing period and a decrease in water availability.

Potato and maize are important staple crops for people in Central Peru, as with beans in Colombia. The vulnerability of these crops to climate change may affect their production and even the maintenance of the diversity of the varieties of these crops found in these countries. The Andean agro-ecosystems have been declared one of the most vulnerable systems of the world, mainly due to native cultivars being adapted to specific niches and environmental levels of agricultural technology are scarce compared to lowland systems. The cultivation of beans and potatoes, therefore, are probably the two most important crops of the Andes and a large number of rural populations depend on the income from these crops. Thus, both progressive adaptation to climate change and current climate risks are essential in these areas.

Chile and Argentina are major producers and exporters of temperate tree fruits in SA, where Brazil is the third largest producer. Fruits and wine are, therefore, important export products for Chile. The U.S., Brazil, Argentina, China and India are the world's largest soybean producers and represent more than 90% of global production.

### **Beans**

Temperatures above 24°C during the stages of flowering and grain formation have negative effects on yield. The bean crop is highly sensitive to deficiencies or water excesses, especially during the flowering phase. Lack of soil moisture is critical in the sub-period between the beginning of flowering and in the physiological maturity, where the water requirement is high.

## Coffee

Extremes of air temperature influence growth, physiological processes and yield of coffee crop. This is apparent in the studies of Camargo and Salati (1966), which show that various biological phases had their development, and /or its growth reduced and even totally paralyzed in extreme temperatures. If the coffee crop is grown in areas with average annual temperatures above 23°C, the development and fruit maturation are accelerated, leading to losses in quality of the final product. Moreover, in regions where temperatures are frequently above 30°C for an extended period and especially during the flowering stage, bud abortion and bad fruit formation can occur (Meireles et al 2009). Figure 44 shows an example of grain ripening, where this process normally occurs slowly in ideal conditions of air temperature (Pezzopane et al 2003). However, in the case of temperature increase, this step could happen very quickly, and consequently, not all grains could reach the maturity stage at the same time. This situation could cause a poor quality of coffee beverage, beyond a drop in the yield.

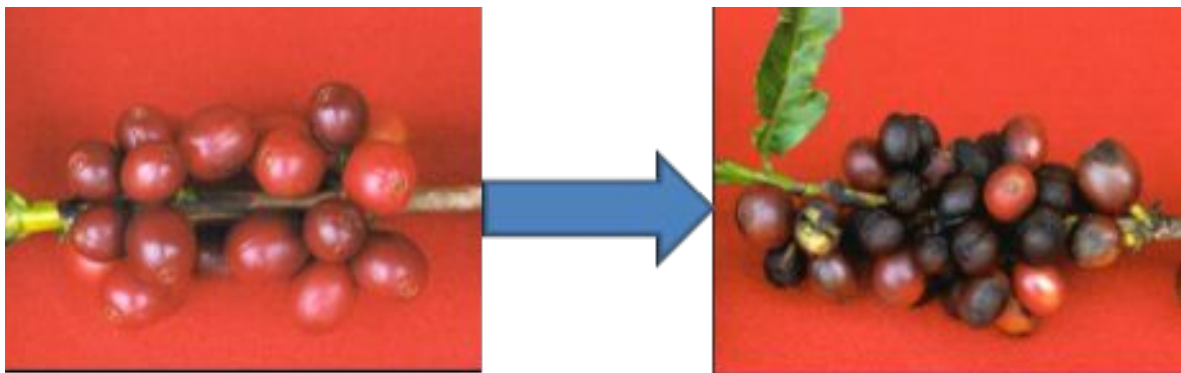


Figure 44. Grain ripening of coffee arabica, where the grains go from "cherry" stage to dried fruits according to air temperature. (Pezzopane et al 2003).

## Potato

Temperatures at night above 20°C reduce the tuber growing process due to breathing increases. In these conditions, the yield is low and the tuber can present bad quality, with possible formation of deformed potato. The potato crop grows well in conditions of moderate water deficit. However, the soil water supply must be readily available to allow uniform and stable growth. An uneven water supply can cause the tubers silking, which depreciates the product.

## Soybean

The soybean crop needs to absorb at least 50% of its weight in water to ensure a good germination. In this phase, the soil water content should not exceed 85% of the maximum total water available and no less than 50%. The need for water increases with plant development, reaching a maximum during the flowering and grain ripening. Significant water deficits during these stages cause physiological changes in the plant, such as stomata closure and leaf roll. As a consequence, this condition can cause premature leaf drop and pod abortion, resulting thus, in the reduction in grain yield. The vegetative growth is small or inactive in temperatures less than or equal to 10°C. Temperatures above 40°C have an adverse effect on growth rate; they also cause flowering disturbances and decrease the pods formation.

## Sugarcane

The ideal temperature for growing varies between 32°C and 38°C however, values between 30°C and 34°C, and especially above 35°C, affect the plant; the growth practically paralyzes when the

temperature is above 38°C. Air temperatures above 38°C reduce the photosynthesis and increase the respiration process. High temperatures can promote reversion of sucrose into fructose and glucose in addition to increased photorespiration thus leading to less accumulation of sugars. During the period of active growth, the rainfall encourages rapid growth of cane, the elongation and the formation of internodes. However, during the ripening, high rainfall is not desirable because it leads to a poor quality of the material, encourages vegetative growth and also promotes an increase of humidity in the tissue. This also affects the harvesting and some operations of transport.

### **Maize**

The maize crop requires sufficient heat and water to obtain a satisfactory yield. Due to a number of existing varieties and new hybrids which are currently being developed, this cereal is cultivated today in a wide range of regions in the world with major climate variations, despite its tropical origin. Temperature is a limiting factor, since the flowering and maturity periods are accelerated with daily average temperatures of 26°C and they are reduced when the value reaches 15.5°C. It is estimated that a minimum of 200 mm of rainfall during the summer is essential for a good yield without irrigation.

### **Wheat**

The wheat crop requires long days for its development; the plant depends on the photoperiod and the temperature, and the flowering grows progressively according to the increase of day length. This crop does not require large quantities of water for development. The zones of satisfactory yield are characterized by low rainfall, but soil water excess causes drenching and can promote diseases and lack of aeration in root zones. High temperatures are an important environmental factor that cause stress and limits the yield for this crop. Heat induces quantitative and qualitative losses in the yield, as well as shortens the cycle time; reduces the leaf area, the height and percentage of fertilization of flowers; accelerates the filling period and senescence, and reduces the average weight of the grains.

### **6.2.3 Agronomic technologies for mitigation and adaptation**

Climate change can have a wide range of effects on agricultural systems and we must adapt to these changes to ensure that agricultural production is not only maintained but is increased to support a growing world population. Climate change mitigation strategies which include interventions to reduce the sources or enhance the sinks of greenhouse gases have a marked management component aiming at conserving natural resources, such as improved fertilizer use and use of water harvesting. These strategies are equally consistent with the concept of sustainability. Adaptation strategies include initiatives and measures to reduce the vulnerability of agro-ecosystems to project climate change, such as changing varieties, alternating the timing or location cropping activities, improving the effectiveness of pest, disease and weed management practices, making better use of seasonal climate forecast, etc (Camargo 2010). Figure 45 shows an example of a strategy that modifies the microclimate and promotes a reduction in air temperature for this crop system (Valentini 2009). This is an adaptation for the occurrence of high temperatures in Brazil.



Figure 45. Coffee crop intercalated with a) Banana and b) Grevillea as a way to evaluate the microclimate in this crop system and adaptation to high temperatures. Source: Valentini (2009); IAC/APTA.

In Mexico, incremental strategies, such as planting varieties better suited to future climate conditions and changing planting dates, have been discussed (Conde et al 2006). The reported studies for SA and CA are extremely important because they guide several studies, not only concerning possible scenarios of climate change, but also adaptation and mitigation in various sectors including agriculture.

## 7. Main results and key advances that can be expected from the climate modelling community in the next few years.

Based on data since 1950, evidence suggests that climate change has already influenced the magnitude and frequency of some extreme weather and climate events globally. However, it remains very difficult to attribute individual events to climate change. Droughts in Amazonia and Northeast Brazil, intense hurricanes in CA, as well as rainfall extremes that have triggered landslides and floods have been attributed to natural climate variability. As climate change impacts become more dramatic, its effect on a range of climate extremes in CA and SA will become increasingly important and will play a more significant role in disaster impacts.

A summary of the projections for both the RCP2.6 and 8.5 is shown in Figure 46, based on an ensemble of 23 models from CMIP5 (Figure 46) by IPCC (Magrin et al 2014). The maps suggest that air temperatures would increase in the region, reaching up to 1-2oC by 2100 on the RCP2.6 (low emissions), and up to 5-6oC for the RCP8.5 (high emissions) over tropical SA over the Amazon region and CA, and with relatively lower warming over Southeastern SA (2-4oC). On rainfall changes, significant increases are projected in southeastern SA and over the Northwest Coast of Peru and Ecuador. Rainfall reductions are projected over the central America-northern SA, eastern Amazonia and central and southern Chile, as well as over eastern Northeast Brazil. At seasonal scales, rainfall reductions during winter and spring in southern Amazonia may indicate a late onset of the rainy season on those regions and a longer dry season. The changes are more intense for the late 21st century and for the RCP8.5.

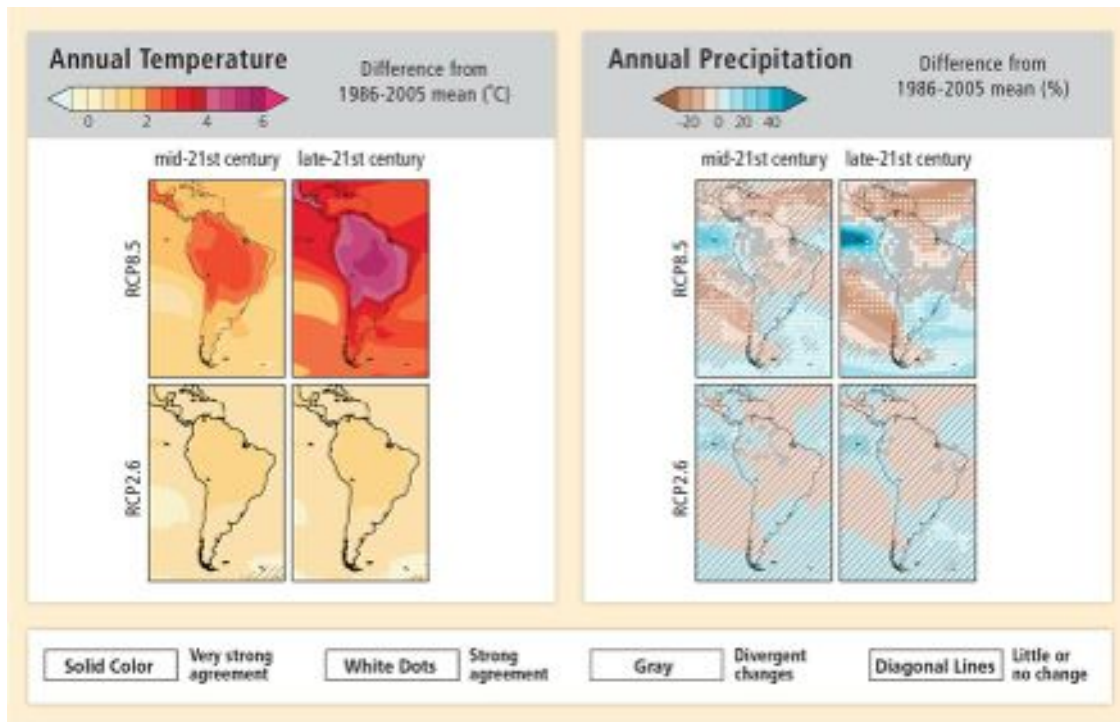


Figure 46. Projected changes in annual average temperature and precipitation. CMIP5 multi-model mean projections of annual average temperature changes (left panel) and average percent change in annual mean precipitation (right panel) for 2046-2065 and 2081-2100 under RCP2.6 and 8.5. Solid colors indicate areas with very strong agreement, where the multi-model mean change is greater than twice the baseline variability, and >90% of models agree on sign of change. Colors with white dots indicate areas with strong agreement, where >66% of models show change greater than the baseline variability and >66% of models agree on sign of change. Gray indicates areas with divergent changes, where >66% of models show change greater than the baseline variability, but <66% agree on sign of change. Colors with diagonal lines indicate areas with little or no change, less than the baseline variability in >66% of models. (There may be significant change at shorter timescales such as seasons, months, or days.). Analysis uses model data and methods building from IPCC WG2 AR5 (Magrin et al 2014).

The influences and interactions, which control the climate of CA and SA, are complex and climate models have difficulty in simulating the observed climate. Temperature climatologies, variability and trends are generally robustly reproduced. GCMs do not perform as adequately in their simulation of regional precipitation patterns, with biases in the model climatologies and further uncertainty in the reproduction of variability and trends. The lack of data in parts of tropical South America and in CA affects the trend assessment and also represents a source of uncertainty in the assessments of trends, and on the assessments of model skill. However, we can affirm that there is better information now available on what is expected in terms of changes in extremes in various regions and sub regions of CA and SA. At times, the problem is not the lack of data but the quality of the data available. We have solved the problems of the lack of observational data using publications from IPCC and other published literature on trends of climate and extremes in CA and SA. We have noticed that there are a smaller number of studies on CA compared to SA, from what was found in international journals.

The use of meteorological reanalysis has allowed for a better knowledge of large-scale circulation anomalies, but are less useful for the analyses of short-term extremes, particularly rainfall extremes.

The spatial and temporal resolution of the models makes resolving the complex climate of the region particularly challenging, especially when dynamic downscaling is performed.

On the models' ability to reproduce climatic short term or seasonal extremes, which can have a significant impact on agriculture, are particularly variable with precipitation-based extremes. The models perform more adequately for temperature-derived indices, but generally tend to underestimate. We have to admit that model projections of the future derived from models are highly uncertain, particularly for precipitation and for regions such as central SA, the Pantanal region and some sections of CA. Precipitation projections vary from significant decreases in precipitation and extended droughts in certain models in some regions, particularly the CA and Northeast Brazil. The ensemble precipitation projections may be particularly useful, since they represent the average of a wide spread and are not constrained by the physical mechanisms which control the model scenarios. The spread among projections can be used as indicator of model predictability. Uncertainty in the projections has a significant controlling influence over agriculture in CA and SA, such that the projections for change in crop cultivation limits are highly variable over space and time and are also subject to uncertainties.

The individual models produce spatially consistent changes in crop domains under continued anthropogenic climate forcing, but the inter-model spread is wide. For crops with lower precipitation growth thresholds, this impact is particularly pronounced, with the growth domain projections produced by the end members of the ensemble having little overlap for some crops. Considering the phenology of certain crops subject to future scenarios can assess the degree of vulnerability of a specific crop production to climate change. For instance, for coffee, higher temperatures accelerate the cycle and, consequently, affect productivity. Temperature trends increase in all models and for all temperature indices, with varying impact on the crops depending on their particular climatic limits of growth. On other hand, the wide divergence in precipitation projections provides a greater challenge to adaptation strategies.

While there have been experiences on the production of high resolution climate change scenarios in SA, mainly from Brazil and Argentina since 2005, few studies on climate change projections for CA are available, though some appear after 2010, mainly by Mexico. Some of those simulations were derived from the PRECIS regional model, consequence of training activities organized in Central American-Caribbean and South America by the UK Met Office Hadley Centre.

As noted in Magrin et al (2014), while more studies have been published on SA climate and impacts for the IPCC AR5 WG2, this growth has not been as strong in CA. However, there has been an increase in literature published on the North American Monsoon and hurricanes impacts in CA and in the Andean region of SA in the last 5 years. This demonstrates the growing knowledge on climate processes in CA and SA. However, the development of capacity for climate modelling has been concentrated in few countries. While Brazil has generated future climate scenarios for the whole of CA and SA regions, other countries have produced scenarios at the country- level (Mexico, Argentina, Chile, Peru, Uruguay and Colombia). Capacity building activities in training for generation of regional climate change scenarios have taken place in the last few years in the region.

In the past we have had training activities with the Eta regional model in SA, but not for CA countries. The Brazilian Government, ECLAC and the Red Internacional de Oficinas sobre Cambio Climatico (RIOCC) from the Spanish Government and the UK government have funded these training activities for SA by the PRECIS initiative. In the future, these activities should continue and cover

CA, perhaps as an initiative of INPE and CIAT-CCAFS. These training activities are important since the production of future climate change simulations is needed for impact studies, particularly on the sectors of water security, food security and energy security, key sectors in the regional economies of CA and SA. We need better interaction with the meteorological services of countries in CA and SA, and institutions such as INPE can assume a major role in training people for the generation and use of regional climate change scenarios for impacts studies.

Lastly, various international projects have been implemented in SA. The Europe South America Network for Climate Change Assessment and Impact Studies-CLARISLPB Project (Boulanger et al 2011), aims at predicting the regional climate change impacts in South America, and at designing adaptation strategies for land use, agriculture, rural development, hydropower. Projects like this and capacity building activities as those previously listed are directed to better understanding model uncertainties and biases, and to model development directed to a better representation physical processes that will lead to a better simulation of seasonal climate extremes—mainly droughts and floods, and for the generation of projections of future climate change scenarios for extremes.



## References

- Aguilar E, Peterson TC, Ramírez Obando P, Frutos R, Retana JA, Solera M, Soley J, González García I, Araujo RM, Rosa A, Santos A, Valle VE, Brunet M, Aguilar L, Álvarez L, Bautista M, Castañón C, Herrera L, Ruano E, Sinay JJ, Sánchez E, Hernández Oviedo GI, Obed F, Salgado JE, Vázquez JL, Baca M, Gutiérrez M, Centella C, Espinosa J, Martínez D, Olmedo B, Ojeda Espinoza CE, Núñez R, Haylock M, Benavides H and Mayorga R. 2005. Changes in precipitation and temperature extremes in Central America and northern South America, 1961–2003. *Journal of Geophysical Research*, 110: D23107. doi:10.1029/2005JD006119
- Alves L, Marengo JA. 2009. Assessment of regional seasonal predictability using the PRECIS regional climate modeling system over South America. *Theoretical and Applied Climatology*. doi:10.1007/s00704-009-0165-2
- Arias PA, Fu R, and Mo KC. 2012. Decadal Variation of Rainfall Seasonality in the North American Monsoon Region and Its Potential Causes. *Journal of Climate*, 25:12, 4258-4274.
- Battisti DS and Naylor RL. 2009. Historical Warnings of Future Food Insecurity with Unprecedented Seasonal Heat. *Science*, 323:5911, 240-244.
- Barros VR. 2010. El Cambio Climático en Argentina (Capítulo 3). In: *Agro y Ambiente: una agenda compartida para el desarrollo sustentable*. Foro de la Cadena Agroindustrial Argentina, Buenos Aires, Argentina, pp. 35.
- Bettolli ML, Vargas WM, and Penalba OC. 2009. Soya bean yield variability in the Argentine Pampas in relation to synoptic weather types: monitoring implications. *Meteorological Applications*, 16:4, 501-511.
- Betts RA, Cox PM, Collins M, Harris PP, Huntingford C, and Jones CD. 2004. The role of ecosystem atmosphere interactions in simulated Amazonian precipitation decrease and forest dieback under global climate warming. *Theoretical and Applied Climatology*, 78:1-3, 157-175.
- Betts RA, Malhi Y, and Roberts JT. 2008. The future of the Amazon: new perspectives from climate, ecosystem and social sciences. *Philosophical Transactions of the Royal Society B-Biological Sciences*, 363:1498, 1729-1735.
- Black TL. 1994. NMC notes, the new NMC mesoscale Eta model: description and forecast examples. *Weather Anal Forecast*, 9:256–278.
- Blázquez J and Nuñez MN. 2013. Analysis of uncertainties in future climate projections for South America: comparison of WCRP-CMIP3 and WCRP-CMIP5 models. *Climate Dynamics*, 41:3-4, 1039-1056.
- Bodas-Salcedo A, Ringer MA, and Jones A. 2008. Evaluation of the Surface Radiation Budget in the atmospheric component of the Hadley Centre Global Environmental Model (HadGEM1). *Journal of Climate*, 21: 4723–4748. doi:10.1175/2008JCLI2097.1
- Boulanger JP, Schlindwein S, Gentile E. 2011. CLARIS LPB WP1: metamorphosis of the CLARIS LPB European project: from a mechanistic to a systemic approach. *CLIVAR exchanges*, 57: 16(3), 7–10.

Cabré M, Solman S, and Nuñez M. 2010. *Creating regional climate change scenarios over southern South America for the 2020's and 2050's using the pattern scaling technique: validity and limitations*. Springer Netherlands. pp. 449-469.

Camargo AP, Salati E. 1966. Determinação da temperatura letal de folhagem de cafeeiro em noite de geada. *Bragantia, Campinas*, 25:2, 61-63.

Camargo M. 2010. The impact of climatic variability and climate change on arabic coffee crop in Brazil. *Bragantia, Campinas*, 69:1, 239:247.

CDKN - Climate and Development Knowledge Network. 2013. *Managing climate extremes and disasters in Latin America and the Caribbean: Lessons from the SREX report*. CDKN. available at: [www.cdkn.org/srex](http://www.cdkn.org/srex)

Chou SC, Nunes AMB, Cavalcanti IFA. 2000. Extended range forecasts over South America using the regional Eta model. *Journal of Geophysical Research*, 105:10147–10160.

Chou SC, Bustamante JF, Gomes JL. 2005. Evaluation of Eta model seasonal precipitation forecasts over South America. *Nonlinear Processes Geophysics*, 12:4, 537–555.

Chou S, Marengo C, Lyra J, Sueiro A, Pesquero G, Alves J, Kay L, Betts G, Chagas R, Gomes D, Bustamante J, Tavares P. 2012. Downscaling of South America present climate driven by 4-member HadCM3 runs. *Climate Dynamics*, 38:3-4, 635-653.

Clarke L, Edmonds J, Jacoby H, Pitcher H, Reill, J, and Richels R. 2007. *Scenarios of Greenhouse Gas Emissions and Atmospheric Concentrations*. Sub-report 2.1A of Synthesis and Assessment Product 2.1 by the US Climate Change Science Program and the Subcommittee on Global Change Research, Department of Energy, Office of Biological & Environmental Research, Washington, 7 DC, USA, 154 pp.

Collins WJ, Bellouin N, Doutriaux-Boucher M, Gedney N, Hinton T, Jones CD, Liddicoat S, Martin G, O'Connor F, Rae J, Senior C, Totterdell I, Woodward S, Reichler T, Kim J, Halloran P. 2008. *Evaluation of the HadGEM2 model*. Hadley Centre Technical Note HCTN 74, Met Office Hadley Centre, Exeter, U.K. Available at: <http://www.metoffice.gov.uk/learning/library/publications/science/climate-science>

Collins W.J, Bellouin N, Doutriaux-Boucher M, Gedney N, Halloran P, Hinton T, Hughes J, Jones C.D, Joshi M, Liddicoat S, Martin G, O'Connor F, Rae J, Senior C, Sitch S, Totterdell I, Wiltshire A, and Woodward S. 2011. Development and evaluation of an Earth-system model – HadGEM2, *Geosci. Model Development Discussions*, 4: 997–1062. doi:10.5194/gmdd-4-997-2011

Conde C, Ferrer R, and Orozco S. 2006. Climate change and climate variability impacts on rainfed agricultural activities and possible adaptation measures. *Atmosfera*, 19:3, 181-194.

Costa LC, Justino F, Oliveira LJC, Sediyaama GC, Ferreira WPM, and Lemos CF. 2009. Potential forcing of CO<sub>2</sub>, technology and climate changes in maize (*Zea mays*) and bean (*Phaseolus vulgaris*) yield in southeast Brazil. *Environmental Research Letters*, 4:1, 014013.

- Costa MH and Pires GF. 2010. Effects of Amazon and Central Brazil deforestation scenarios on the duration of the dry season in the arc of deforestation. *International Journal of Climatology*, 30:13, 1970-1979.
- Cox PM, Betts RA, Jones CD, Spall SA, and Totterdell IJ. 2000. Acceleration of global warming due to carbon-cycle feedbacks in a coupled climate model. *Nature*, 408:6809, 184-187.
- Cox PM, Betts RA, Collins M, Harris PP, Huntingford C, Jones CD. 2004. Amazonian forest dieback under climate-carbon cycle projections for the 21st century. *Theoretical Applied Climatology*, 78:137-156. doi:10. 1007/s00704-004-0049-4.
- Donat MG., Alexander LV, Yang H, Durre I, Vose R, Dunn RJH, Willett KM, Aguilar E, Brunet M, Caesar J, Hewitson B, Jack C, Klein Tank AMG, Kruger AC, Marengo JA, Peterson TC, Renom M, Oria Rojas C, Rusticucci M, Salinger J, Sanhoury Elrayah A, Sekele SS, Srivastava AK, Trewin B, Villarreal C, Vincent LA, Zhai P, Zhang X, and Kitching S. 2013. Updated analyses of temperature and precipitation extreme indices since the beginning of the twentieth century: The HadEX2 dataset. *Journal of Geophysical Research: Atmospheres*, 118:5, 2098-2118.
- Ek MB, Mitchell KE, Lin Y, Rogers E, Grummen P, Koren V, Gayno G, Tarpley JD. 2003. Implementation of NOAA land surface advances in the National centers for environmental prediction operational mesoscale Eta model. *Journal of Geophysical Research*, 108:8851. doi: 10.1029/2002JD003246
- ECLAC. 2010a. *Economics of Climate Change in Latin America and the Caribbean. Summary 2010*. (LC/G.2474). United Nations, ECLAC, Santiago de Chile, Chile. pp. 107.
- ECLAC. 2010b. *El progreso de América Latina y el Caribe hacia los Objetivos de Desarrollo del Milenio. Desafíos para lograrlos con igualdad*. (LC/G 2460). Economic Commission for Latin America and the Caribbean (ECLAC), Santiago de Chile, Chile, pp.25. Available at: <http://www.eclac.org/publicaciones/xml/1/39991/portada-indice-intro.pdf>
- ECLAC. 2010c. *The Economics of Climate Change in Central America: Summary 2010*. (LC/MEX/L.978). United Nations, ECLAC. pp.146.
- ECLAC. 2010d. *Economics of Climate Change in Latin America and the Caribbean. Summary 2010*. United Nations, Economic Commission for Latin America and the Caribbean (ECLAC), Santiago, Chile, pp. 107.
- Ericksen P, Thornton P, Notenbaert A, Cramer L, Jones P, and Herrero M. 2011. Mapping hotspots of climate change and food insecurity in the global tropics. In: *CCAFS Report no. 5*. Technical Report. CGIAR Research Program on Climate Change, Agriculture and Food Security (CCAFS), Copenhagen, Denmark.
- Espinoza JC, Ronchail J, Frappart F, Lavado W, Santini W, and Guyot J.L. 2013. The Major Floods in the Amazonas River and Tributaries (Western Amazon Basin) during the 1970-2012 Period: A Focus on the 2012 Flood. *Journal of Hydrometeorology*, 14:3, 1000-1008.

- Espinoza JC, Guyot JL, Ronchail J, Cochonneau G, Filizola N, Fraizy P, Labat D, de Oliveira E, Julio Ordonez J, and Vauchel P. 2009a. Contrasting regional discharge evolutions in the Amazon basin (1974-2004). *Journal of Hydrology*, 375:3-4, 297-311.
- Espinoza JC, Ronchail J, Guyot JL, Cochonneau G, Naziano F, Lavado W, De Oliveira E, Pombosa R, and Vauchel P. 2009b. Spatio-temporal rainfall variability in the Amazon basin countries (Brazil, Peru, Bolivia, Colombia, and Ecuador). *International Journal of Climatology*, 29:11, 1574-1594.
- Espinoza JC, Ronchail J, Guyot JL, Junquas C, Vauchel P, Lavado W, Drapeau G, and Pombosa R. 2011. Climate variability and extreme drought in the upper Solimões River (western Amazon Basin): Understanding the exceptional 2010 drought. *Geophysical Research Letters*, 38:13, L13406.
- Espinoza JC, Lengaigne M, Ronchail J, and Janicot S. 2012. Large-scale circulation patterns and related rainfall in the Amazon Basin: a neuronal networks approach. *Climate Dynamics*, 38:1-2, 121-140.
- Falvey M. and Garreaud RD. 2009. Regional cooling in a warming world: Recent temperature trends in the southeast Pacific and along the west coast of subtropical South America (1979–2006). *Journal of Geophysical Research*, 114, D04102.
- FAO. 2012. *The State of Food Insecurity in the World 2012. Economic growth is necessary but not sufficient to accelerate reduction of hunger and malnutrition*. FAO, WFP and IFAD; Rome, Italy.
- Fels SB, Schwarzkopf MD. 1975. The simplified exchange approximation: a new method for radiative transfer calculations. *Journal of Atmospheric Science*, 32:1475–1488.
- FEWS NET. 2013. *Special Report Central America. Coffee sector shocks and projected food security impacts in Central America*. Famine Early Warning Systems Network (FEWS NET). Washington. pp.3.
- Garreaud RD and Falvey M. 2009. The coastal winds off western subtropical South America in future climate scenarios. *International Journal of Climatology*, 29:4, 543-554.
- Giorgi F. 2002. Variability and trends of sub-continental scale surface climate in the twentieth century. Part I: observations. *Climate Dynamics*, 18:8, 675-691.
- Gutiérrez D, Bertrand A, Wosnitza-mendo C, Dewitte B, Purca S, Peña C, Chaigneau A, Tam J, Graco M, Grados C, Fréon P, and Guevara-carrasco R. 2011a. Sensibilidad del sistema de afloramiento costero del Perú al cambio climático e implicancias ecológicas [Climate change sensitivity of the Peruvian upwelling system and ecological implications]. *Revista Peruana Geatmosférica*. 3: 1-24.
- Gutiérrez D, Bouloubassi I, Sifeddine A, Purca S, Goubanova K, Graco M, Field D, Mejanelle L, Velazco F, Lorre A, Salvattecchi R, Quispe D, Vargas G, Dewitte B, and Ortlieb L. 2011b. Coastal cooling and increased productivity in the main upwelling zone off Peru since the mid-twentieth century. *Geophysical Research Letters*, 38, L07603.
- Haylock MR, Peterson TC, Alves L.M, Ambrizzi T, Anunciação YMT, Baez J, Barros VR, Berlato M.A, Bidegain M, Coronel G, Corradi V, Garcia VJ, Grimm AM, Karoly D, Marengo JA, Marino MB, Moncunill DF, Nechet D, Quintana J, Rebello E, Rusticucci M, Santos JL, Trebejo I, and

- Vincent LA. 2006. Trends in Total and Extreme South American Rainfall in 1960–2000 and Links with Sea Surface Temperature. *Journal of Climate*, 19, 1490–1512.
- Hoyos LE, Cingolani AM, Zak MR, Vaieretti MV, Gorla DE, and Cabido MR. 2012. Deforestation and precipitation patterns in the arid Chaco forests of central Argentina. *Applied Vegetation Science*, 16:2, 260-271.
- ICO. 2013. *Report on the outbreak of coffee leaf rust in Central America and Action Plan to combat the pest.* (ED 2157/13). International Coffee Organization (ICO), London, UK. pp.6.
- Imbach P, Molina L, Locatelli B, Roupsard O, Mahé G, Neilson R, Corrales L, Scholze M, and Ciais P. 2012. Modeling potential equilibrium states of vegetation and terrestrial water cycle of Mesoamerica under climate change scenarios. *Journal of Hydrometeorology*, 13:2, 665-680.
- IPCC. 2007. Summary for Policymakers. In: *Climate Change 2007: The Physical Science Basis. Contribution of Working Group I to the Fourth Assessment Report of the Intergovernmental Panel on Climate Change* [Solomon S, Qin D, Manning M, Chen Z, Marquis M, Averyt K.B, Tignor M, Miller H.L (eds.)]. Cambridge University Press, Cambridge, United Kingdom and New York, NY, USA.
- IPCC. 2013. Summary for Policymakers. In: *Climate Change 2013: The Physical Science Basis. Contribution of Working Group I to the Fifth Assessment Report of the Intergovernmental Panel on Climate Change* [Stocker T.F, D Qin, G.K Plattner, M Tignor, S.K Allen, J Boschung, A Nauels, Y Xia, V Bex and P.M Midgley (eds.)]. Cambridge University Press, Cambridge, United Kingdom and New York, NY, USA.
- IPCC SREX. 2012. Managing the Risks of Extreme Events and Disasters to Advance Climate Change Adaptation. In: *A Special Report of Working Groups I and II of the Intergovernmental Panel on Climate Change.* [Field C.B, Barros V, Stocker T.F, Qin D, Dokken D.J, Ebi K.L (eds.)]. Cambridge University Press, Cambridge, UK, and New York, NY, USA, pp. 582.
- IPCC. 2014. Summary for Policymakers. In: *Climate Change 2014: Impacts, Vulnerability and Adaptation. Part A: Global and Sectoral Aspects. Contribution of Working Group 2 to the Fifth Assessment Report of the Intergovernmental Panel on Climate Change* [Field C, Barros V.R, Dokken D.J, Mach K.J, Mastrandrea M.D, Bilir T.E, Chatterjee M, Ebi K.L, Estrada Y.O, Genova R.C, Girma B, Kissel E.S, Levy A.N, MacCracken S, Mastrandrea P.R, and White L.L (eds.)]. Cambridge University Press, Cambridge, United Kingdom and New York, NY, USA. pp. 1-32.
- Janjic ZI. 1979. Forward-backward scheme modified to prevent two grid-interval noise and its application in sigma coordinate models. *Contrib Atmos Phys*, 52:69–84.
- Janjic ZI. 1994. The step-mountain Eta coordinate model: further developments of the convection, Viscous sub layer and turbulence closure schemes. *Monthly Weather Review*, 122:927–945.
- Joetzer E, Douville H, Delire C, Ciais P. 2013. Present-day and future Amazonian precipitation in global climate models: CMIP5 versus CMIP3. *Climate Dynamics*, p.1-16.
- Jones C, Carvalho LMV. 2013. Climate change in the South American Monsoon System: present climate and CMIP5 projections. *Journal of Climate*, 5:26, 6660-6678.

Jones CD, Hughes JK, Bellouin N, Hardiman SC, Jones GS, Knight J, Liddicoat S, O'Connor FM, Andres RJ, Bell C, Boo KO, Bozzo A, Butchart N, Cadule P, Corbin KD, Doutriaux-Boucher M, Friedlingstein P, Gornall J, Gray L, Halloran PR, Hurtt G, Ingram WJ, Lamarque JF, Law RM, Meinshausen M, Osprey S, Palin EJ, Parsons Chini L, Raddatz T, Sanderson MG, Sellar AA, Schurer A, Valdes P, Wood N, Woodward S, Yoshioka, and Zerroukat M. 2011. The HadGEM2-ES implementation of CMIP5 centennial simulations. *Geoscience Model Development*, 4, 543–570. doi:10.5194/gmd-4-543-2011

Kim H-J, Wang B, Ding Q. 2008. The global monsoon variability simulated by CMIP3 coupled climate models. *Journal of Climate*, 20, 4497-4525. doi: 10.1175/2008JCLI2041.1

Kitoh A, Endo H, Krishna Kumar K, Cavalcanti IFA, Goswami P, and Zhou T. 2013. Monsoons in a changing world: A regional perspective in a global context. *Journal of Geophysical Research: Atmospheres*, 118:8, 3053-3065.

Knutti R, Seclacek J. 2013. Robustness and uncertainties in the new CMIP5 climate model projections. *Nature Climate Change*, 5: 3, p.369-373.

Kosaka Y, and Xie S. 2013. Recent global-warming hiatus tied to equatorial Pacific surface cooling. *Nature*, (published online 28 August 2013).

Lacis AA, Hansen JE. 1974. A parameterization of the absorption of solar radiation in earth's atmosphere. *Journal of Atmospheric Science*, 31:118–133.

Lavado CWS, Ronchail J, Labat D, Espinoza JC, and Guyot JL. 2012. Basin-scale analysis of rainfall and runoff in Peru (1969-2004): Pacific, Titicaca and Amazonas drainages. *Hydrological Sciences Journal-Journal Des Sciences Hydrologiques*, 57:4, 625-642.

Lapola DM, Schaldach R, Alcamo J, Bondeau A, Msangi S, Priess JA, Silvestrini R, and Soares BS. 2011. Impacts of Climate Change and the End of Deforestation on Land Use in the Brazilian Legal Amazon. *Earth Interactions*, 15:16, 1-29.

Lenton TM, Held H, Kriegler E, Hall JW, Lucht W, Rahmstorf S, Schellnhuber HJ. 2008. Tipping elements in the Earth's climate system. *Proceedings of the National Academy of Sciences of the USA*, 105:1786-1793. doi\_10.1073\_pnas.0705414105.

Lewis SL, Brando PM, Phillips OL, van der Heijden GMF, and Nepstad D. 2011. The 2010 Amazon Drought. *Science*, 331:6017, 554-554.

Lobell DB. and Field CB. 2007. Global scale climate - crop yield relationships and the impacts of recent warming. *Environmental Research Letters*. 2:1, 014002.

Lobell DB, Burke MB, Tebaldi C, Mastrandrea MD, Falcon WP, and Naylor RL. 2008. Prioritizing climate change adaptation needs for food security in 2030. *Science*, 319:5863, 607-610.

Lopes CA, da Silva GO, Cruz EM, Assad ED, and Pereira ADS. 2011. An analysis of the potato production in Brazil upon global warming. *Horticultura Brasileira*, 29:1, 7-15.

Magrin G, García CG, Choque DC, Giménez JC, Moreno AR, Nagy GJ, Nobre C, and Villamizar A. 2007. Latin America. In: *Climate Change 2007: Impacts, Adaptation and Vulnerability. Contribution*

of Working Group II to the Fourth Assessment Report of the Intergovernmental Panel on Climate Change. [Parry M.L, O.F Canziani, J.P Palutikof, P.J van der Linden, and C.E Hanson (eds.)]. Cambridge University Press, Cambridge, UK, pp. 581-615.

Magrin GO, Travasso MI, Rodríguez GR, Solman S, and Núñez M. 2009. Climate change and wheat production in Argentina. *International Journal of Global Warming*, 1:1, 214-226.

Magrin G, Marengo J, Boulanger JP, Buckeridge M.S, Castellanos E, Poveda G, Scarano FR, Vicuña S. 2014. Central and South America. In: *Climate Change 2014: Impacts, Adaptation and Vulnerability. Contribution of Working Group II to the Fifth Assessment Report of the Intergovernmental Panel on Climate Change*. In Press, Cambridge University Press, Cambridge, UK.

Malhi Y, Roberts JT, Betts RA, Killeen TJ, Li W, and Nobre CA. 2008. Climate change, deforestation, and the fate of the Amazon. *Science*, 319:5860, 169-172.

Malhi Y, Aragao LEOC, Galbraith D, Huntingford C, Fisher R, Zelazowski P, Sitch S, McSweeney C, and Meir P. 2009. Exploring the likelihood and mechanism of a climate-change-induced dieback of the Amazon rainforest. *Proceedings of the National Academy of Sciences of the USA*.

Marengo JA. 2004. Interdecadal variability and trends of rainfall across the Amazon basin. *Theoretical and Applied Climatology*, 78:1-3, 79-96.

Marengo JA, Nobre CA, Tomasella J, Oyama MD, Sampaio de Oliveira G, de Oliveira R, Camargo H, Alves LM, and Brown IF. 2008. The Drought of Amazonia in 2005. *Journal of Climate*, 21:3, 495-516.

Marengo JA, Jones R, Alves LM, and Valverde MC. 2009a. Future change of temperature and precipitation extremes in South America as derived from the PRECIS regional climate modeling system. *International Journal of Climatology*, 29:15, 2241-2255.

Marengo JA, Rusticucci M, Penalba O, and Renom M. 2009b. An intercomparison of observed and simulated extreme rainfall and temperature events during the last half of the twentieth century: part 2: historical trends. *Climatic Change*, 98:3-4, 509-529.

Marengo JA, Ambrizzi T, da Rocha R, Alves L, Cuadra S, Valverde M, Torres R, Santos D, and Ferraz S. 2010. Future change of climate in South America in the late twenty-first century: intercomparison of scenarios from three regional climate models. *Climate Dynamics*, 35:6, 1073-1097.

Marengo JA, Pabón JD, Díaz A, Rosas G, Ávalos G, Montealegre E, Villacis M, Solman S, and Rojas M. 2011. Climate Change: Evidence and Future Scenarios for the Andean Region, Chapter 7. In: *Climate Change and Biodiversity in the Tropical Andes*. [Herzog K, Martínez R, Jørgensen P.M, and Tiessen H (eds.)]. MacArthur Foundation, IAI, START, São Jose dos Campos, São Paulo, Brazil. pp. 110-127.

Marengo JA, Chou SC, Kay G, Alves LM, Pesquero JF, Soares WR, Santos DC, Lyra AA, Sueiro G, Betts R, Chagas DJ, Gomes JL, Bustamante JF, and Tavares P. 2012. Development of regional future climate change scenarios in South America using the Eta CPTEC/HadCM3 climate change

projections: Climatology and regional analyses for the Amazon, São Francisco and the Paraná River Basins. *Climate Dynamics*, 38:9-12, 1829-1848.

Marengo JA, Alves LM, Soares WR, Rodriguez DA, Camargo H, Paredes M, and Diaz Pablo A. 2013. Two contrasting seasonal extremes in tropical South America in 2012: Flood in Amazonia and drought in Northeast Brazil. *Journal of Climate*, 26:22, 9137-9154.

Marin FR, Pellegrino GQ, Assad ED, Nassif DSP, Viana MS, Soares FA, Cabral LL, and Guiatto D. 2009. *Cenários futuros para cana-de-açúcar no Estado de São Paulo baseados em projeções regionalizadas de mudanças climáticas*. Proceedings of XVI Congresso Brasileiro de Agrometeorologia, 22-25 September 2009, Gran Darrell Minas Hotel, Eventos e Convenções – Belo Horizonte, Minas Gerais, Brazil, pp. 5.

Martin GM, Bellouin N, Collins WJ, Culverwell ID, Halloran PR, Hardiman SC, Hinton TJ, Jones CD, McDonald RE, McLaren AJ, O'Connor FM, Roberts MJ, Rodriguez JM, Woodward S, Best MJ, Brooks ME, Brown AR, Butchart N, Dearden C, Derbyshire SH, Dharssi I, Doutriaux-Boucher M, Edwards JM, Falloon PD, Gedney N, Gray LJ, Hewitt HT, Hobson M, Huddleston MR, Hughes J, Ineson S, Ingram WJ, James PM, Johns TC, Johnson CE, Jones A, Jones CP, Joshi MM, Keen AB, Liddicoat S, Lock AP, Maidens AV, Manners JC, Milton SF, Rae JGL, Ridley JK, Sellar A, Senior CA, Totterdell IJ, Verhoef A, Vidale PL, and Wiltshire A. 2011. The HadGEM2 family of Met Office Unified Model climate configurations. *Geoscience Model Development*, 4, 723–757.

Masiokas MH, Villalba R, Luckman BH, Lascano ME, Delgado S, and Stepanek P. 2008. 20th-century glacier recession and regional hydroclimatic changes in northwestern Patagonia. *Global and Planetary Change*, 60:1-2, 85-100.

Maurer E, Adam J, and Wood A. 2009. Climate model based consensus on the hydrologic impacts of climate change to the Rio Lempa basin of Central America. *Hydrology and Earth System Sciences*, 13:2, 183-194.

Meireles E JL. et al. 2009. *Fenologia do Cafeeiro: Condições Agrometeorológicas e Balanço Hídrico do Ano Agrícola 2004–2005*. Embrapa Café, Documentos, 2. Brasília, *Embrapa Informação Tecnológica*. P.43.

Menendez C, de Castro M, Boulanger J-P, D'Onofrio A, Sanchez E, Soërensson AA, Blazquez J, Elizalde A, Jacob D, Le Treut H, Li ZX, Nunez MN, Pessacq N, Pfeiffer S, Rojas M, Rolla A, Samuelsson P, Solman SA, Teichmann C. 2010. Downscaling extreme month-long anomalies in southern South America. *Climate Change*, 98:379–403. doi:10.1007/s10584-009-9739-3

Mesinger F, Janjic' ZI, Nic'kovic' S, Gavrilov D, Deaven DG. 1988. The step-mountain coordinate: model description and performance for cases of Alpine lee cyclogenesis and for a case of Appalachian redevelopment. *Monthly Weather Review*, 116:1493–1518.

Meza FJ and Silva D. 2009. Dynamic adaptation of maize and wheat production to climate change. *Climatic Change*, 94: 1-2, 143-156.

Mitchell TD, Jones PD. 2005. An improved method of constructing a database of monthly climate observations and associated high-resolution grids. *International Journal of Climatology*, 25: 693–712. doi:10.1002/joc.1181



- Moss RH, Edmonds JA, Hibbard KA, Manning MR, Rose SK, van Vuuren DP, Carter TR, Emori S, Kainuma M, Kram T, Meehl GA, Mitchell JFB, Nakicenovic N, Riahi K, Smith SJ, Stouffer RJ, Thomson AM, Weyant JP, Willbanks TJ. 2010. The next generation of scenarios for climate change research and assessment. *Nature*, 463, 747–756.
- Narayan N, Paul A, Mulitza S, and Schulz M. 2010. Trends in coastal upwelling intensity during the late 20th century. *Ocean Science*, 6:3, 815-823.
- Nakicenovic N, Alcamo J, Davis G, De Vries B, Fenhann J, Gaffin S, Gregory K, Grubler A, Jung TY, Kram T, La Rovere EL, Michaelis L, Mori S, Morita T, Pepper W, Pitcher H, Price L, Riahi K, Roehrl A, Rogner HH, Sankovski A, Schlesinger M, Shukla P, Smith S, Swart R, Van Rooijen S, Victor N, Dadi Z. 2000. *Special report on emissions scenarios*, Cambridge University Press, UK.
- Nunez M, Solman S, Cabre´ M. 2006. Mean climate and annual cycle in a regional climate change experiment over Southern South America. II: climate change scenarios (2081–2090). In: *Proceedings of 8 ICSHMO, 24–28 April 2006*. Foz do Iguacu, Brazil. pp 325–331.
- Pesquero JF, Chou SC, Nobre CA, Marengo JA. 2009. Climate downscaling over South America for 1961–1970 using the Eta model. *Theoretical and Applied Climatology*. doi:10.1007/s00704-009-0123-z
- Pezzopane JRM, Pedro Júnior MJ, Thomaziello RA, Camargo MBP. 2003. Escala para avaliação de estádios fenológicos do cafeeiro Arábica. *Bragantia*, 62:3, 499-505.
- Pisnichenko AI and Tarasova TA. 2009. Climate version of the ETA regional forecast model: Evaluating the consistency between the ETA model and HadAM3P global model. *Theoretical Applied Climatology*.
- Podestá G, Bert F, Rajagopalan B, Apipattanavis S, Laciana C, Weber E, Easterling W, Katz R, Letson D, and Menendez. 2009. Decadal climate variability in the Argentine Pampas: regional impacts of plausible climate scenarios on agricultural systems. *Climate Research*, 40:2-3, 199-210.
- Quintana JM and Aceituno P. 2012. Changes in the rainfall regime along the extratropical west coast of South America (Chile): 30-43° S. *Atmósfera*, 25:1, 1-12.
- Ramirez-Villegas J, Salazar M, Jarvis A, and Navarro-Racines C.E. 2012. A way forward on adaptation to climate change in Colombian agriculture: perspectives towards 2050. *Climatic Change*, 115:3-4, 611-628.
- Rauscher SA, Seth A, Qian J-H, Camargo SJ. 2006. Domain choice in an experimental nested modeling prediction system for South America. *Theoretical and Applied Climatology*, 86:229–246.
- Rauscher SA, Seth A, Liebmann B, Qian J-H, Camargo SJ. 2007. Regional climate model simulated timing and character of seasonal rains in South America. *Monthly Weather Review*, 135:2642–2657.
- Resende N, Giarolla A, Rodrigues D, Tavares PS, Chou SC. 2011. Ocorrência da doença ferrugem-do-café (hemileia vastatrix) em algumas regiões de São Paulo, baseada nas projeções climáticas do modelo Eta/cptec (cenário A1B-IPCC/SRES). In: *XVII Congresso Brasileiro de Agrometeorologia, 2011, Guarapari*. Anais. Sociedade Brasileira de Agrometeorologia.

- Rodrigues D, Tavares PS, Giarolla A, Chou SC, Resende N, Camargo MBP. 2011. Estimativa da ocorrência de temperatura máxima maior que 34 C durante o florescimento e maturação do cafeeiro baseada no modelo Eta/CPTEC 40km Cenário A1B. In: *XVII Congresso Brasileiro de Agrometeorologia, 2011, Guarapari*. Anais. Sociedade Brasileira de Agrometeorologia.
- Rosenzweig C. 2007. Crops and livestock. In ML Parry (eds.) Chapter 1: Assessment of Observed Changes and Responses in Natural and Managed Systems. *Climate change 2007: impacts, adaptation and vulnerability: contribution of Working Group II to the fourth assessment report of the Intergovernmental Panel on Climate Change*. Cambridge University Press (CUP): Cambridge, UK: Print version: CUP.
- Ruane AC, Cecil LD, Horton RM, Gordón R, McCollum R, Brown D, Killough B, Goldberg R, Greeley AP, and Rosenzweig C. 2013. Climate change impact uncertainties for maize in Panama: Farm information, climate projections, and yield sensitivities. *Agricultural and Forest Meteorology*, 170:0, 132-145.
- Salazar LF, Nobre CA, Oyama MD. 2007. Climate change consequences on the biome distribution in tropical South America. *Geophysical Research Letters*, 34:L09708.
- Sampaio G, Nobre C, Costa MH, Satyamurty P, Soares-Filho BS, Cardoso M. 2007. Regional climate change over eastern Amazonia caused by pasture and soybean cropland expansion. *Geophysical Research Letters*, 34:L17709.
- Satyamurty P, da Costa CPW, Manzi AO, and Candido LA. 2013. A quick look at the 2012 record flood in the Amazon Basin. *Geophysical Research Letters*, 40:7, 1396-1401.
- Satyamurty P, de Castro AA, Tota J, da Silva Gularte LE, and Manzi AO. 2010. Rainfall trends in the Brazilian Amazon Basin in the past eight decades. *Theoretical and Applied Climatology*, 99:1-2, 139-148.
- Schulz N, Boisier J.P, and Aceituno P. 2012. Climate change along the arid coast of northern Chile. *International Journal of Climatology*, 32:12, 1803-1814.
- SENAMHI. 2007. *Escenarios de cambio climático en la Cuenca del Río Urubamba para el año 2100* [Climate change scenarios in the Urubamba River Basin by 2100]. [Rosas G, Avalo, G, Díaz A, Oria C, Acuña D, Metzger L and Miguel R. (eds.)]. Servicio Nacional de Meteorología e Hidrología (SENAMHI), Lima, Perú. Segunda edición: octubre de 2005, pp. 120.
- Seth A, Rauscher SA, Camargo SJ, Qian J-H, Pal JS. 2007. RegCM3 regional climatologies for South America using reanalysis and ECHAM global model driving fields. *Climate Dynamics*, 28:461-480. doi:10.1007/s00382-006-0191-z
- Seth A, Rojas M, Rauscher SA. 2010. CMIP3 projected changes in the annual cycle of the South American Monsoon. *Climatic Change*, 98: 331-357. doi: 10.1007/s10584-009-9736-6
- Sillmann J, Kharin VV, Zwiers FW, Zhang X, and Bronaugh D. 2013. Climate extremes indices in the CMIP5 multimodel ensemble: Part 2. Future climate projections. *Journal of Geophysical Research: Atmospheres*, 118: 2473-2493. doi:10.1002/jgrd.50188.

Silva VDPR, Campos JHBC, Silva MT, and Azevedo PV. 2010. Impact of global warming on cowpea bean cultivation in northeastern Brazil. *Agricultural Water Management*, 97:11, 1760-1768.

Sitch S, Huntingford C, Gedney N, Levy PE, Lomas M, Piao SL, Betts R, Ciais P, Cox P, Friedlingstein P, Jones CD, Prentice IC, and Woodward FI. 2008. Evaluation of the terrestrial carbon cycle, future plantgeography and climate-carbon cycle feedbacks using five Dynamic Global Vegetation Models (DGVMs). *Global Change Biology*, 14:9, 2015-2039.

Smith SJ and Wigley TML. 2006. Multi-Gas Forcing Stabilization with the MiniCAM. *The Energy Journal*, Special Issue, 3, 373–391.

Solman S, Nunez M, Cabre MF. 2007. Regional climate change experiments over southern South America. I: present climate. *Climate Dynamics*, 30:533–552. doi:10.1007/s00382-007-0304-3

Taylor KE, Stouffer RJ, Meehl GA. 2012. An overview of CMIP5 and the experiment design. *Bulletin of the American Meteorological Society*, 485–498.

Tavares PS, Giarolla A, Chou SC, Rodrigues D, Resende N. 2010. Projeções futuras da duração do ciclo da cultura da soja baseadas no modelo regional Eta/CPTEC 40km (cenário A1B). In: *XVI Congresso Brasileiro de Meteorologia, 2010*, Belém. Anais, XVI Congresso Brasileiro de Meteorologia, Sociedade Brasileira de Agrometeorologia.

Teixeira EI, Fischer G, van Velthuizen H, Walter C, and Ewert F. 2013. Global hot-spots of heat stress on agricultural crops due to climate change. *Agricultural and Forest Meteorology*, 170:206-215.

Torres RR, Marengo JA. 2013. Uncertainty assessments of climate change projections over South America. *Theoretical and Applied Climatology*, 112, 253-272.

Urrutia R, Vuille M. 2009. Climate change projections for the tropical Andes using a regional climate model: temperature and precipitation simulations for the end of the 21st century. *Journal of Geophysical Research*, 114, D02108.

Valentini LSP. 2009. *Avaliações microclimáticas em cafezais nos sistemas de monocultivo e arborizados com seringueira e coqueiro-anão na região de Mococa-SP*. Dissertação (Mestrado em Agricultura Tropical e Subtropical), Instituto Agronômico de Campinas. 58p.

Van Vuuren DP, Edmonds J, Kainuma M, Riahi K, Thomsonm A, Hibbard K, Hurtt GC, Kram T, Krey V, Lamarque JF, Masui T, Meinshausen M, Nakicenovic N, Smith SJ, Rose SK. 2011. The representative concentration pathways: an overview. *Climatic Change*, 109, 5 – 31.

Villacis M. 2008. *Ressources en eau glaciaire dans les Andes d'Equateur en relation avec les variations du climat: le cas du volcan Antisana*. [Resources of water ice in the Andes of Ecuador in relation to climate variations: the case of Antisana volcano.]. Diss. PhD, Université Montpellier, Montpellier. 256 pp.

Vincent L, Peterson T, Barros VR, Marino MB, Rusticucci M, Miranda G, Ramirez E, Alves LM, Ambrizzi T, Baez J, Barbosa de Brito JI, Berlato M, Grimm AM, Jaido dos Anjos R, Marengo JA, Meira C, Molion L, Muncunil DF, Nechet D, Rebello E, Abreu de Sousa J, Anunciação YMT, Quintana J, Santos J, Ontaneda G, Baez J, Coronel G, Garcia VL, Varillas IT, Bidegain M, Corradi V,

- Haylock MR, Karoly D. 2005. Observed trends in indices of daily temperature extremes in South America, 1960–2002. *The Journal of Climate*, 18:5011–5023.
- Vuille M, Francou B, Wagnon P, Juen I, Kaser G, Mark BG, and Bradley RS. 2008. Climate change and tropical Andean glaciers: Past, present and future. *Earth-Science Reviews*, 89:3-4, 79-96.
- Walter LC, Rosa HT, and Streck NA. 2010. Simulação do rendimento de grãos de arroz irrigado em cenários de mudanças climáticas [Simulating grain yield of irrigated rice in climate change scenarios]. *Pesquisa Agropecuaria Brasileira*, 45:11, 1237-1245.
- Wang G, Sun S, and Mei R. 2011. Vegetation dynamics contributes to the multi-decadal variability of precipitation in the Amazon region. *Geophysical Research Letters*, 38, L19703.
- Zhao Q, Black TL, Baldwin ME. 1997. Implementation of the cloud prediction scheme in the Eta model at NCEP. *Weather Forecast*, 12:697–712.
- Zhang Y, Fu R, Yu H, Qian Y, Dickinson R, Silva Dias MAF, da Silva Dias PL, and Fernandes K. 2009. Impact of biomass burning aerosol on the monsoon circulation transition over Amazonia. *Geophysical Research Letters*, 36, L10814.
- Zullo J, Pinto HS, Assad ED, and Heuminski de Avila AM. 2011. Potential for growing Arabica coffee in the extreme south of Brazil in a warmer world. *Climatic Change*, 109:3-4, 535-548.



RESEARCH PROGRAM ON  
**Climate Change,  
 Agriculture and  
 Food Security**



The CGIAR Research Program on Climate Change, Agriculture and Food Security (CCAFS) is a strategic initiative of CGIAR and the Earth System Science Partnership (ESSP), led by the International Center for Tropical Agriculture (CIAT). CCAFS is the world's most comprehensive global research program to examine and address the critical interactions between climate change, agriculture and food security.

**For more information, visit [www.ccafs.cgiar.org](http://www.ccafs.cgiar.org)**

Titles in this Working Paper series aim to disseminate interim climate change, agriculture and food security research and practices and stimulate feedback from the scientific community.

CCAFS is led by:

Strategic partner:



Research supported by:

